

Friction, wear and mechanical properties of electron beam modified PTFE-based rubber compounds

Der Fakultät Maschinenwesen

der

Technical Universität Dresden

zur

Erlangung des akademischen Grades

Doktoringenieur (Dr.-Ing.)

angenommene Dissertation

M. Sc.- Eng. Khan, Mohammad Sohail
geb. am: 01.02.1977 in Peshawar, Pakistan

Tag der Einreichung:	15.10.2008
Tag der Verteidigung:	19.03.2009
Gutachter:	Prof. Dr.rer.nat.habil. Gert Heinrich Prof. Dr.-Ing.habil. Hans-Joachim Radosch Prof. Dr.-Ing. Edmund Haberstroh
Vorsitzender:	Prof. Dr.-Ing.habil. Rüdiger Lange

Acknowledgements

It is a great pleasure for me that the hard work, dedication and energy invested during last three years for the completion of PhD thesis have been acclaimed by the scientific community with great enthusiasm. I am grateful to my thesis-supervisor, colleagues, friends and my family for making it possible for me.

Firstly, I would express my deep gratitude to Prof. Gert Heinrich as being my thesis-supervisor. A humble person and a kind teacher who is always willing in helping, providing opportunities, and exposing students to the scientific environment on a large scale. Under his auspices and supervision, the task was accomplished efficiently. It produced significant results and can be verily considered as one of my well-earned academic achievements. The completion of my thesis work would have been dispensable with out his support and kind supervision. Afterwards, I am grateful to my respected colleagues, Dr. Dieter Lehmann and Dr. Uwe Gohs with whom I worked closely and learned enormously. The expertise and vast experience of Dr. Lehmann in chemical modification of PTFE powder coupled with the endless adventure of Dr. Gohs in electron treatment of polymers proved a substantial help to me in exploring solution to incomprehensible and complicated problems. I am also indebted to pay my appreciation and thankfulness to Dr. Rainer Franke from IMA GmbH for his continuous support both experimentally and theoretically in studying the tribological aspects of the research work. Their scientific cognition and experience was undoubtedly beneficial.

I would also like to greatly commend especially my colleagues including Dr. Eva Ürögi, Dr. Amit Das, Rene Jurk and Dr. Klaus Werner Stöckelhuber with whom I have spent great time both in and off the work and were often involved in discussion on different subject matters. I am very much thankful to their full support and co-operation during the course of my research work. Besides this, I am indebted to the departmental co-workers of Composite Materials along with Dr. Edith Mäder, Ms. Gudrun Schwarz, Ms. Anne Hofmann and the administration of the Leibniz Institute of Polymer Research Dresden.

I am thankful to members and co-workers of other departments who have helped me in my research work. Uwe Geißler for particle size analysis, Carola Kutschera for chemical analysis, Gudrun Adam for FTIR analysis, Ute Reuter for TEM, Holger Scheibner and Robert Sommerschuh for mechanical testing and many others for providing assistance. Last, but not least, I thank my LORD and my parents and family for educating me with aspects from both arts and sciences, for unconditional support and encouragement to pursue my interests, even when the interests went beyond the boundaries of language, field and geography.

Contents

1. Introduction	1
1.1. Aim of the work	3
1.2. Scope of the thesis	4
2. Theoretical approach	6
2.1. PTFE powder in tribological applications – state of the art	6
2.2. Friction and wear	8
2.2.1. Friction and wear of rubber-like materials	9
2.2.2. Friction and wear of solid polymeric materials	12
2.2.3. Practical objectives of tribology	15
2.3. Polytetrafluoroethylene (PTFE)	16
2.3.1. Polymerization and manufacturing	16
2.3.2. Structure and properties	18
2.3.3. Micropowders	18
2.4. Chemically coupled PTFE compounds	19
2.5. Radiation and crosslinking processes	21
2.5.1. Radiation-induced modification processes	21
2.5.2. Crosslinking of rubber compounds	23
2.6. Structure and properties of rubber	25
3. Design of experiments	28
3.1. Material description	28
3.1.1. PTFE powder	28
3.1.2. Rubber and additives	28
3.2. Electron modification of PTFE powder	29
3.3. Characterization of PTFE powder	31
3.3.1. Spectroscopic analyses	31
3.3.2. Contact angle measurement	31
3.3.3. Particle size and distribution	31
3.3.4. Scanning electron microscopy (SEM)	31
3.4. Sample preparation and characterization techniques	32

3.4.1.	Crosslinking processes	33
3.4.2.	Rheometric analysis	34
3.4.3.	Physical and dynamic mechanical properties	34
3.4.4.	Differential scanning calorimetry (DSC)	35
3.4.5.	Microstructure and dispersion	35
3.5.	Tribological measurements	36
3.5.1.	Pin on disk tribometer	36
3.5.2.	Surface characterization	38
3.5.2.1.	Surface topography/roughness	38
3.5.2.2.	X-ray photoelectron spectroscopy (XPS)	38
3.5.2.3.	Wear scar analysis	38
3.6.	Chloroprene rubber	38
3.6.1.	Chemical coupling analysis	39
3.6.2.	Estimation of crosslinking density: stress-strain measurements	39
4.	Results and discussion	43
4.1.	Characterization of PTFE powder: Effects of electron modification	43
4.2.	Characterization of peroxide-cured PTFE-EPDM	48
4.2.1.	Influence of PTFE loading and irradiation dose	48
4.2.1.1.	Cure analysis	48
4.2.1.2.	Compatibility and dispersion behavior	50
4.2.1.3.	Physical properties	53
4.2.1.4.	Friction and wear behavior	56
4.2.1.4.1.	Analysis of the wear mechanism	58
4.2.1.4.2.	Physical-wear property relationship	60
4.2.1.5.	Conclusions	61
4.2.2.	Influence of irradiation dose at constant PTFE loading	62
4.2.2.1.	Curing characteristics	62
4.2.2.2.	Physical properties	63
4.2.2.3.	Friction and wear properties	65
4.2.2.4.	Conclusions	71
4.2.3.	PTFE micropowder filled EPDM	72
4.2.3.1.	Physical and dynamical mechanical properties	72
4.2.3.2.	Microstructure and dispersion analysis	75

4.2.3.3.	Friction and wear properties	77
4.3.	Electron beam cross linked PTFE-EPDM	79
4.3.1.	Characterization with respect to chemical coupling	80
4.3.2.	Characterization of friction and wear properties	85
4.3.3.	Conclusions	88
4.4.	Chemically coupled PTFE-CR compounds	89
4.4.1.	Structure-properties characterization	89
4.4.2.	Chemical coupling analysis	93
4.4.2.1.	FTIR spectroscopy	93
4.4.2.2.	Plausible chemical coupling mechanism	95
4.4.3.	Compatibility and dispersion	96
5.	Conclusions & Outlook	98
	References	101
	Curriculum Vitae	110

Nomenclature

PTFE	Polytetrafluoroethylene
EPDM	Ethylene-propylene-diene-monomer
CR	Chloroprene rubber
(-COOH)	Carboxylic acid group
(-COF)	Carbonyl fluoride group
E-beam	Electron beam
kGy	kiloGray
μ	Friction coefficient
k	Specific wear rate
phr	Parts per hundred of rubber
t_{90}	Optimum cure time
ΔM	Apparent crosslinking density
C_1 (Mooney-Rivlin constant)	Number of network chains per unit volume of rubber
C_2 (Mooney-Rivlin constant)	Number of the effectively elastic trapped entanglements
σ_B	Tensile strength at break
ϵ_B	Elongation at break
E'	Storage modulus
Tan delta (E''/E')	Mechanical energy dissipation
σ_{red}	Reduced stress
$f(\lambda)$	Deformation function

1. Introduction

Elastomers derived from "elastic polymers" are special class of polymeric materials composed of long, chain-like crosslinked molecules with exceptional elastic mechanical properties. The high elastic memory, high ultimate elongation and low elastic modulus in comparison to engineering thermoplastics recommend elastomers in wide range of special purpose applications. More than half of all rubber produced worldwide is consumed alone in the production of automobile tires while the rest is utilized in mechanical goods such as mountings, seals, gaskets, belts, and hoses, and consumer products.

Although, natural rubber with the longest history of use as elastomer is still one of the most important industrial polymer, it now competes with synthetic elastomers such as ethylene-propylene-diene-monomer (EPDM), chloroprene (CR), styrene-butadiene-rubber (SBR) and acrylonitrile-butadiene-rubber (NBR) because of the diversity of the properties offered by these man made compounds over a wide range of applications. Versatility in polymer design and performance requirement has also resulted in the development of new synthesis routes, processing procedures and rubber formulations to meet specific demands. Although, it helped to a greater extent in acquiring the desired properties by variation of the physical characteristics such as resiliency, flexibility, extensibility and durability, they are unable to deliver solution to few inherent disadvantages associated with elastomers. One such drawback is the significantly poor friction and wear property of rubber compound. This characteristic of rubber compound is not only required for tire performance but also for non-tire rubber goods where the elastomeric structure is in direct contact with relatively hard counter-surface.

For this reason, a renewed interest can be noticed for rubber tribology because of the property requirement for rubber in engineering applications such as dynamic and static sealing, gaskets, automotive weather stripping etc [1]. Figure 1 shows a variety of sealing and gasket components which are feasible for different applications in a typical automotive engine unit. For friction and wear purpose, this necessitates exploring on how the requested performance can be fulfilled by the formulation of rubber compounds for specific requirement. For this reason, addition of Polytetrafluoroethylene (PTFE) powder as a potential friction-modifier additive has gained a huge interest due to its significantly low friction coefficient. However, these efforts have not been wholly successful especially in rubbers due the difficulty of obtaining homogeneous mixtures and higher PTFE loading. This problem was the result of PTFE unique properties, most probably its highly hydrophobic and inert surface which resists

wetting and compatibility. As such, uniform mixing and chemical coupling of PTFE in rubbers has not been achieved with any commercially significant success. There is indeed a strong motivation to probe into new techniques and procedures for the use of PTFE powder as solid lubricant in vast range of rubber compounds for tribological applications. Beside property requirements, this motivation is also encouraged by the demand for adapting sustainable technologies by replacing polymeric components in tribological applications where fluid and grease lubricants fail or possesses potential risk to surrounding environment.

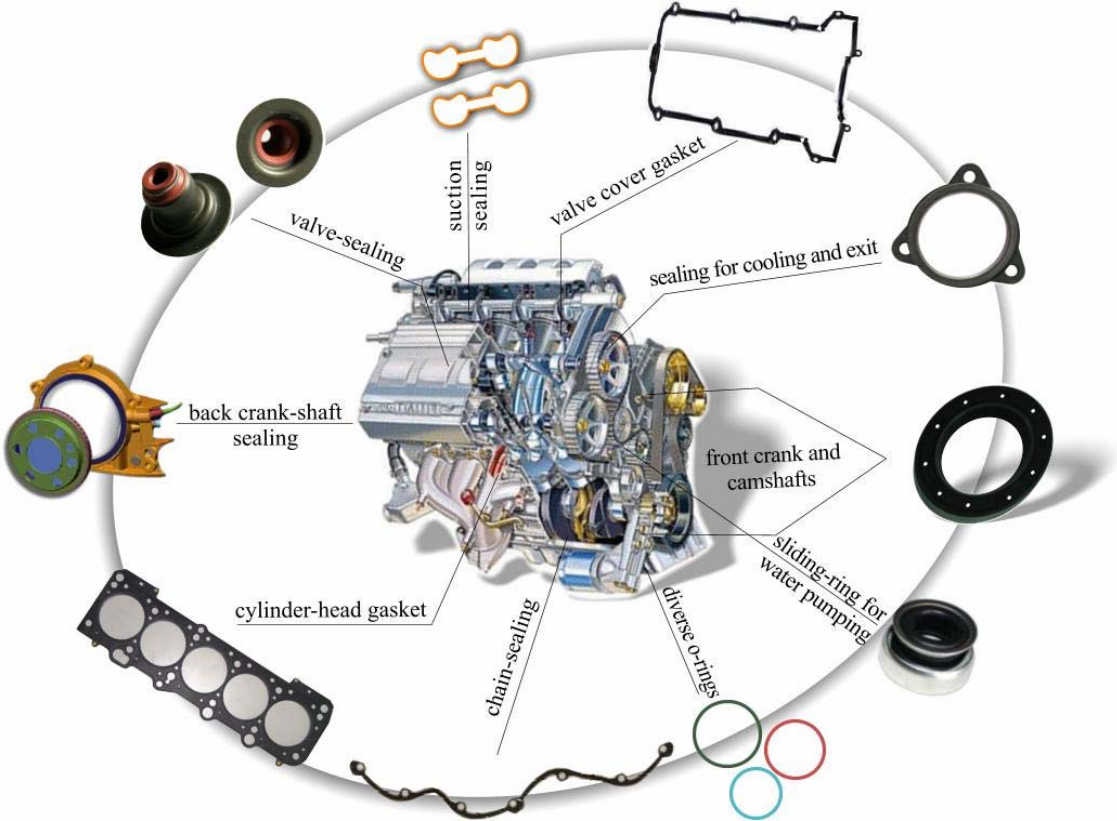


Figure 1. Dynamic and static sealing in motor engine [1]

In the present work friction and wear properties of PTFE filled EPDM rubber are investigated. With the help of electron irradiation, the inherent poor wetting and dispersion of PTFE powder is enhanced. Electron irradiation provides a wide range of advantages for the modification of inert PTFE surface. Chain scission of PTFE powder generates radical which are either trapped as persistent radicals in the crystalline structure of PTFE or in the presence of atmospheric conditions react partially with oxygen to form carbonyl fluoride groups (-COF) and later with water vapour to form carboxylic acid groups (-COOH). The presence of such reactive radicals and functional groups promote PTFE as an attractive choice for

effective use of PTFE powder in a wide range of polymers. Taking advantage of these specific radiation-induced modifications, chemical coupling of PTFE powder with speciality rubber matrixes such as EPDM and CR is achieved by a simple reactive-mixing process. Beside tribological properties, the corresponding chemical coupling of modified PTFE powder with rubber matrixes can significantly improve engineering properties of the rubber compounds.

1.1. Aim of the work

The extremely low friction properties of PTFE are well known, but so far there is no work disclosed in the literature concerning investigation on the friction and wear behaviour of this material in different types of rubber matrixes. In this context, the main aim of the present work was to impart low-friction and self-lubricating properties to rubber compounds by addition of PTFE powder.

In this work two different kinds of rubber matrixes have been investigated i.e. EPDM and CR. Although, bulk of the current investigation is devoted to understanding the friction and wear behaviour of PTFE filled EPDM compounds, a minor segment but significantly important both from the application and academic point of view has been dedicated to exploring novel compounds based on PTFE powder in technical rubbers, such as CR. For this reason the current thesis has been designed specifically to answer the following three important questions. These three points also constitute the main objectives of the research thesis.

- a) Is it possible to improve friction and wear properties of host rubber matrixes by incorporating PTFE powder with desired mechanical properties?
- b) Which dominant mechanism/s are involved concerning friction, wear and mechanical properties of PTFE based rubber compound?
- c) Is there any influence of morphology, dispersion and chemical coupling of PTFE powder on the mentioned properties of rubber compound?

For this reason different aspects of the work have been investigated. The main tasks of the current work have been divided into five different directions as formulated below.

- Modification of PTFE powder with the help of electron irradiation for chemical coupling with rubber matrixes.
- Optimization of PTFE loading (both modified/non-modified PTFE powder) required not only for friction and wear properties but also for the desired mechanical and dispersion properties.
- Investigating the effects of radiation-induced changes in PTFE powder on friction, wear and mechanical properties of PTFE based EPDM compound.
- Designing of experimental set-up for the preparation of PTFE-based rubber compounds for investigating the influence of morphology, dispersion and chemical coupling of PTFE powder on rubber compound.
- Is there any influence of morphology, dispersion and chemical coupling on friction, wear and mechanical properties of rubber compound and which related mechanism/s are dominant?

1.2. Scope of the thesis

In Chapter 2, a detailed but relevant theoretical background in the context of the thesis has been provided. A detailed overview related to the properties, structure and use of PTFE powder in tribological as well as in different applications has been provided. Besides this, some insight into basics of the friction and wear mechanisms of rubber-like materials have also been presented. This section provides the basis of the work. The aim was to combine, analyze and at the same time extract known information relevant to the present thesis and utilize this information in achieving the desired aim.

Chapter 3 is concerned with the detailed description of the instrumentation and experimental procedures adapted in the present work. The experimental section was designed to provide overview of the sample preparation, electron modification technique and various other characterization techniques with special emphasis on the determination of the friction, wear and mechanical properties of PTFE based rubber compounds.

In Chapter 4, results along with the discussion have been presented. This chapter has been divided into four distinct subchapters. **Chapter 4.1** discusses the characterization of modified PTFE powder in comparison with non-modified PTFE powder with the aim to study the effects of electron irradiation on chemical structure of PTFE powder using techniques such as Fourier Transform Infra red Spectroscopy (FTIR), Electron Spin Resonance (ESR) etc. The characterization of PTFE-EPDM rubber compounds have been discussed in details in **Chapter 4.2**. The effects of electron modification on properties of peroxide crosslinked EPDM and optimization of PTFE loading for desired properties have been investigated. The effects of electron modification, irradiation dose and PTFE loading on physical, friction and wear properties have been determined. Further, the chemical compatibility and dispersion of PTFE powder with EPDM is characterized by Transmission Electron Microscopy (TEM), Scanning Electron Microscopy (SEM) and by Differential Scanning Calorimetry (DSC). **Chapter 4.3** focuses on using electron irradiation instead of peroxide for crosslinking of EPDM filled with 30 phr to investigate the influence of morphology, dispersion and chemical coupling PTFE powders on physical, friction and wear properties. **Chapter 4.4** discusses a new class of chemically coupled PTFE filled CR compounds. A new approach to the coupling reaction mechanism is proposed based on the Lewis acid concept which is also applicable to crosslinking of CR in the presence of MgO and ZnO. Some new findings and results which have not been previously investigated for CR rubber are reported. Finally, the most relevant results are summarized and some general conclusions are drawn in **Chapter 5**. In addition, an outlook on future work and an overview of possible applications for this promising material is presented in **Chapter 6**.

2. Theoretical approach

2.1. PTFE in tribological applications – state of the art

It has long been a desire to combine the properties of an elastomer and PTFE. Past efforts to produce compositions with beneficial combined properties have not been wholly successful. In addition, the past attempts to incorporate PTFE into rubber, have been generally limited to attempts and compositions containing no more than 20 wt% of PTFE loading. Such compositions have failed to provide a sufficient combined benefit from the properties of PTFE and elastomers to have great commercial importance. Higher PTFE loadings could not be obtained because of the difficulty in achieving homogeneous dispersion in elastomer composition. This was mainly due to the result of PTFE unique properties, most probably due its highly hydrophobic surface which resist wetting and adhesion. Because of these properties, homogeneous dispersion and chemical coupling of PTFE powder both in natural and synthetic rubbers have not been achieved in compositions with any commercially significant incorporation of PTFE due to the associated "poor wetting" and "dispersion" of PTFE powder.

The extremely low friction properties of PTFE are well known, but there is little work disclosed in the literature on compounding this material with different types of elastomers. Initially, PTFE was used in speciality polymers such as silicone and fluorosilicone rubber for sealing and dynamic applications owing to their superior temperature and chemical resistance. However, their relatively low tear strength and abrasion resistance restrict their useful application. For this reason, Crandell used PTFE as a reinforcing additive to improve the tear resistance of silicone rubbers [2] while by late 60's it was further used in fluoroelastomers [3, 4]. Although the fibrillation of the high molecular weight PTFE during shearing action inside the roll mills effectively reinforces elastomers, it also leads to deterioration of some other mechanical properties. For this reason the practical level of application of the addition of high molecular weight PTFE powder is limited. Although, the compounding of elastomers with PTFE powder may produce vulcanizates with reduced frictional properties, the required PTFE loading to affect even a marginal improvement so diminishes the physical properties of the vulcanizate that the practical applications of these compounds are severely limited. Simply, if a material could be found which would reduce the surface frictional properties and not appreciably deteriorate or, in other words, improve the physical properties of the vulcanizate,

such an approach would be attractive. Consequently, this approach to producing low-surface-friction elastomers based on neoprene and silicone compounds resulted both in low physical and friction properties due to the poor compatibility of PTFE powder [5]. Alternatively, efforts were also dedicated to provide low-friction surface coatings to elastomers and thermosets substrates by depositing thin PTFE film coating while maintaining intact the bulk properties of the compounds. The attempt was successful in case of metals coating but a failure for elastomers due to inability of elastomeric substrate to sustain high temperature PTFE film coating [5, 6]. PTFE powder was also used in styrene-butadiene rubber (SBR), acrylonitrile-butadiene-rubber (NBR) and butyl rubber (IIR). The principal cause of the great improvement in tensile and tear strength was believed to be due to the formation of oriented PTFE fibers in the elastomer matrix [7]. Fluoro-elastomers and PTFE powder were also compounded and kneaded until PTFE is fibrillated to be used as adhesive agent, a sealing agent, a packing material or a reinforcing material in instruments employed in corrosive environments [8]. New elastomer-PTFE compositions and compounding procedures were developed in improving mechanical properties (tensile strength, modulus) of low-strength Ethylene Propylene (EP) and silicone elastomers by effective fibrillation of PTFE powder. Similarly, in the case of high-strength rubbers such as Nitrile and NBR as low as 2-6 wt% of PTFE powder was incorporated in improving the vulcanizate strength and modulus. These compositions could be useful for example, for O-rings, seal lips (for hydraulic and pneumatic cylinders), seals for pumps, valves etc. The improvement in the desired properties of the composition with such a low PTFE loading was attributed to the formation of network of entangled fibers due to high shearing of the PTFE powder during compounding. The fibrillated PTFE provides a high ratio between fiber length and fiber diameter (aspect ratio). On the other hand, finely ground particulate PTFE (lacking fibrillation effect) was also modified by special purpose etching procedures to enhance interaction with the rubber matrix. This helped to improve the tensile strength and modulus of elasticity of rubber compounds [9, 10]. With growing demands for high performance compounds for sealing applications (gaskets etc), different processing techniques and procedures were also employed in which the crosslinked domains of silicone, fluorosilicone etc as minor components were introduced in the bulk of stretched PTFE films and sheets [11, 12].

2.2. Friction and wear

Tribology derived from the Greek *tribos*, meaning to rub, is defined in 1967 as a science and technology of interactive surfaces in relative motion. The fundamental aspects related to interacting surfaces mainly focuses on *friction*, *wear* and *lubrication*. In this work emphasis has been devoted to study friction and wear behaviour under dry conditions (solid state) without any lubrication. Therefore, tribology due to lubrication is not discussed.

Friction is a force that resists relative motion between two surfaces in contact. The friction coefficient is the ratio between the friction force (F_R) and the normal force (F_N):

$$\mu = \frac{F_R}{F_N} \quad (1)$$

It is generally recognized that the frictional force between two surfaces in relative motion comprises two principal components. The first arises due to adhesion over the area of real contact while the second component, known as the ploughing, displacement, or deformation, results from the interpenetration of asperities of the two bodies, necessitating the displacement of material during sliding. A particularly common situation is when hard asperities on one solid penetrate into the surface of the softer body. Thus, the frictional force F is given by:

$$F_{\text{total}} = F_{\text{adhesion}} + F_{\text{displacement}} \quad (2)$$

The importance of adhesion between two solids in sliding contact has been emphasized by Bowden and Tabor [13] in explaining the tribological phenomena. The adhesive friction component depends on the chemistry of the tribo surfaces at the sliding interface. The displacement component is subdivided by Kraghelskii into four distinct types [14]: elastic displacement, plastic displacement, shearing-cutting of the bulk material and shearing of surface films. The relative importance of the contribution of each of the above to the total frictional force depends on the type of motion involved (sliding or rolling), the surface topography and the physical and mechanical properties of the material themselves.

Wear is defined as the unwanted loss of solid material from sliding surfaces due to mechanical interaction. The classifications of the wear occurring in different situations are:

- a) Abrasive wear – caused by the presence on one or both surfaces, by the presence of hard particles between the surfaces, or by hard particles embedding in one of them.
- b) Adhesive wear – the transfer of material from one surface to another during relative motion as a consequence of adhesive forces.
- c) Erosive wear – caused by relative motion between a solid and particles entrained in a fluid.

- d) Fatigue wear – the detachment of particles as a result of cyclic stress variations.
- e) Corrosive wear – a process in which the chemical reaction with the environment is the rate-determining factor [15].

2.2.1. Friction and wear of rubber-like materials

A completely different situation arises when a rubber-like material slides against a hard counter-surface e.g., in rubber sealing, wiper blades or the contact between a tire and the metallic rim [16]. Rubber friction in such a tribological system differs in many ways from the frictional properties of most other solids. The reason for this is the very low elastic modulus of rubber and the high internal friction exhibited by rubber over a wide frequency range. The pioneering studies of Grosch have concluded that rubber friction in many cases is directly related to the internal friction of the rubber, i.e., it is mainly a bulk property of the rubber. It has been shown that rubber surfaces sliding on silicon carbide paper and glass surfaces result in friction coefficients with the same temperature dependence as that of the complex elastic modulus $E(\omega)$ of the rubber [17]. The friction force between rubber and a hard-rough counter-surface has two contributions commonly described as the adhesion and hysteretic components as shown schematically in Figure 2.

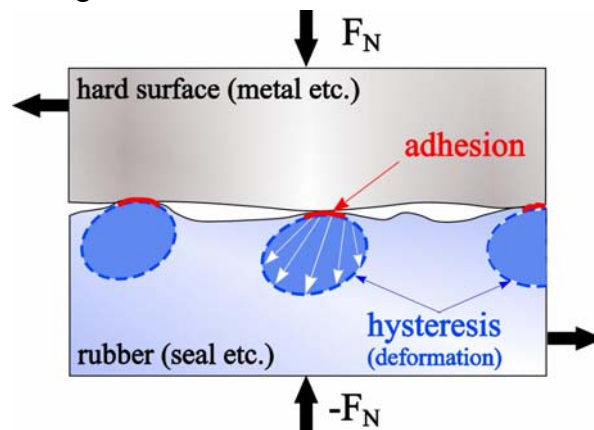


Figure 2. Schematic of the adhesion and hysteresis (deformation) components in rubber against hard surfaces

The hysteretic component results from the internal friction of the rubber. The asperities of the hard counter-surface during sliding exert oscillating forces on the rubber surface. This leads to cyclic deformations of the rubber and simultaneously to energy ‘dissipation’ via the internal damping of the rubber. This contribution to the friction force have the same temperature dependence as that of the elastic modulus $E(\omega)$ (a bulk property). The adhesion component is important only for sufficiently clean and smooth surfaces.

Velocity and Temperature effects on rubber friction

Another important parameter of rubber friction is the dependency of friction coefficient on sliding velocity and temperature. The most extensive and systematic study so far on the dependency of rubber friction on velocity and temperature has been reported by Grosch [17]. He measured the effects of velocity, temperature, and surface roughness for rubber sliding on optically smooth glass. Grosch observed that the rubber friction increases nonlinearly with velocity, much like the shear thinning behaviour of high viscous polymers. Furthermore, at each sliding velocity, friction decreases with increasing temperature. Irrespective of the precise mode of friction (rolling, sliding), the effects of velocity and temperature are likely to be closely interrelated. Figure 3 shows results for the friction of acrylonitrile-butadiene-rubber (NBR) against glass as a function of speed at various temperatures.

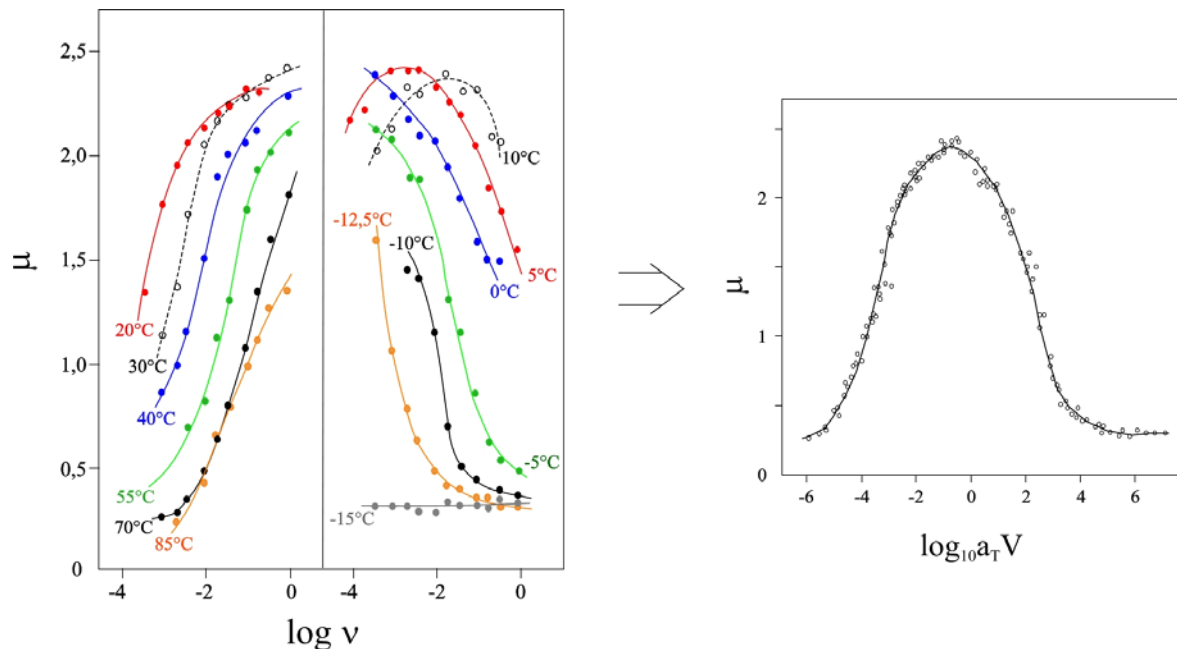


Figure 3. Construction of master curve for NBR sliding against glass [17]

It was determined that the curves were in fact segments of a single master curve which describes the friction coefficients of the sliding velocity at a selected reference temperature (T_0). This family of curves can be fitted together to form a master-curve as shown in Figure 3 by a transformation of the Williams-Landel-Ferry (WLF) equation:

$$\log a_T = -8.86(T-T_0)/(101.5+T-T_0) \quad (3)$$

where: a_T is the temperature-dependent parameter [dimensionless]
 T is the contact or ambient temperature [$^{\circ}\text{C}$]

T_0 is the Reference temperature defined as: $T_0 \sim T_g + 50 \text{ }^\circ\text{C}$ where T_g is the glass transition temperature of the polymer [$^\circ\text{C}$]

The master curve is derived from the experimental results by translating the curve obtained at a temperature T horizontally by an amount $\log a_T$ to fit the reference curve at temperature T_0 . The strong influence of visco-elasticity on rubbers causes the friction coefficient to initially rise with sliding velocity before declining. This is in contrast to most other materials where the static friction coefficient (friction coefficient in micro-sliding) is always greater than the kinetic friction coefficient. One important advantage which can be obtained by transforming velocity and temperature effects on friction is that it becomes possible to isolate the effect of velocity on friction at constant temperature. Experimentally, this cannot be achieved because of the effects of frictional heating at high sliding velocities. As an example, Figure 4 shows some results in which experimental values of friction and temperature are plotted against velocity for a particular rubber at three different loads. The coefficient of friction appears to decrease with increasing speed. However, if the curves are superposed to constant temperature by WLF transform, the left hand line shows that the friction now increases with velocity. The original decrease was therefore a temperature rather than a velocity effect. Moreover, the fact that after transformation all the points for the three loads lie on the same curve further shows that the original, apparent increase in friction with load was merely a consequence of the different temperatures associated with each load.

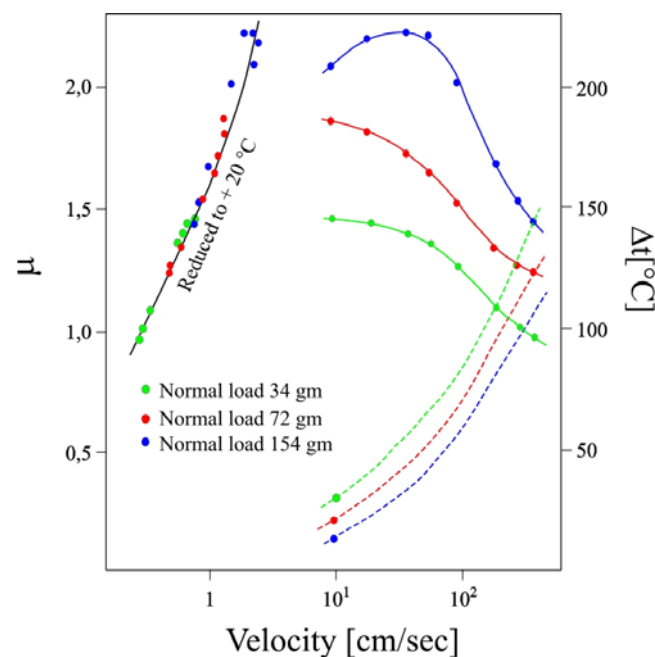


Figure 4. Coefficient of friction (full lines); and temperature rise (dotted lines) for a needle-thermocouple sliding on carbon black-filled natural rubber [14]

2.2.2. Friction and wear of solid polymeric materials

The term polymers were never intended to be bearing or wear-resistant materials and in fact are usually unsuitable for tribological purpose. Hence, the number of polymers with valuable tribological properties is limited. Table 1 shows the most important polymers used for tribological applications along with their tribological characteristics [18].

Table 1. Tribological characteristics of typical polymers

Polymer	Tribological characteristics
Polytetrafluoroethylene (PTFE)	Low friction but high wear rate; usually blended with other polymers or reinforced as a composite material. High operating temperature limit (excess of 150°C).
Polyamide	Moderate coefficient of friction and low wear rate. Medium performance bearing material. Wear accelerated by water. Relatively low temperature limit.
Polyacetals	Performance similar to nylon. Durable in rolling contacts.
Polyetheretherketone (PEEK)	High operating temperature limit. Resistant to most chemical reagents. Suitable for high contact stress. High coefficient of friction in pure form.
Ultra high molecular weight polyethylene (UHMWPE)	Very high wear resistance even when water is present. Moderate coefficient of friction. Good abrasive wear resistance. Relatively low temperature limit.
Polyurethanes	Good resistance abrasive wear and to wear under rolling conditions. Relatively high coefficient of friction in sliding.
Polyimide	High performance polymers, suitable for high contact stresses and high operating temperatures.
Epoxides and phenolics	Used as binders in composite materials.

Most polymer surfaces are worn by a harder counterface during contact. A basic feature of almost all polymers is that a transfer film is formed when sliding against a harder counterface which has a strong influence on the tribology of polymers. The polymer which provides a classic example of transfer films formation is *PTFE*. Although there is probably a strong adhesion between a metallic surface and any other polymer, the special molecular structure

of PTFE cause a mechanism of film transfer which is particular to PTFE. A block of PTFE in contact with a harder counterface loses material as a series of laminae resulting in low friction but a high wear rate due to its characteristic molecular structure [19]. In tribology, PTFE is a well-known and commonly used polymer for solid lubrication. PTFE can be used also as an additive to improve lubricant and tribological properties of thermoplastics, coatings, greases, and inks. Concentrations ranging from 1 up to 20 wt% give in better wear resistance and release properties. Figure 5 shows wear rate and friction coefficient of unfilled polymers, polymer blends, and polymer composites used in tribological studies [20].

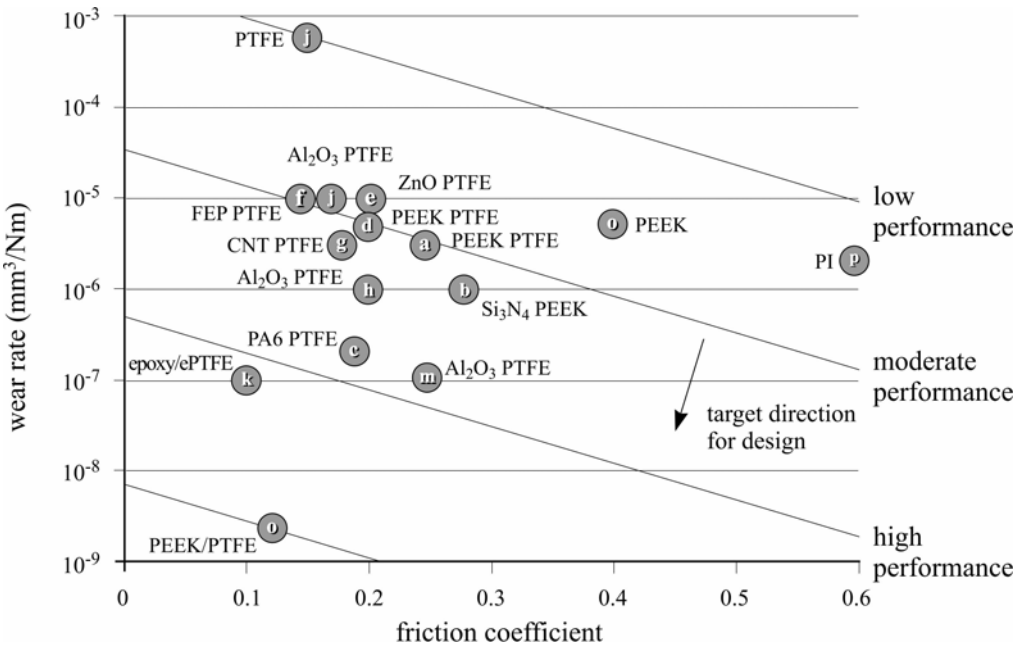


Figure 5. A multivariate plot of wear rate versus friction coefficient

As can be seen PTFE has significantly low friction coefficient but high wear rate. High performance engineering polymers like PEEK and polyimide (PI) have good wear resistance but high friction coefficient. In general, neat polymers lack the tribological performance required for most application. For this reason and especially in the case of high wear rate and low friction coefficient materials like PTFE, are extensively used as antifriction additives, bulk matrixes or in conjunction with various kinds of nanoparticles to obtain high performance solid lubricating polymeric composites. Fundamental studies addressed the tribology of rubbers already some decades ago [21–27]. Though these pioneering works contributed to our state-of-knowledge on this field markedly, many questions related to the friction and wear of rubbers remained open. Numerous investigators in recent years have studied the frictional behaviour of elastomers. The bulk of their endeavors have been directed

towards understanding the influence of this behaviour on the skidding characteristics of tires and towards deriving suitable mechanisms for the frictional behaviour under these conditions [28-34].

Nowadays, a renewed interest can be noticed for rubber tribology because of the property requirements for rubbers in engineering applications. This necessitates exploring on how the requested performance can be met by the formulation of the rubber. Different formulations have been investigated, e.g. fluoroelastomer matrix into which silica-based glass fibers is incorporated. The glass fibers serve to reinforce the elastomer and also serve as friction modifiers to provide desired coefficients of friction [35]. Fluoroelastomers were also used by filling with carbon fibers for improved tribological performances at elevated temperatures [36]. The fluoroelastomer is compounded with particles of a relatively hard material, such as beads and fibers of glass, ceramics and carbon black [35-37]. Various kinds of friction modifiers including fibrous (glass, carbon, asbestos etc) and powdered fillers (molybdenum disulfide, silica, graphite etc) have also been incorporated in various combinations in producing epoxy-rubber based compounds [38]. Beside this, tribological works on rubbers containing novel reinforcing fillers, such as organophilic clay [39] and carbon nanofibers and carbon nanotubes have also been studied [40, 41]. EPDM rubbers filled with carbon black were also studied in different test configurations. It was found that with increasing carbon black content the specific wear rate was reduced irrespective of the testing configuration. However, the coefficient of friction depends on rubber composition, test duration and the type of testing rig [42, 43]. Depending on the test conditions and the concentration of carbon black, the abrasion resistance could be significantly reduced for Isoprene rubber. The enhanced wear resistance is attributed to the increase in the strength and hardness of the matrix by adding carbon black [44]. More recently friction tests were performed on synthetic wiper rubber samples (EPDM and CR rubber) with several modulus and tangent modulus [45]. A good rubber formulation and an adapted surface treatment and coating can improve these phenomena. The rubber formulation should include the modulus and the tangent modulus, which have an influence on dry friction. This wiping is only possible by a good understanding of the tribological, mechanical and vibroacoustic parameters that control completely the contact.

2.2.3. Practical objectives of tribology

In simple terms it appears that the practical objective of tribology is to minimize the two main disadvantages of solid to solid contact; friction and wear, but this is not always the case. In some situations, as illustrated in Figure 6 shows the minimizing friction and maximizing wear or minimizing wear and maximizing friction or maximizing both friction and wear is desirable. For example, reduction of wear but not friction is desirable in brakes and lubricated clutches, reduction of friction but not wear is desirable in pencils, increase in both friction and wear is desirable in erasers. The necessity of tribology in automotive, petroleum, metallurgy, ship and rail, power plants and heavy mechanical industries is of significant importance for greater plant efficiency, better performance, fewer breakdowns, and significant savings. The other important reason of controlled or maintained tribology is the economical aspect. The first recognition on importance of the tribology applications is by the British ‘Jost Report’ as early as 1966, in which it was estimated that improvements in lubrication and maintenance in industry could save the British economy 500 million pounds sterling per year [46]. Subsequently, similar investigations have been carried out in West Germany, Japan, Canada and USA and similar figures for savings in the range 1.3 to 1.6% of GNP were suggested [47, 48]. It is generally believed that the economic losses to friction and wear are up to 4% of GNP in developed countries, about 8.5 billion pounds for the UK in 2001, and that up to 1% of these losses can potentially be saved by the application of known techniques to reduce friction and wear in machines [49].

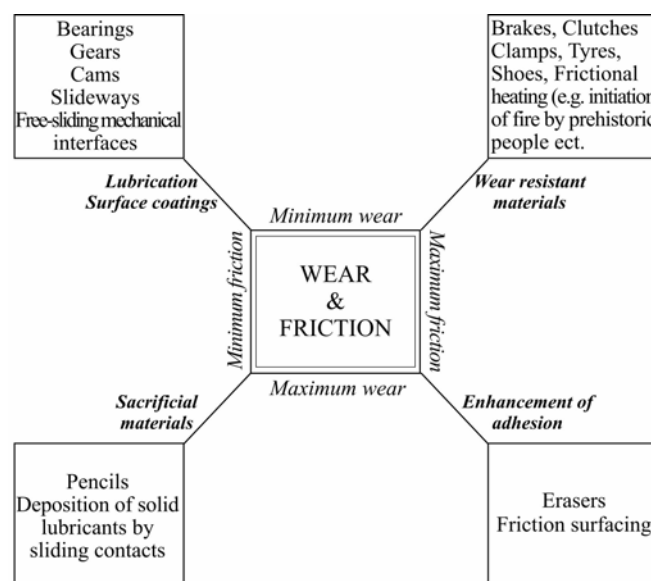


Figure 6. Practical objectives of tribology [18]

2.3. Polytetrafluoroethylene (PTFE)

2.3.1. Polymerization and manufacturing

Polytetrafluoroethylene (PTFE), a homopolymer of tetrafluoroethylene (TFE) monomer is a highly crystalline white to translucent solid polymer with extremely high molecular weight (range 10^6 - 10^7 g/mol) and viscosity (10^{10} - 10^{12} Poise at 380°C). Polymerization of TFE monomer gives the perfluorinated straight-chain high polymer PTFE with the chemical formula $(\text{CF}_2\text{-CF}_2)_n$. TFE (molecular weight 100 g/mol) is a colourless, tasteless, odourless non-toxic gas. It is stored as a liquid and polymerized usually above its critical temperature 33.3°C and below its critical pressure 3.94 MPa. Besides being used for polymerization of PTFE homopolymer it could also be used in the copolymerization with hexafluoropropylene, ethylene, perfluorinated ether, and as a co monomer in a variety of terpolymers. Figure 7 shows the main steps involved in the manufacture of TFE monomer.

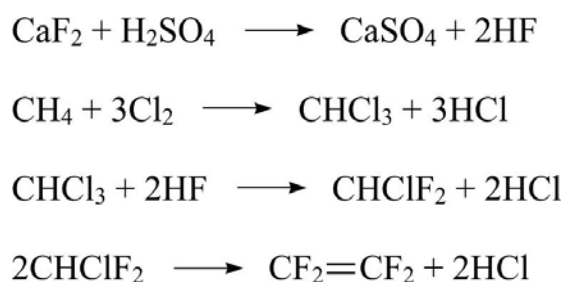


Figure 7. Basic manufacturing steps involved in TFE production

Hydrogen fluoride is manufactured by the first step while chloroform and other chloromethanes are produced in succeeding steps. Chloroform is then fluorinated with hydrogen fluoride to chlorodifluoromethane which upon pyrolysis produces tetrafluoroethylene. Although the polymerization mechanism is not a typical emulsion type, some of the principles of emulsion polymerization are applied. The two products are distinctly different, even though both are chemically high molecular weight PTFE polymers. Table 2 shows processing, properties and uses of various grades of PTFE in different applications such as electrical, mechanical and chemical [50].

Table 2. Applications of Polytetrafluoroethylene Resins

Resin grade	Processing	Description	Main uses
Granular			
- agglomerates	molding preforming sintering ram extrusion	free-flowing powder	gaskets, packing, seals, electronic components, bearings, sheet, rod, heavy-wall tubing; tape and molded shapes for nonadhesive applications
- coarse	molding preforming sintering	granulated powder	tape, molded shapes, non-adhesive applicatons
- finely divided	molding preforming sintering	powder for highest quality, void - free moldings	molded sheets, tape, wire wrapping, tubing, gaskets
- presintered	ram extrusion	free-flowing powder granular	rods and tubes
Fine powder			
- high reduction ratio	paste extrusion	agglomerated powder	wire coating, thin - walled tubing
- medium red. ratio	paste extrusion	agglomerated powder	tubing pipe, overbraided hose, spaghetti tubing
- low reduction ratio	paste extrusion	agglomerated powder	thread-sealant tape, pipe liners, tubing, porous structures
Dispersion			
- general purpose	dip coating	aqueous dispersion	impregnation, coating, packing
- coating	dip coating	aqueous dispersion	film, coating
- stabilized	coagulation	aqueous dispersion	bearings

Commercial PTFE is manufactured by two different polymerization techniques:

- **suspension polymerization** – either little or no dispersion agent is used and vigorous agitation is maintained. A precipitated resin commonly referred to as *granular resin* is produced.
- **emulsion polymerization** - a sufficient amount of dispersing agent and mild agitation is employed. This produces small colloidal particles dispersed in the aqueous reaction medium. In this procedure, called aqueous dispersion polymerization, precipitation of the resin particles is avoided. The coagulated dispersion produced by emulsion polymerization is often called as *fine-powder* or *PTFE dispersion*.

2.3.2. Structure and properties

The exceptional thermal and chemical stability of PTFE originate in the strength of its primary chemical bonds. The carbon-fluorine bond energy is the highest currently known among organic compounds [51, 52]. In addition, the fluorine atoms also strengthen the main chain carbon-carbon bond. Another factor that contributes to the unique character of PTFE is the crowding of the fluorine atoms around the main chain, which forces a helical conformation of the polymer backbone in the crystal lattice (Figure 8) [53, 54]. The dense packing of the relatively large fluorine atoms yields an impenetrable shield protecting the carbon backbone from chemical attack, and increases the stiffness of the molecular chain. Due to the relatively smooth molecular profile of the helical chains, the PTFE crystal structure essentially consists of a hexagonal packing of cylinders [55].

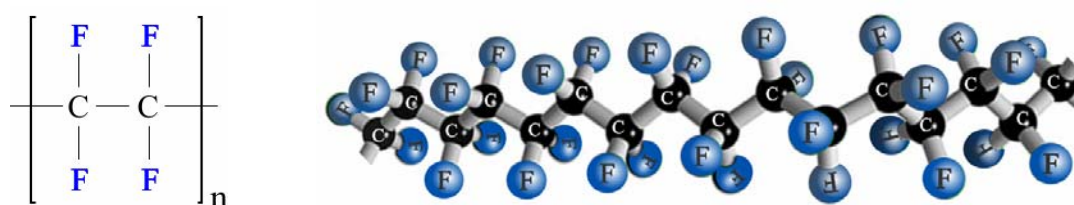


Figure 8. Chemical and molecular structure of PTFE

The limited contact area between the chains in the crystal lattice results in weak intermolecular interactions and a high chain mobility. The latter, in turn, is responsible for the outstanding low friction characteristics of PTFE, and, somewhat unexpected, for the high melting point of PTFE (327°C), as the high chain mobility in the solid state results in a low entropy of fusion. That high chain mobility also is the origin of a wide range of mechanical properties, such as a relatively low yield stress, high fracture toughness down to cryogenic temperatures and susceptibility to plastic creep (so-called “cold flow”) [56].

2.3.3. Micropowders

The PTFE micropowders, also called waxes, are tetrafluoroethylene homopolymers with molecular weights significantly lower than that of normal PTFE. The molecular weight for micropowders varies from 2.5×10^4 to 2.5×10^5 g/mol, where as that of normal PTFE is of the order of 10×10^6 g/mol. Micropowders are usually white in colour and are friable. The average

agglomerate particle size is between 5 μm and 10 μm while the primary particles are approximately 0.2 μm in diameter. These micropowders are commonly used as additives in a wide variety of applications for example where chemical resistance, weathering resistance and a wide temperature application range may be required. Most importantly the low friction properties of micropowders are obviously of significant advantage in many applications.

Micropowders are added to variety of materials used in industry, where they provide non stick and sliding properties. They are incorporated into the product by blending and grinding. The PTFE micropowders are commonly used in plastics, elastomers, inks, lubricants, and finishes lacquer. Lubricants containing micropowders are used for bearings, valve components, and other moving parts where sliding friction must be minimalised or eliminated. Nonstick finishes that required good release properties, e.g., in the food and packaging industry, commonly use PTFE micropowders.

In some applications, the high heat stability of micropowder can be utilised over a reasonably wide temperature range. The maximum service temperature is normally 260°C, provided the crystalline melting point is between 320°C and 335°C. Exposure above 300°C leads to degradation and possible evolution of toxic decomposition products. The particulate morphology of PTFE micropowder in printing inks provides desirable gloss to the printed product. Its inherent lubricity results in good wear and slip properties and surface smoothness. The chemical resistance of micropowder is as high as that of high molecular weight PTFE. It is therefore used in applications requiring service in a strong or corrosive chemical environment such as concentrated mineral acids and alkalies. It is also not attacked by organic solvents, which contributes to good weatherability [50].

2.4. Chemically coupled PTFE compounds

The chemically coupled PTFE based compounds were initially produced from irradiated PTFE micropowders and polyamide (PA) in a reactive extrusion process. High shear rate under melt processing conditions was necessary to obtain a good distribution and re-agglomeration of the PTFE micropowder. To achieve coupling reaction, an enhanced interaction between the carboxylic acid groups on the surface of the PTFE microcrystals and the amide groups of the molten polyamide matrix is necessary. The mechanism of the block copolymer formation by transamination reactions is shown in Figure 9. It was further investigated that the chemical coupling of PTFE with other matrix polymers, in particular rubber composition, a further modification of the carboxylic acid functionalised PTFE with

other functional groups is necessary. This can be done by transforming COOH groups into amide groups by the reaction of the irradiated PTFE micropowders with ϵ -caprolactam.



R- : H₂N- and/or Ac-NH-
 PA_{1,2} : polyamide chain segments

Figure 9. Mechanism of the formation of PTFE-PA-blockcopolymers [57]

For chemical coupling of electron irradiated PTFE powder with rubber compounds the presence of olefinic double bonds is necessary. Taking advantage of the persistent free radicals, formed by electron irradiation of PTFE, direct coupling of olefinic unsaturated matrix polymers like styrene-butadiene-styrene block copolymers (SBS), acrylonitrile-butadiene-styrene block-copolymers (ABS), acrylonitrile-butadiene rubber (NBR), ethylene-propylene-diene terpolymer (EPDM) etc. during a reactive extrusion process is possible. These radically coupled PTFE-rubber compounds have been previously investigated by Lehmann et. al. for tribological applications [58, 59]. The radically coupled PTFE elastomeric compounds were produced by low-temperature reactive processing technique. The olefinically unsaturated polymers such as SBS, NBR and EPDM are radically coupled during reactive blending. During mixing the reactive perfluoroalkyl-(peroxy) radicals react with these olefinically unsaturated polymers. Figure 10 shows the schematics of the radical coupling of the unsaturated diene containing elastomers [60, 61].

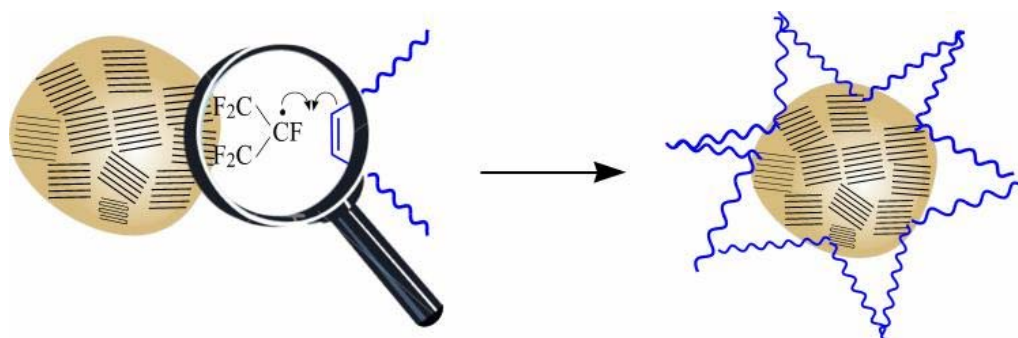


Figure 10. Radical coupling mechanism of modified PTFE radicals and the unsaturated diene EPDM

First investigations exhibit that coupling activity depends on the morphology of the PTFE powder, irradiation dose and processing conditions such as temperature etc. The coupling

activity of the PTFE powder with rubbers was determined by Fourier Transform Infrared spectroscopy. The PTFE powder was separated from the soluble rubber matrix in a good solvent during successive centrifugation process. The insoluble or extracted PTFE powder shows strong adsorption bands of the coupled rubber matrix. On the basis of these results, Haberstroh et. al later demonstrated the development of novel materials based on carbon black filled NBR recipe containing irradiated PTFE micropowder for high performance tribological applications by simple and competitive irradiation and shear mixing processes [62].

2.5. Radiation and crosslinking processes

For the last fifty years, radiation processing by gamma rays, electron beams (E-beam) or X-rays has been an effective technique in improving end-use properties of various kinds of polymers. The main applications for modification of polymer materials through radiation are crosslinking, degradation and grafting. For irradiation technologies, gamma rays from radioactive isotopes such as cobalt 60, high energy electrons from electron accelerators, and X-rays converted from high energy electrons are used. When gamma rays, electrons or X-rays interacts with a polymer material, its energy is absorbed by the polymer material and reactive species such as excited atoms, molecules, ions and free radicals are generated. In the presence of these reactive species various specific transfers of energy and complex chemical reactions take place.

2.5.1. Radiation-induced modification processes

The three fundamental processes that results from electron modification of polymers are degradation, crosslinking, and grafting. Crosslinking and degradation occur simultaneously. The ratio of their kinetics depends on chemical structure of the polymer to be modified as well as treatment conditions [61]. In general, polymers are divided into those that predominantly crosslink and those that predominantly degrade.

Degradation: the molecular weight of the polymer is reduced through chain scission. Some of the polymers that undergo degradation at room temperature include PTFE, polypropylene (PP) and cellulose. Although degradation usually brings about deterioration of mechanical properties of polymers and needs to be avoided in many cases (e.g., radiation sterilization), some good applications have been found for chain scission of polymers by radiation. A well-

known example of applications for degradation is the production of fine PTFE powders by simple and easy degradation i.e. **particle size reduction** for Fine Powders, **melt flow rate adjustments** (high molecular weight to low molecular weight compounds and for **compatibility improvement for coupling** with other polymers [63]. When a polymer such as PTFE is irradiated in air, the oxygen and moisture in the air cause oxidation in addition to degradation. The generation of polar functional groups such as the carboxylic acid groups on PTFE can help to improve the compatibility of PTFE with other polymers. Schematic of the radiation-induced degradation of PTFE in presence of oxygen is shown in the Figure 11. Beside special purpose surface modification techniques [64], E-beam irradiation provides wide range of advantages for the modification of inert PTFE surface [65]. E-beam irradiation generates free radical and functional groups in PTFE due to chain scission. In the presence of air, these radiation-induced radicals react partially with oxygen to form carbonyl fluoride groups (-COF) which further reacts with water vapour to form carboxylic acid groups (-COOH) on the surface of PTFE [66-71].

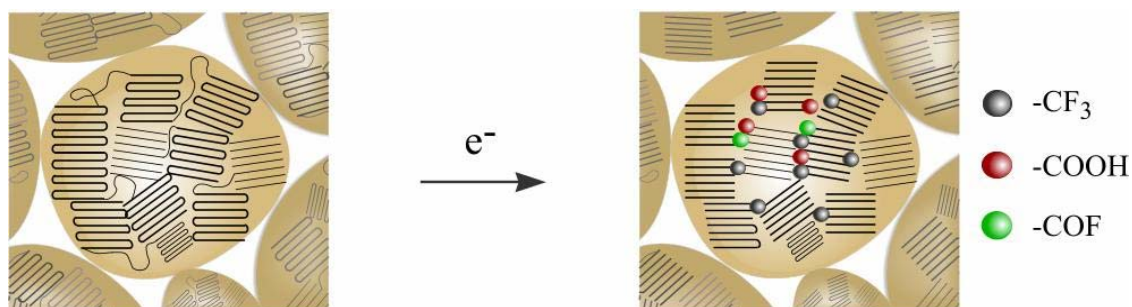


Figure 11. Radiation-induced degradation of PTFE

Crosslinking: Irradiation is also employed to crosslink elastomers by intermolecular chemical bonding of polymer chains to form a three-dimensional network. These methods like peroxide crosslinking lead to C–C bonds. As opposed to peroxide or sulfur curing, no heating of the material is necessary. Radiation crosslinking provides range of advantages and applications because it can improve the mechanical, thermal and chemical properties of the bulk materials. Its applications include crosslinking of insulating wire and cable, heat-shrinkable products, plastic pipes (PE pipes) and partial crosslinking of rubber tires etc. Polymers having relatively unhindered main chains tend to crosslink on irradiation (e.g., polyethylene). More highly substituted polymers with a quaternary carbon atom and natural products tend to degrade on irradiation. (e.g., polypropylene, polymethacrylate, Polytetrafluoroethylene)

Grafting: where a new monomer is polymerized and grafted onto the base polymer chain.

With the help of electron spin resonance, it was observed that the primary type of radical formed during the peroxide cross-linking of EPR is tertiary while allylic radicals are most prevalent in EPDM [76]. The main factors which influence the peroxide cure efficiency of EPR and EPDM are monomer, Ethylene/Propylene content, randomness of monomer distribution, polymer molecular weight and molecular weight distribution, peroxide, coagent, fillers, oils and antidegradants [72, 75-77]. One disadvantage of the use of peroxide for crosslinking is the undesired interference with additives where they act as radical scavengers, which leads to a reduction of the crosslinking efficiency. The efficiency of the crosslinking mode depends not only on the chemical composition of the polymer, but also on the presence of additives, such as antioxidants, which are generally incorporated to reduce excessive degradation while curing at high temperature and during subsequent aging. Electron beam modified PTFE powder as additive in EPDM greatly affects peroxide-induced crosslinking process. This behaviour will be discussed in the results and discussion section.

b) Electron irradiation crosslinking

One of the main advantages of the electron irradiation crosslinking compared to peroxide crosslinking is the rate of the network formation which can occur within a relatively short time at ambient temperature. Some authors have shown that the distribution of the crosslinks is more uniform in radiation than in peroxide crosslinked samples [74]. The mechanical properties of the networks are drastically depending on the crosslinking mode. One reason for that is the nature of the chemical bonds formed between the chains and the functionality of the crosslinks. The other is attributed to the differences of heterogeneity i.e. distribution of crosslinks and defects in the networks [78-80]. Grobler et al. found for polyisoprene, that the heterogeneity of the network decreased in the following order: conventional sulphur > efficient sulfur > peroxide > γ -rays irradiation (because of the low dose rate and oxygen induced degradation) [81]. Banik et al. studied the structural modification of fluoroelastomers by electron beam and also its impact on the dynamic mechanical properties [82-84]. Crosslinking of EPDM by a conventional technique and electron irradiation is expected to generate different types of network, which could be reflected on the properties [85]. Properties such as hardness, tensile strength, elongation at break, permanent set, tear strength, etc., change by different amounts during curing or during the subsequent buildup of a denser network [86].

The addition of antioxidants as with peroxide crosslinking has a negative effect on the crosslinking efficiency, due to the influence on radical deactivation and chain scission.

Identical behaviour has been shown when irradiation is used as the crosslinking mode [87]. In the review by Böhm and Tveekrem, results are given reported by Bauman who studied the effect of various “antirads” on the yield of crosslinks and scissions in natural rubber. In both cases the yields decreased [88]. Abdel-Aziz and Bafar [89] have shown the effect of various antioxidants on the thermal stability of the networks. Regardless of the treatment (peroxide curing, electron beam curing or mixed treatment), the presence of antioxidant strongly decreases the crosslinking efficiency and induces an increased scission/crosslinking competition [90].

E-beam effects in improving end-properties of a variety of polymers for different applications have been thoroughly investigated [91-94]. Beside this, the effect of E-beam processing parameters such as dose rate and oxygen on radiation crosslinking of filled rubber e.g. silica filled fluorosilicone rubber [95] as well as in rubber blends have been studied [96].

2.6. Structure and properties of rubbers

EPDM Rubber

Ethylene-propylene rubbers use the same chemical building blocks or monomers as polyethylene (PE) and polypropylene (PP) thermoplastic polymers. These ethylene and propylene monomers are combined in a random manner to produce rubbery and stable polymers called ethylene-propylene rubber (EPR). A wide family of ethylene-propylene elastomers can be produced ranging from amorphous to semi-crystalline structures. A third, non-conjugated diene monomer can be terpolymerized in a controlled manner to maintain a saturated backbone and place the reactive unsaturation in a side chain for vulcanization or polymer modification. The terpolymers are referred to as, ethylene-propylene-diene-monomer (EPDM). An EPDM polymer structure is illustrated in Figure 13. The two most widely used diene termonomers are primarily ethylidene norbornene (ENB) followed by dicyclopentadiene (DCPD). EPDM rubbers are valuable for their excellent resistance to heat, oxidation, ozone and weather aging due to their stable, saturated polymer backbone structure. As non-polar elastomers, they have good electrical resistivity, as well as resistance to polar solvents, such as water, acids, alkalis, phosphate esters and many ketones and alcohols. Amorphous or low crystalline grades have excellent low temperature flexibility with glass transition points of about -60°C. These polymers respond well to high filler and plasticizer

loading, providing economical compounds. They can develop high tensile and tear properties, excellent abrasion resistance, as well as improved oil swell resistance and flame retardance.

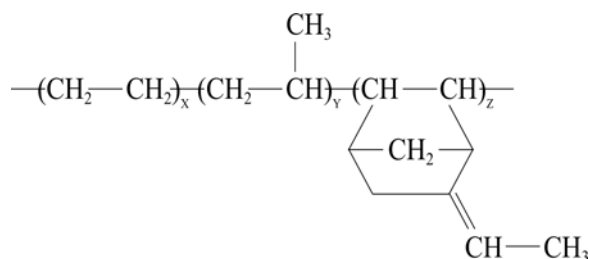


Figure 13. Chemical structure of EPDM unit

Versatility in polymer design and performance has resulted in broad usage in automotive weather-stripping and seals, glass-run channel, radiator, garden and appliance hose, tubing, belts, electrical insulation, roofing membrane, rubber mechanical goods, plastic impact modification, thermoplastic vulcanizates and motor oil additive applications [97, 98].

Chloroprene rubber

However, besides coupling of unsaturated olefinic compounds, modified PTFE can also be coupled to other technical rubber compounds such as chloroprene for high performance applications for the development of sealing and gaskets materials with improved physical and tribological properties. Polychloroprene is highly regular in structure and consist primarily of trans-units; however, there are sufficient cis-units to disturb the backbone symmetry and maintain a rubbery state. Figure 14 shows the structural units of commercially available chloroprene.

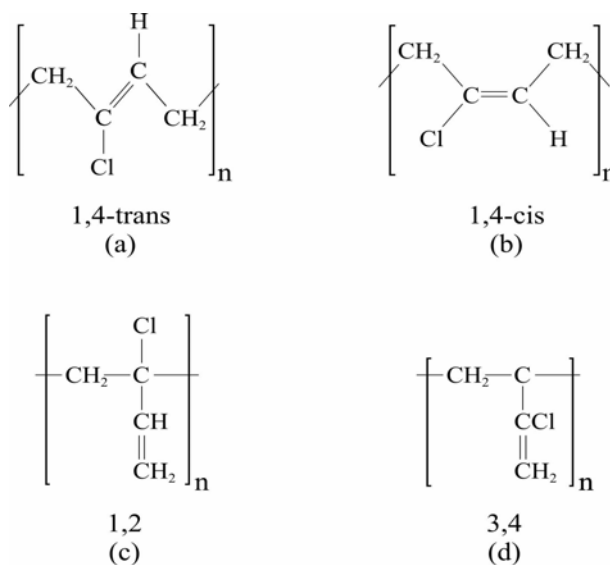


Figure 14. Structure units in the polychloroprene chain (typical commercial rubber grade)

In this polymer the 1,4-addition, in particular the 1,4-trans-addition, is dominant. In addition, small portions of the 1, 2 and 3, 4 structures are also present. The amounts of the different structural units depend on the polymerization temperature [99]. Chloroprene finds many technological applications from special purpose mechanical and automotive goods to general purpose seals, gaskets, pads and cable wires etc. It has excellent physical, ozone, aging and chemical resistance properties [100]. Similarly as in the case of PTFE radical coupling to EPDM, coupling of the PTFE powder to chloroprene could be achieved either in the presence of specially modified functional groups during reactive mixing at low temperature or in the presence of crosslinking coagents at high temperature.

3. Design of experiments

3.1. Material description

3.1.1. PTFE powder

PTFE powder (Algoflon L100X), an emulsion grade received from Solvay Solexis S.p.A., Bollate, Italy, is an agglomerated white PTFE powder with bulk density and surface area of 0.25-0.44 g cm⁻³ and 26 g m⁻², respectively. PTFE micropowders including Zonyl[®] MP1100 (emulsion) and Zonyl[®] MP1200 (suspension polymerization) are commercially electron beam modified (500 kGy) grades produced by Dupont, Wilmington, Delaware, USA.

3.1.2. Rubber and additives

Both EPDM (Buna EP G 6850) with ethylidene norbornene (ENB) and ethylene content of 7.7 and 51 wt%, respectively, and chloroprene (Bayprene[®] 216) having medium crystallization tendency shown in Table 3 were supplied from Lanxess Deutschland GmbH, Leverkusen, Germany.

Table 3. Properties of the rubbers investigated

Rubbers	Mooney viscosity (1+4) [MU]	Ash content [wt%]	specific gravity [g cm ⁻³]
EPDM	60 @ 125°C	0.2	0.86
Chloroprene	49 @ 100°C	0.5	1.23

The curative for EPDM crosslinking is peroxide di-(2-tert-butylperoxy- isopropyl benzene) with the trade name Perkadox[®] 14-40 MB GR. It was kindly supplied by Akzo Nobel Polymer Chemicals, AE Amersfoort, The Netherlands while coagent based on Zinc Dimethacrylate (Saret[®] SR634) was used from Sartomer Company, Exton Pennsylvania (PA), USA. Curing additives for chloroprene ZnO, MgO, Stearic acid and Ethylenethiourea were supplied from ACROS Organics, Geel, Belgium. Table 4 shows the rubber composition of two different rubbers i.e. EPDM and CR. The corresponding curatives were added to the rubber compound in the order shown in Table 4. The processing of rubber compounds will be discussed in section 3.4.

Table 4. Recipe of rubber composition

Material	Loading [phr [#]]	Material	Loading [phr [#]]
EPDM	100	Chloroprene	100
PTFE	10. 20. 30...60	PTFE	10. 20. 30...60
Peroxide	5	ZnO	5
Co-agent	7.5	MgO	4
		Stearic acid	0.5
		Ethylenethiourea	1

[#] phr is parts per hundred rubber

3.2. Electron beam modification of PTFE powder

PTFE powder was modified with absorbed doses of 20, 100, 200, 300, 400 and 500 kGy using electron beam accelerator ELV-2 from Budker Institute of Nuclear Physics, Novosibirsk, Russia, installed at the Leibniz Institute of Polymer Research Dresden. Figure15 shows the schematics of the ELV-2.

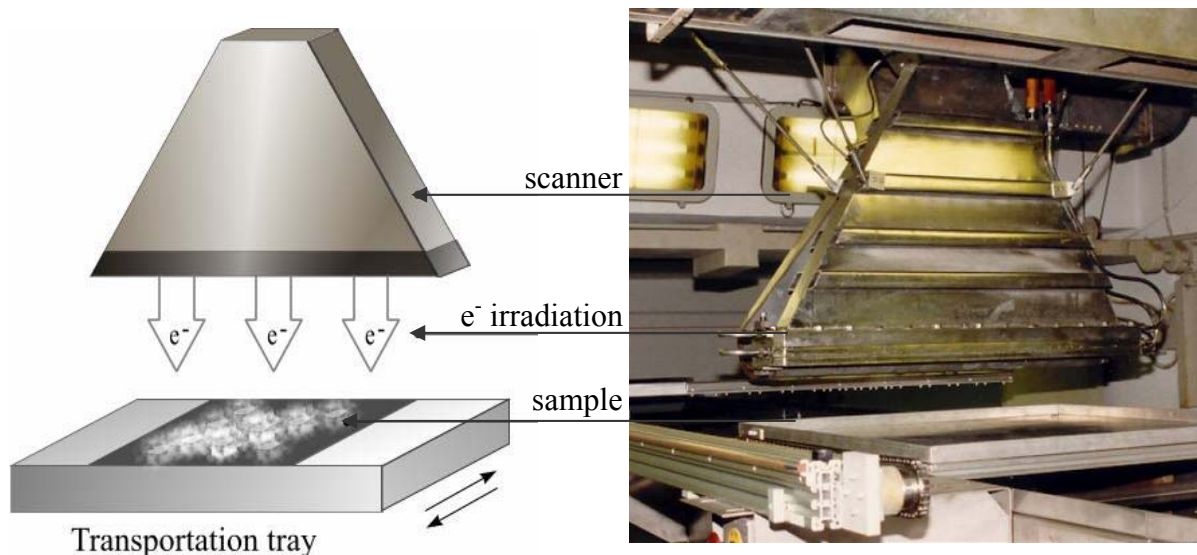


Figure 15. Schematics of the radiation zone showing the high energy electrons scanned through electron accelerator (ELV-2)

Figure 12 shows the processing parameters and steps involved in the modification of PTFE powder with 100 kGy dose. The electron treatment was carried out in air and at room temperature with an absorbed dose of 2.5 kGy per pass and at an average dose rate of 10 kGy/h. The tray passes under electron beam accelerator. Each pass delivers 2.5 kGy, e.g. for 20 kGy, 8 passes are required ($8 \times 2.5 = 20$ kGy). Similarly to achieve 100 kGy, further 80 kGy (33 passes) is added to the previously 20 kGy (8 passes). Therefore, for 100 kGy, a total of $33+8 = 41$ passes are required as shown in Figure 16.

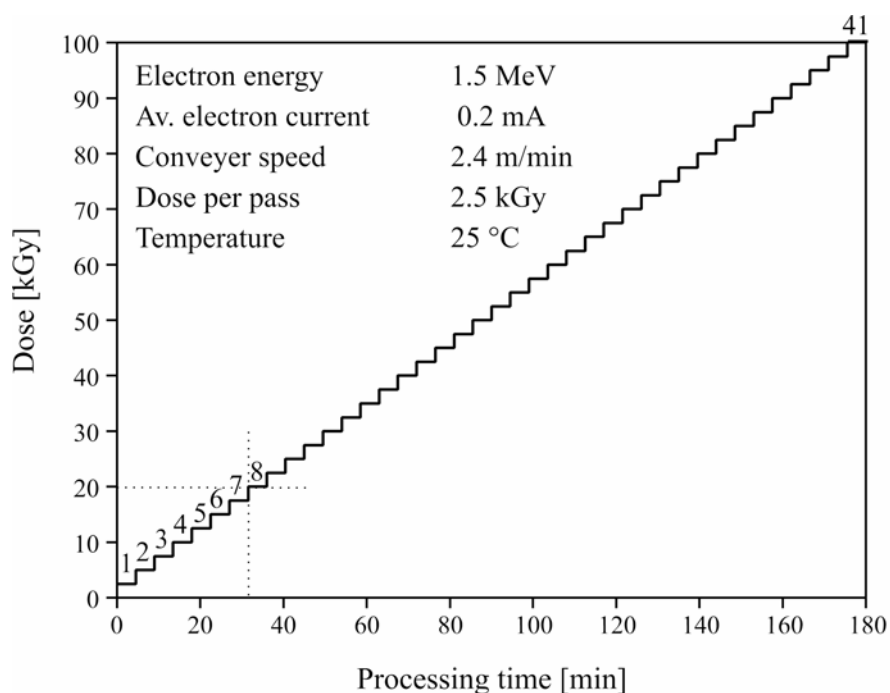


Figure 16. Processing parameters and number of steps involved in the modification of PTFE powder with 100 kGy dose

An optimum processing time of 180 mins are required for a complete cycle of 100 kGy dose. A shut down time of at least 8 hrs was necessary after every 100 kGy addition to allow sufficient diffusion of oxygen in the PTFE powder. The total time for the whole process from 20 to 500 kGy requires approximately 50 hrs including 8 hrs shutdown intervals after every 100 kGy addition. To achieve 500 kGy, the doses were added to the PTFE powder in 100 kGy steps to the batch. These treatment parameters were considered in order to avoid excess temperature rise which might favour deactivation of the radical formation as well as to control agglomerate size and chemical structure via absorbed dose. Further information on electron accelerator (ELV-2) facility can be found in [65].

3.3. Characterization of PTFE powder

3.3.1. Spectroscopic analysis

Electron Spin Resonance (ESR)

The number of free radicals was determined with the help of MiniScope MS200 electron spin resonance (ESR) instrument from Magnettech Limited, Berlin, Germany. Spin numbers for each absorbed dose were calculated after four hours of electron treatment.

Fourier Transform Infrared Spectroscopy (FTIR)

Fourier Transform Infrared Spectrometer (FTIR) spectra were recorded on Vertex 80v (Bruker) FTIR spectrometer ($4000\text{--}400\text{ cm}^{-1}$, resolution = 2 cm^{-1} , 32 scans per measurement) from Bruker Optik GmbH, Ettlingen, Germany in transmission mode on $10\text{ }\mu\text{m}$ thin PTFE foils to observe the chemical changes induced in PTFE powder having exposed to different absorbed doses.

3.3.2. Contact angle measurement

The contact angle measurements were performed on (1 mm thin, diameter 20 mm) PTFE discs with the help of OCA 40 Micro contact angle meter from DataPhysics Instruments GmbH, Filderstadt, Germany. The rounded discs were prepared by compressing PTFE powder at room temperature under a pressure of 1.0 MPa. Sessile drop method was performed to determine the wettability of PTFE discs modified similarly as discussed in section 3.2. The discs were used to obtain smooth and comparable surfaces for contact angle measurement.

3.3.3. Particle size and distribution

The particles size and their distribution were determined with the help of the particle size analyzer, Sympatec HELOS HO367 from Sympatec GmbH, Clausthal-Zellerfeld, Germany, having a measuring range of $0.5/0.9\text{--}175\text{ }\mu\text{m}$. The primary and mean agglomerate size of PTFE powder was $70\text{--}80\text{ nm}$ and $17.7\text{ }\mu\text{m}$, respectively, as received from the supplier.

3.3.4. Scanning electron microscopy (SEM)

Post and pre-irradiation structure morphology of the PTFE powder was determined with the help of LEO 435 scanning electron microscope (SEM – acceleration voltage 20 kV) from LEO Electron Microscopy Ltd, Cambridge, England. SEM examination was also performed on the cryogenically surface fractured samples for the dispersion analysis of PTFE powder in EPDM.

3.4. Samples preparation and characterisation techniques

Rubbers and PTFE powder were first pre-mixed in an internal mixer (PolyLab Haake Rheomix) from Thermo Electron GmbH, Karlsruhe, Germany for 5 mins at a temperature of 100°C and at a rotor speed of 50 rpm as shown in Figure 15.

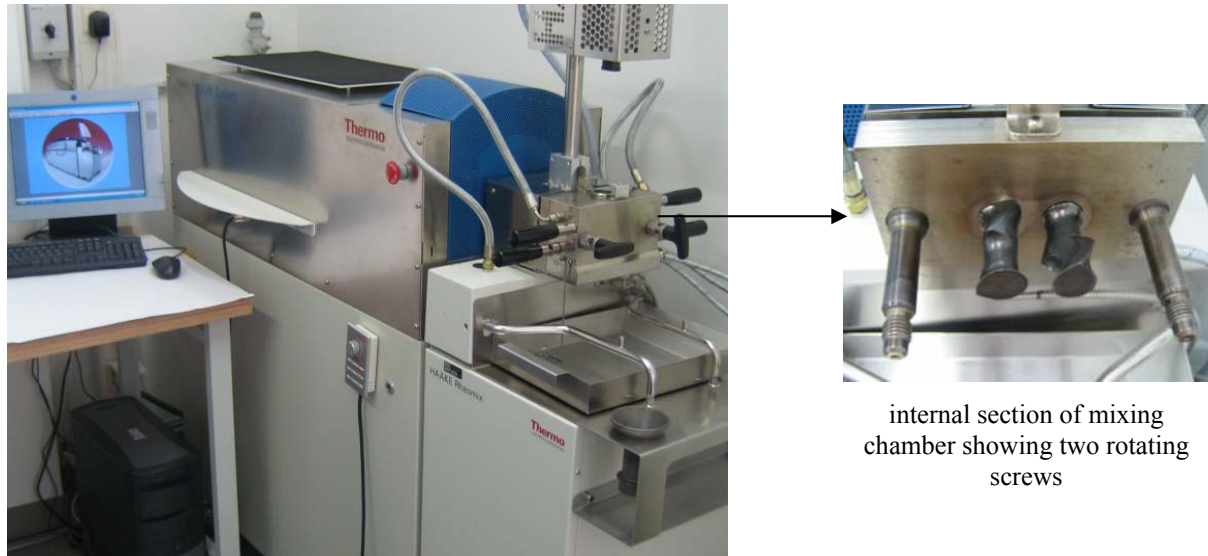


Figure 17. Internal mixer: PolyLab Haake Rheomix for rubber and PTFE mixing

Figure 18 shows two different crosslinking routes i.e. a) thermal and b) electron irradiation crosslinking. In case of EPDM, beside thermal, crosslinking of EPDM was also performed with E-beam and is discussed in the following section 3.4.1. The reason for choosing E-beam crosslinking for EPDM will be discussed in results and discussion.

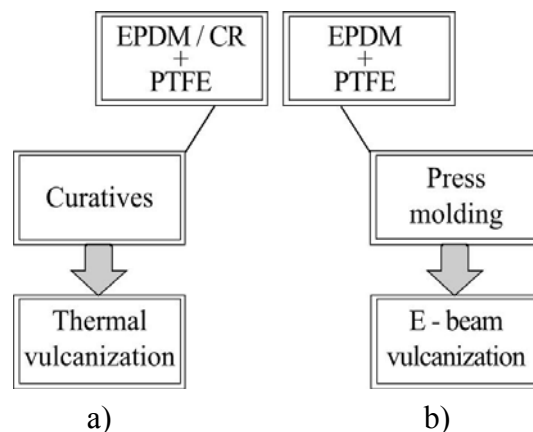
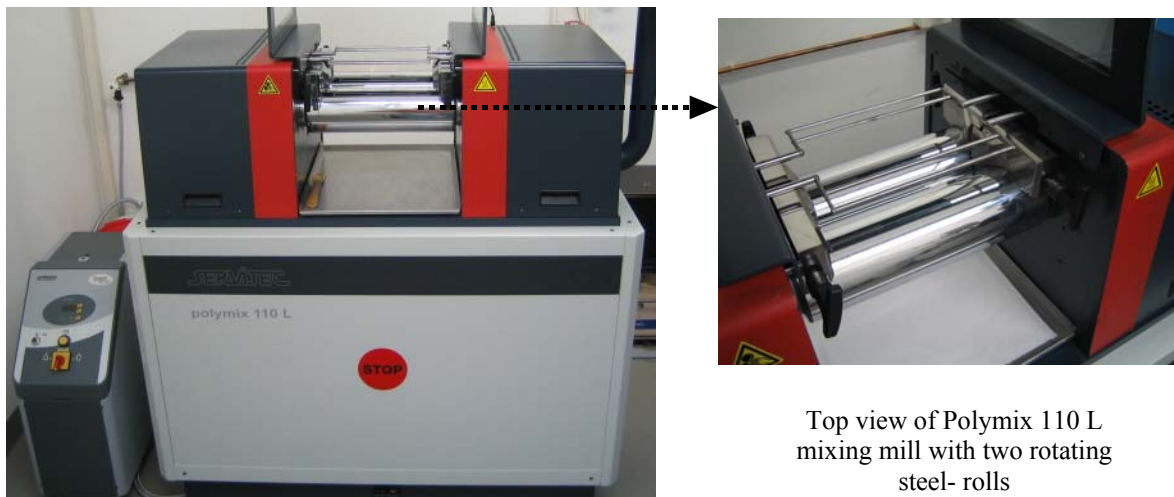


Figure 18. Schematics of the a) thermal and b) electron irradiation crosslinking

3.4.1. Crosslinking processes

Thermal (EPDM, CR)

In case of thermal crosslinking the corresponding curatives were added to each of the EPDM and CR rubber on a two roll laboratory mill (Polymix 110L, SERVITEC Maschinenservice GmbH, Wustermark, Germany) at room temperature as shown in Figure 19. A constant friction ratio of 1.2 was maintained between the milling rolls. Approximately 2 mm sheets were drawn out from the mill and cured in a hot press (FONTUNE Holland) from Fortijne Grotnes BV, AC Vlaardingen, Holland at a pressure of 10 MPa at a temperature of 170°C and 160°C for EPDM and CR rubber, respectively, up to their corresponding optimum cure time (t_{90}).



Top view of Polymix 110 L mixing mill with two rotating steel-rolls

Figure 19. Two roll laboratory mill Polymix 110L for mixing and incorporating curatives

Electron irradiation (EPDM)

In case of crosslinking with electron irradiation, material from internal mixer was placed in between thin non-sticking polyesters films for press molding at a temperature of 150°C and a pressure of 5 MPa in an electrically heated press for 3 min to obtain rubber blocks of dimension 110 x 110 x 2 mm. The molded samples of PTFE filled EPDM were then irradiated for crosslinking with 200 kGy in atmospheric conditions and at room temperature of 25°C. Crosslinking with 200 kGy was accomplished in 5 passes with an absorbed dose of 40 kGy per pass and at an average dose rate of 25 kGy/min. The processing time was 8 mins with an electron energy and current of 1.5 MeV and 4 mA, respectively.

3.4.2. Rheometric analysis

The processing characteristics including optimum cure time (t_{90}) and delta torque ($\Delta M = M_h - M_l$, maximum– minimum torque) were determined with the help of rubber process analyzer (Scarabaeus SIS V50) from Scarabaeus Mess- und Produktionstechnik GmbH, Langgöns, Germany shown in Figure 20. Approximately 4.5 g circular shaped samples were punched out from the uncured compounds and placed between the two oscillating discs of SIS V50 maintained at their corresponding t_{90} values. The test was run at an amplitude and frequency of 0.5 degree and 1.67 Hz, respectively. The torque value was monitored as a function of time. The time corresponding to the development of 90% of the maximum torque i.e. optimum cure time (t_{90}) was calculated from their respective rheographs.

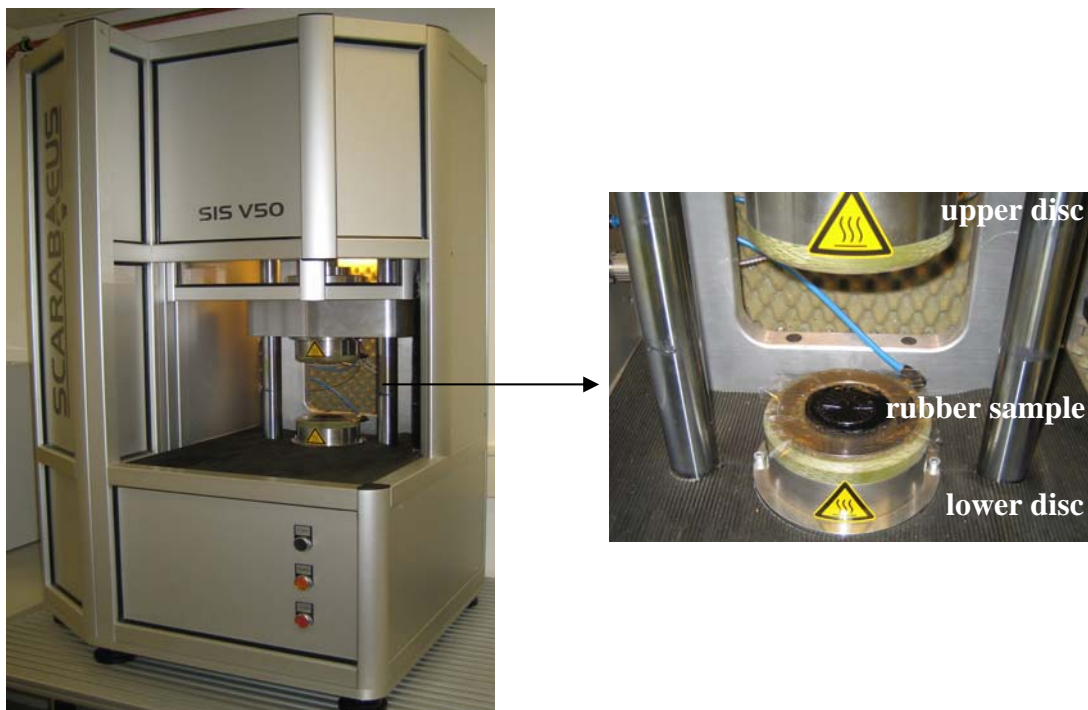


Figure 20. Rubber process analyzer for the determination of processing characteristics of rubber compound

3.4.3. Physical and dynamic mechanical properties

Physical properties

Mechanical properties including tensile strength at break, percentage elongation at break and modulus at 100% and 300% elongation were determined according to ISO 527 at a cross-head speed of 200 mm/min using tensile testing machine from Zwick GmbH, Ulm Germany. Hardness values were measured according to DIN 53505, using a Shore (A) Durometer from

Heinrich BAREISS GmbH, Oberdischingen, Germany. Indentations were made at several points for each specimen for measurements of average hardness values. Compression properties were determined according to DIN ISO 815 while tear resistance was calculated according to DIN 53507 at a test speed of 100 mm/min.

Dynamic mechanical thermal analysis (DMTA)

The frequency-temperature dependent viscoelastic mechanical properties of the vulcanizate including storage (E'), loss modulus (E'') and tan delta (E''/E') were measured with the help of a dynamic mechanical analyzer, EPLEXOR[®] 150 N from Gabo Qualimeter Testanlagen GmbH, Germany using a 2 mm thick rectangular rubber vulcanizate block having an area of 15 mm x 8 mm. The temperature scans were run from -100°C to 150°C at a heating rate of 4 Kmin^{-1} . The measurements were done in tension mode with strain and frequency being set to 0.5 % and 10 Hz, respectively.

3.4.4. Differential scanning calorimetry (DSC)

DSC studies of the PTFE-EPDM composites were carried out using NETSCH DSC 204 from NETZSCH-Gerätebau GmbH, Selb, Germany to analyze the influence of absorbed dose on the compatibility and dispersion in EPDM from the crystallization studies. All experiments were performed under atmospheric conditions and at a heating rate of $10\text{ K}\cdot\text{min}^{-1}$ above the melting temperature of PTFE up to 330°C . The results obtained were expressed as input energy versus temperature.

3.4.5. Microstructure and dispersion

Transmission electron microscopy (TEM)

TEM micrographs of the modified and non-modified PTFE filled EPDM were recorded on transmission microscope model EM910 from Carl Zeiss, Oberkochen, Germany.

Scanning electron microscopy (SEM)

SEM studies were carried on tensile fractured samples. The SEM observations were done with the help of LEO 435 from LEO Electron Microscopy Ltd, England. The samples were first sputter-coated with gold for 6 s before being used for observation.

3.5. Tribological measurements

3.5.1. Pin-on-disk tribometer

A pin on disk tribometer according to ASTM G 99 – 2005 (ISC 200 from Implant Sciences, Wakefield, USA) was used as shown in Figure 21. Hardened carbon balls (type 100 KU 15 KL3, Wälzlager-technik Dresden, Germany) made of steel 100Cr6 (German standard 100 Cr 6, near AISI L3 steel) with a diameter of 15 mm served as counterpart. The balls were heat treated with a hardness of 59 ± 1 HRC. The surface of the steel balls were grinded with an arithmetic average roughness of $R_a = 0.47 \mu\text{m}$. The ball slides against EPDM gum and PTFE filled EPDM vulcanizates. The vulcanizate specimens (samples) were manufactured as square plates with dimensions 40mm x 40mm, thickness $h = 2\text{mm}$ and bonded on the steel disc using double-sided tesafilm®. A sliding speed, $v = 0.05 \text{ms}^{-1}$ was applied. The diameter of the circle rotation was 10mm in each case. The tribological investigations were performed with a constant load of $F_N = 1 \text{N}$ over a testing time of $t_B = 2\text{h}$. The tests were carried out at a temperature of 22.9°C and a relative humidity of 31 %. For each material, a single test was performed.

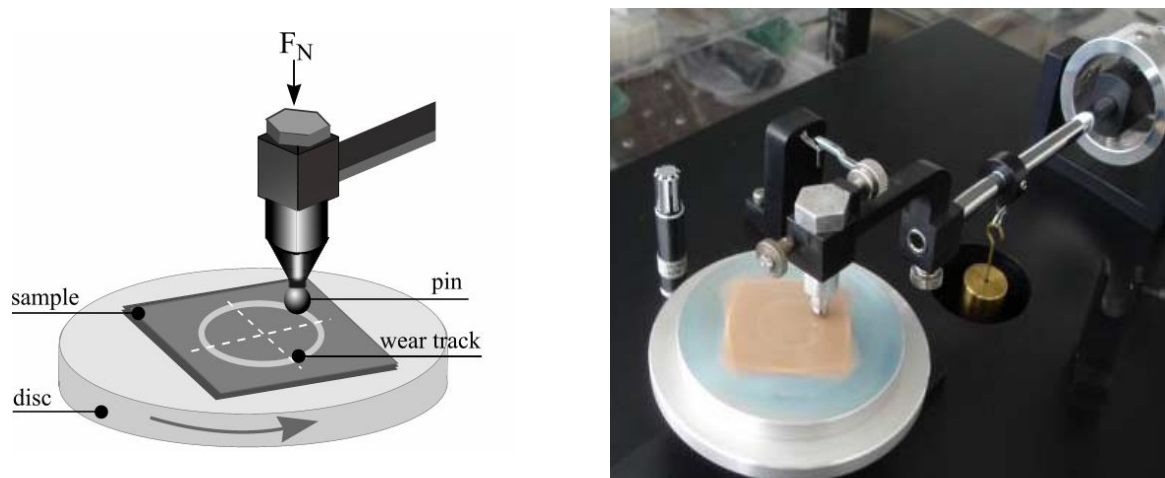


Figure 21. Schematic (left) of the pin-on-disk tribometer (right) illustrating the testing set-up for the friction and wear characterization of rubber sample (mounted on disk) against a counter-surface (pin/steel ball)

The wear scar shape was measured with a profilometer (Perthometer CONCEPT 6.2, Mahr, Göttingen, Germany) at the end of each test. The shape was measured at four different locations, in each case the point was shifted around an angle of 90° . Figure 22 shows a characteristic plot of a wear scar. For determination of the specific wear rate (k), the cross-

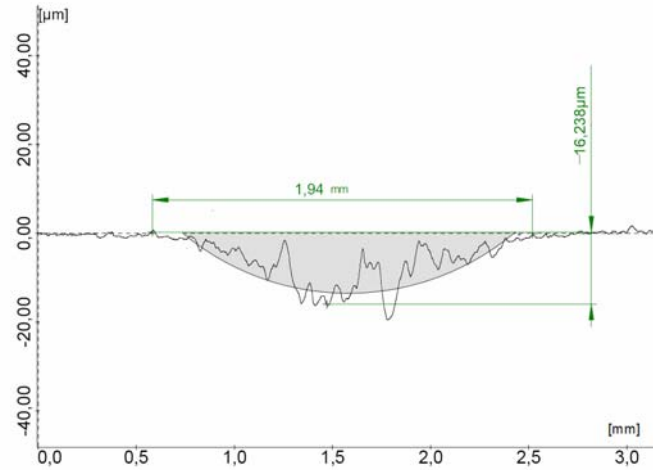


Figure 22. Typical wear scar profile showing the wear cross-section area

sectional area of the wear scar was calculated by approximating the wear scar shape with a segment of circle. Specific wear rate was calculated as:

$$k = \frac{W_V [mm^3]}{F_N \cdot s [N \cdot m]} \quad (4)$$

where W_V is the volume of the removed material, F_N is the normal load and s is the sliding distance. The friction coefficient (μ) was determined directly by measuring the tangential force with a strain gauge load cell. During the test, friction coefficient (μ) was recorded continuously with a sampling rate of 100 Hz. In case of stick slip effect, the experimental data strongly fluctuated as shown in Figure 23. For a better comparison between different types of materials, the average values of friction coefficients (μ) are reported. For all series the mass wear loss of the counterpart ball was lower than the detection limit of the weighing balance (RC 1 from Satorius AG, Göttingen, Germany) which works with an accuracy of 0.1 mg.

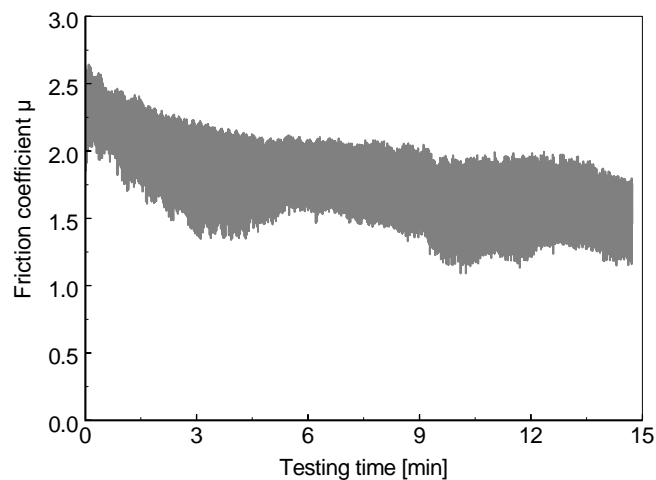


Figure 23. Friction coefficient as a function of time shows strong stick slip effect

3.5.2. Surface characterization

3.5.2.1. Surface topography/roughness

The vulcanizates surface topography was examined using an imaging measuring instrument for the optical analysis of surface roughness with the help of MicroGlider from FRT, Germany. Surface roughness was performed at three different locations. The measuring area of each location was 10 mm x 10 mm. Surface roughness was determined as mean of the three locations.

3.5.2.2. X-ray photoelectron spectroscopy (XPS)

X-ray photoelectron spectroscopy (XPS) was performed for the surface chemical analysis prior to sliding contact of the vulcanizates filled with modified and non-modified PTFE powder. The fluorine to carbon (F/C) ratio on the surfaces were determined using Axis Ultra (Kratos Analytical, England) with a mono Al K α X-ray source. Analysis area of XPS was estimated to be circular, approximately 1.0 mm in diameter.

3.5.2.3. Wear scar analysis

SEM was also performed on the wear scars after loading to observe the changes caused by the counter-surface after repeated sliding and to assess the failure mechanism involved in wear of the different vulcanizates. Instrument described in section 3.3.4 was used for analysis.

3.6. Chloroprene rubber

It has been discussed previously in detail that chemical coupling of PTFE powder to rubber matrixes is a prerequisite for effective use of PTFE powder in rubber compounds. In general, chemical coupling enhances the chemical compatibility of the modified PTFE powder with rubber compounds. This helps in homogeneous dispersion and ultimately in improvement of final properties of the rubber compound. The structure-property effects resulting from the chemical coupling between PTFE and rubber matrix result in significant improvement of the desired properties. For EPDM, it has already been established that PTFE powder modified by electron irradiation readily reacts with unsaturated diene containing rubber compounds by radical coupling mechanism as discussed in section 2.4. Unlike non-polar EPDM, the chemistry of polar compounds such as Chloroprene (CR) rubber suggests that the unsaturated double bonds are sufficiently deactivated by highly electronegative chlorine atom so that the direct chemical coupling with PTFE powder by radical coupling mechanism is not possible.

There is indeed a strong motivation to expand the incorporation of PTFE powder in technical rubber compounds. For this reason PTFE powder was modified and the coupling activity with CR rubber is investigated.

3.6.1. Chemical coupling analysis

The chemical coupling between modified PTFE powder and Chloroprene rubber (CR) was investigated using FTIR spectroscopy. PTFE filled CR samples (without adding curatives) were produced in internal mixer as discussed in section 3.4. Sufficient shear blending of PTFE powder and CR was considered. For IR investigations, PTFE powder was separated from CR in the following steps:

- a) About 5 g CR-PTFE blend is dissolved in 50–70 ml chloroform (CHCl_3). Stirring was done at 50°C . The dispersion containing dissolved CR and fine dispersed PTFE particles was centrifuged and the solution above the solid sediment decanted.
- b) About 50 ml solvent (CHCl_3) was added to the solid residue and the mixture stirred over night using a magnet stirrer. The dispersion was centrifuged and the solution above the solid residue decanted. The cleaning steps were repeated five times.
- c) Following cleaning procedure, further 50 ml methanol was added to the solid residue. The mixture was stirred over night, the methanol solution was decanted and the solid residue dried at 80°C under vacuum.
- d) Investigation of the dried solid by FTIR spectroscopy:
The solid PTFE powder was pressed to a $10\ \mu\text{m}$ thin film and investigated for IR as discussed in section 3.3.1.

For FTIR analysis it was necessary that the solution/dispersion is free of CR gels. The presence of CR absorptions in modified PTFE spectrum as opposed to non-modified PTFE provides an indication of a chemical coupling. It was possible to separate CR from PTFE without the formation of insoluble gels. In the presence of gel content the mentioned separation procedure fails to evidence any indication of chemical coupling between CR and PTFE. The centrifugation procedure must allow complete separation of gel content.

3.6.2. Estimation of crosslinking density: stress-strain measurements

The structure–property relationship was analyzed from the stress–strain behaviour described by a phenomenological expression of the form suggested by Mooney [101] and Rivlin [102],

$$\frac{\sigma}{\lambda - \lambda^{-2}} = C_1 + C_2\lambda^{-1} \quad (5)$$

where σ is the applied stress, λ is the extension ratio and C_1 and C_2 are the Mooney-Rivlin (MR) constants related to network structure and the flexibility of the network chains. C_1 is directly proportional to the number of network chains per unit volume of the rubber. The elastically active cross-linking density is given by:

$$\nu = 2C_1 / RT \quad (6)$$

where R is the gas constant and T is absolute temperature. The value of C_2 can be related to the number of the elastically effective trapped entanglements, to the number of steric obstructions and other network defects. In the case of filled systems, the two latter effects provide a substantial contribution to C_2 than the influence of trapped entanglements [103]. For filled systems the estimated or apparent cross-linking density can be analyzed with the help of the Mooney-Rivlin equation using the assumption that the hard filler particles do not undergo deformation. This means that the macroscopic strain is lower than the intrinsic strain (local elongation of the polymer matrix). Thus, in the presence of hard particles the macroscopic strain is usually replaced by a true intrinsic strain:

$$\lambda = 1 + \varepsilon X \quad (7)$$

where ε is the macroscopic elongation and X is an amplification factor. The latter can be defined as

$$X = 1 + 2.5\phi_f + 14.1\phi_f^2 \quad (8)$$

where ϕ_f is the volume fraction of the spherical filler particles. This definition is based on the Guth-Gold equation [104]:

$$G = G_0(1 + 2.5\phi_f + 14.1\phi_f^2), \quad (9)$$

where G_0 is the modulus of the matrix. This equation is based on the Einstein's equation for the viscosity of a suspension of spherical rigid particles. Hence, the Guth-Gold equation takes into account the effect of hydrodynamic reinforcement arising from the inclusion of rigid

particles into the polymer matrix. For PTFE powder, the intrinsic strain is deduced from Eq (7) by defining $X = 1$, i.e.

$$\lambda = 1 + \varepsilon \quad (10)$$

This assumption is based on the fact that PTFE agglomerates are soft and deformable particles in comparison to conventional (hard) fillers such as carbon black and silica for which Eq (7) has been originally derived. The morphological analysis (shown later) also reveals that PTFE agglomerates can be considered as soft deformable particles. Therefore, it is assumed that the particles are deformed with the same extension ratio as applied to the bulk sample. According to the Mooney-Rivlin equation the plot of reduced stress, $\sigma_{red} = \sigma / (\lambda - \lambda^{-2})$, as a function of inverse extension ratio, λ^{-1} , should yield a linear curve, from which the values of C_1 (y-intercept) and C_2 (slope) can be readily obtained from the stress-strain curves [105].

Testing Procedure

A series of six stress-strain cycles with a cross-head rate of 600 mm/min was applied to specimens having a parallel length of 25 mm and a cross section of 1 x 4mm² on tensile testing machine. The samples were continuously stretched in six hysteresis cycles up to 60 % of their elongation at break values as shown in Figure 24. This procedure is an established one and widely practiced in the elastomeric compounds reinforced with fillers such as carbon black and silica which tend to build a strong filler-filler network. In case of PTFE powder a pronounced networking is not expected because of the microscopically large and chemically inert PTFE agglomerates. Therefore, it is expected that any contribution to the overall crosslink density should arise solely from the effective chemical coupling between the PTFE powder and the chloroprene matrix. After the sixth cycle, a tensile test (dotted line) was performed with a cross-head rate of 25 mm/min in order to estimate the true deformation (λ) of the specimen. For this purpose, an optical 2D deformation analysis system based on a grating technique (ARAMIS[®] from GOM mbH, Germany) and coupled with a 1.3 mega pixel camera is used. For optical analysis it is necessary to imprint a random pattern on the sample surface. ARAMIS[®] software compares the optical images of different load steps to calculate the displacement and the deformation of the sample. Figure 25 shows the schematics of the procedure adapted for estimating deformation in the specimen. A detailed description using ARAMIS[®] for deformation analysis is given in [106].

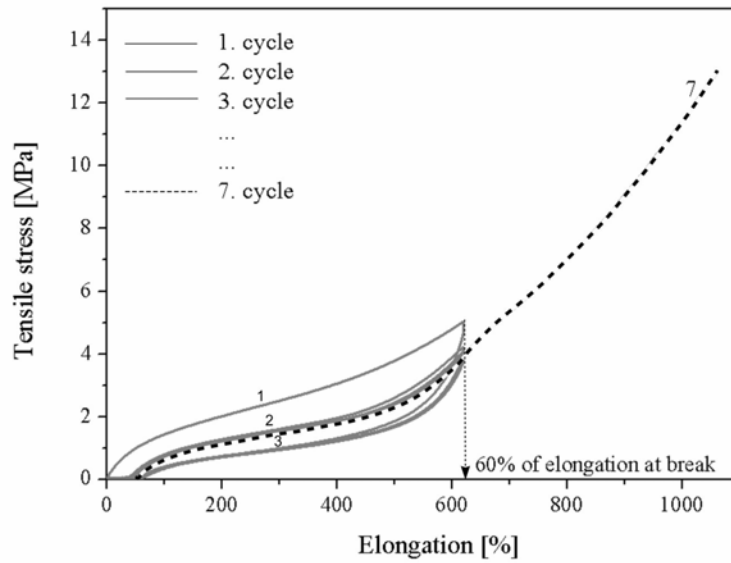


Figure 24. Typical stress-strain curves of the chloroprene composites. The first six hysteresis cycles are shown with filled lines while the seventh curve (dotted line) was investigated using optical method

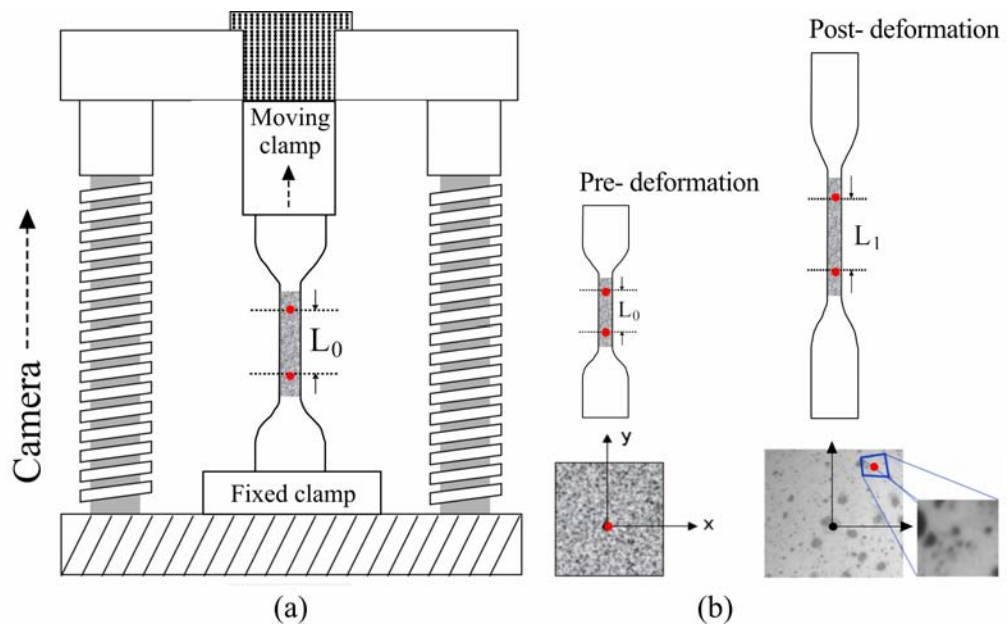


Figure 25. Schematics showing the (a) tensile testing rig holding the sample between clamps for uniaxial deformation (b) deformation stages in the sample recorded with optical imaging system

4. Results and discussion

4.1. Characterization of PTFE powder: Effects of electron modification

Figure 26 shows the ESR spectra of the electron beam irradiated and non-irradiated PTFE powder (L100X). The ESR spectra show a systematic increase in the signal with increasing absorbed irradiation dose. Non-modified PTFE powder produced no signal due to the absence of reactive free radicals. The increase in signal indicates that the radical concentration is increased with increasing absorbed dose or modification. 500 kGy irradiated PTFE powder having the highest spin numbers shows the highest number of radical concentration. Electron beam treatment generates persistent reactive free radicals and functional groups on the surface due to degradation of PTFE powder by chain scission.

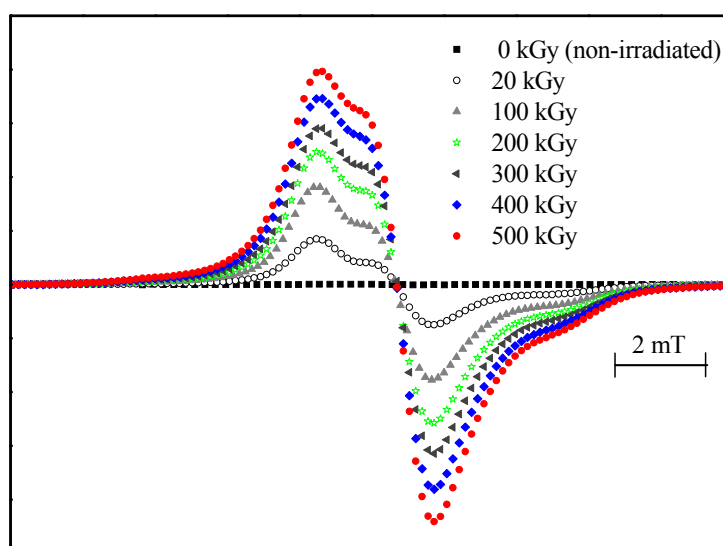


Figure 26. Electron spin resonance (ESR) spectra of PTFE powder irradiated with different absorbed doses

It has been reported that PTFE in the presence of air undergoes C-F and C-C scission during energy rich electron modification process [107, 108]. C-F scission results in secondary radicals while C-C scissions produce primary free radicals. These free radicals react with atmospheric oxygen to yield stable perfluoroalkylperoxy radicals. Beside these peroxy radicals, carbonyl fluoride groups are also formed which hydrolyse in the presence of atmospheric moisture to form carboxylic acid groups (-COOH). The complete reaction mechanism can be found in [109].

Chemical changes introduced in PTFE after exposure to electron treatment were monitored by FTIR spectroscopy. Figure 27 shows several new bands in the infrared spectrum of modified PTFE.

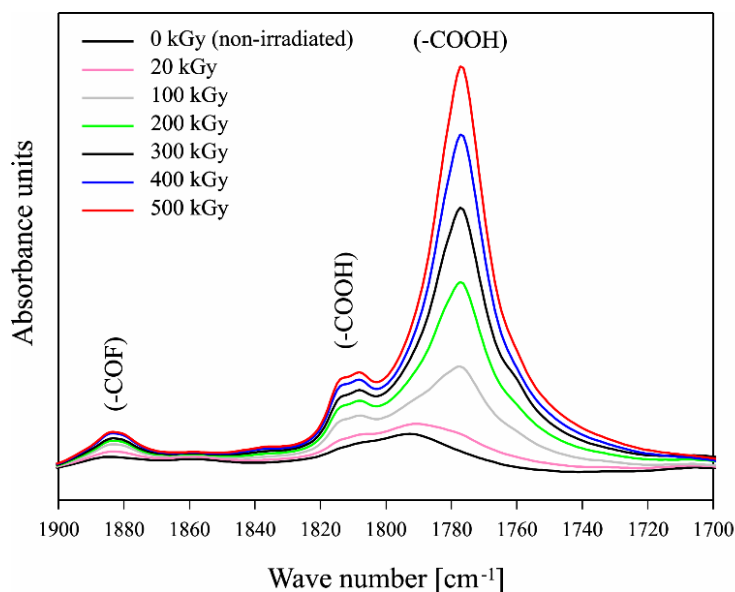


Figure 27. Infrared spectra ($1900\text{-}1700\text{ cm}^{-1}$) of PTFE powder after modification to different irradiation doses in comparison to non-irradiated PTFE

The peak at 1884 cm^{-1} was identified with carbonyl fluoride groups (-COF) while 1810 cm^{-1} are free and 1777 cm^{-1} associated carboxylic acid groups (-COOH). Figure 28 shows the influence of absorbed dose on the mean agglomerate size of PTFE powder.

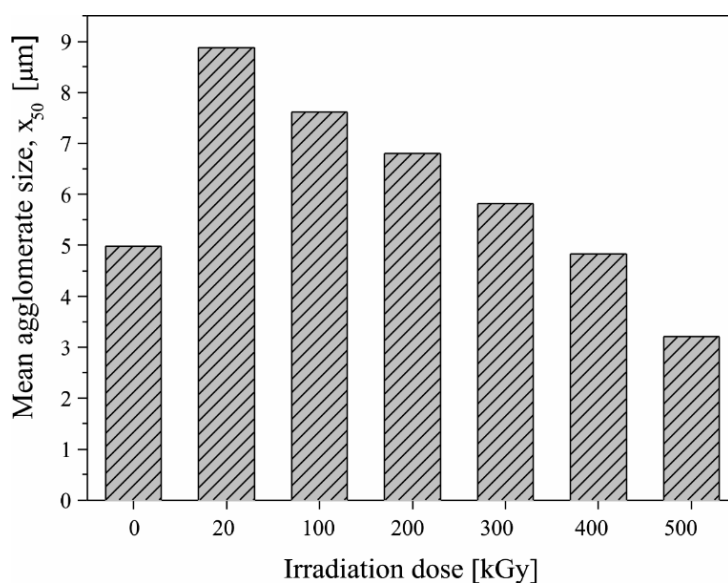


Figure 28. Mean agglomerate size of PTFE powder as a function of absorbed dose

It can be seen that mean agglomerate size of PTFE powder decreased systematically with absorbed irradiation dose. It suggests that mean agglomerate size of PTFE powder can be controlled via absorbed dose. The decrease in agglomerate size is due to chain scission of PTFE powder. High molecular weight PTFE is reduced to low molecular weight PTFE. The highest absorbed dose of 500 kGy shows the smallest mean agglomerate size. The mean agglomerate size delivered by the supplier of virgin non-modified PTFE powder was 17.7 μm compared to our determined agglomerate size of 5.0 μm . This might be due to the ability of PTFE powder to re-agglomerate as can be seen in the particle size distribution in Figure 29. The particle size distribution suggests that non-irradiated PTFE powder has a broad particle size distribution compared to 500 kGy irradiated PTFE powder. The non-irradiated PTFE powder shows a characteristic bimodal distribution compared to unimodal distribution of 500 kGy irradiated PTFE powder. This specific bimodal distribution clearly signifies that non-irradiated PTFE powder is mainly composed of bigger agglomerates which tend to re-agglomerate. On the contrary, 500 kGy irradiated PTFE powder indicates finely dispersed smaller agglomerate particles.

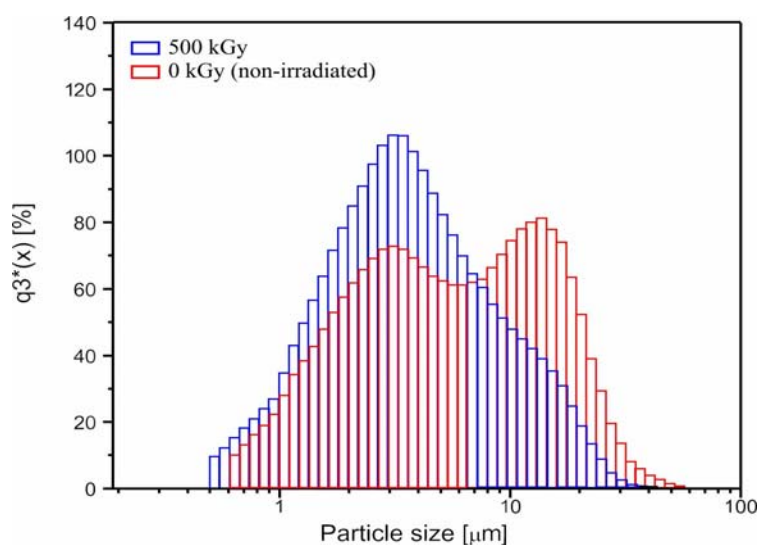


Figure 29. Percentage density distribution (q_3) as a function of particle size of 0 and 500 kGy irradiated PTFE powder

This can also be seen in the SEM micrographs of 500 kGy irradiated PTFE powder. Effect of absorbed dose on the agglomerate morphology of (a) non-irradiated and (b) 500 kGy irradiated PTFE powder is shown in Figure 30. It is evident that the agglomerate size and morphology of these powders are apparently distinguishable from each other. Non-irradiated PTFE powder are huge solid-structured agglomerates formed by the random re-agglomeration

of PTFE agglomerates. In comparison, 500 kGy irradiated PTFE powder shows fine homogeneous coarse particles dispersed individually over the area without the formation of huge agglomerates.

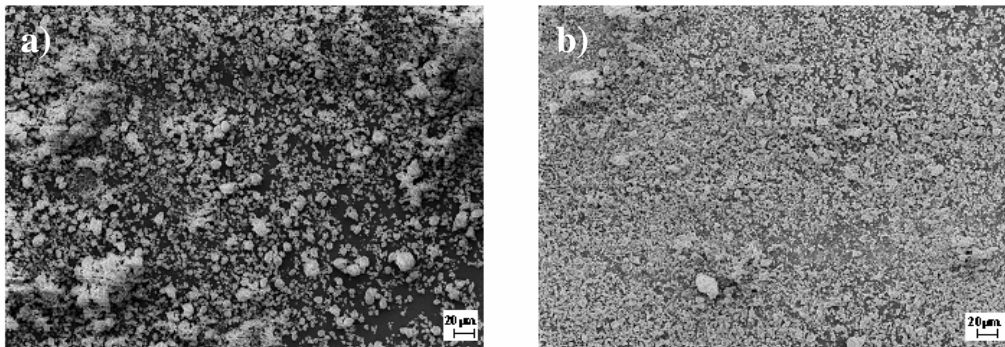


Figure 30. SEM micrographs of (a) non- and (b) 500 kGy irradiated PTFE powder

Figure 31 shows result of the contact angle measurements on PTFE powders having different absorbed doses in comparison to 0 kGy (non-modified) PTFE powder. The horizontal line indicates contact angle value of a typical commercial PTFE. It is observe that the water contact angles of modified PTFE discs are lower than non-modified PTFE disc and is systematically decreasing with increasing absorbed dose. The water contact angle of 111° of non-irradiated PTFE powder indicates its inherently hydrophobic behaviour. Post-modification to different absorbed doses result in the decrease in contact angle from 114.8° to 92° for 500 kGy PTFE powder. That is, compared with non-modified PTFE, the wettability of 500 kGy is significantly increased.

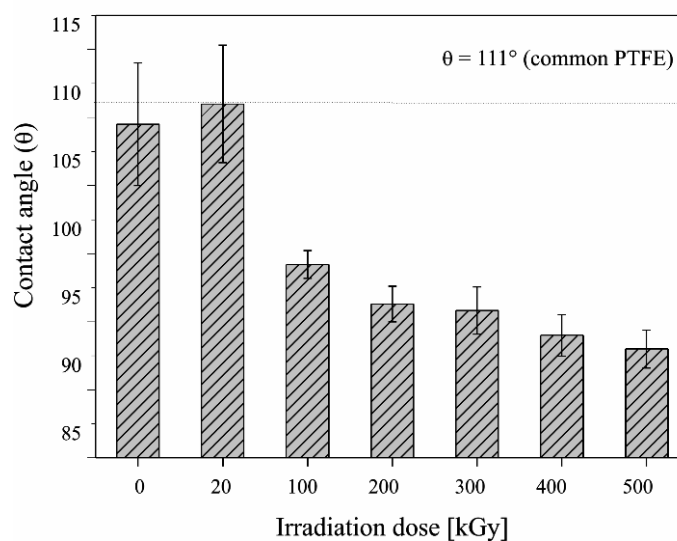


Figure 31. Effect of the absorbed dose on the contact angle of irradiated PTFE discs in comparison to non-irradiated PTFE. The horizontal line indicates contact angle value of a commercial PTFE

The increase in wettability is due to the strong interaction between water and the hydrophilic groups (COF/COOH) generated on the surface of PTFE powder after electron treatment in the presence of air. As can be seen, increasing absorbed dose results in lower contact angles due to the generation of oxygen containing groups on the PTFE surface. Lower contact angles correspond to higher surface energy and thus higher adhesion and higher interfacial compatibility. As shown in Figure 27 an increasing absorbed dose results in higher concentration of C=O groups (1777 cm^{-1}). This shows that the chemical structure of PTFE powder was changed due to electron treatment.

Conclusions

PTFE powder is prone to chain scission and chemical changes even at a low irradiation dose. The radiation-induced chemical changes in PTFE powder (L100X) determined by Electron Spin Resonance (ESR) and Fourier Transform Infrared (FTIR) spectroscopy shows increasing concentration of persistent trapped radicals and carboxylic functional groups ($-\text{COOH}$) with increasing irradiation dose. The morphological variations of PTFE powder including its decreasing mean agglomerate size with irradiation dose was investigated by particle size and Scanning Electron Microscopic (SEM) analysis. Water contact angles indicate that the wettability of the modified PTFE powder increases significantly in comparison with non-modified PTFE powder. With increasing absorbed dose the wettability of the modified PTFE powder increases systematically in accordance with the ($-\text{COOH}$) concentration.

4.2. Characterization of peroxide-cured PTFE-EPDM

The effects of electron modification on properties of EPDM along with the optimization of PTFE loading for desired properties are investigated in the following chapter. For preliminary investigations, PTFE powder L100X was modified with absorbed doses of 20, 100 and 500 kGy and incorporated in EPDM as 10, 20, 30....up to 60 phr loading. PTFE based EPDM compounds have been characterized with respect to the effect of electron modification, irradiation dose and PTFE loading on physical, friction and wear properties. Further, the chemical compatibility and dispersion of PTFE powder with EPDM is characterized by Transmission Electron Microscopy (TEM), Scanning Electron Microscopy (SEM) and by Differential Scanning Calorimetry (DSC). As known, the inherent poor wetting and dispersion of PTFE restricts its effective application especially in rubber composition. In the present chapter, it has been shown that with the help of electron irradiation the inherent hydrophobic and incompatible PTFE surface can be successfully functionalized to enhance its dispersion and simultaneously compatibility with EPDM by radical coupling mechanism.

4.2.1 Influence of PTFE loading and irradiation dose

4.2.1.1. Cure analysis

An oscillating disc rheometer discussed in section 3.4.2 is a useful tool for monitoring the cure characteristics of a rubber compound. The delta torque (ΔM) is one of the most important parameters that is provided by the curing curve. These curves will be used to measure the effects of PTFE powder (additive) on cure efficiency of EPDM filled with varying PTFE loadings and irradiation doses. Figure 32 shows delta torque or apparent crosslink density (ΔM) values expressed in deci-Newton-meter [dNm] as a function of PTFE loading for various compounds in comparison with EPDM gum. As can be seen, ΔM decreases with irradiation dose at constant PTFE loading. However, at constant irradiation dose and increasing PTFE loading, comparatively distinct delta torque behaviour is observed. For PTFE^{0kGy}-EPDM and PTFE^{20kGy}-EPDM, an increase in ΔM is observed while for PTFE^{100kGy}-EPDM and PTFE^{500kGy}-EPDM it decreases with PTFE loading. PTFE^{500kGy}-EPDM shows ΔM even less than EPDM gum. However, in some cases EPDM gum has ΔM even higher than or equal to PTFE^{20kGy}-EPDM.

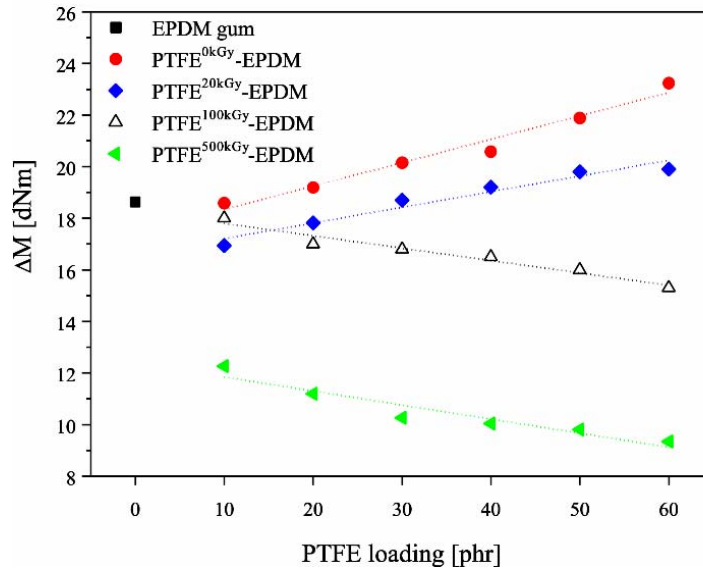


Figure 32. Delta torque (ΔM) values as a function of PTFE loading

It should be noticed that delta torque (ΔM) is only a measure of an apparent crosslink density of compounds. It is beyond the scope of the present work to investigate in detail the effective crosslink (physical and chemical). However, for a qualitative assessment it can be concluded that an apparent crosslink density decreases or is influenced by the electron beam irradiation of PTFE powder. PTFE^{500kGy}-EPDM vulcanizates show much lower delta torque and hence apparent crosslink densities. It can be inferred that the state of cure and crosslinking efficiency are strongly dependent on irradiation dose. Table 5 shows the optimum curing time (t_{90}) as a function of PTFE loading and irradiation dose for different PTFE filled EPDM compounds.

Table 5. Optimum curing time of PTFE filled EPDM vulcanizates

Filler loading [phr]	Optimum cure time, t_{90} [min]			
	0 kGy	20 kGy	100 kGy	500 kGy
Gum	14.8	-	-	-
10	15.2	13.6	15.3	11.1
20	14.8	14.0	15.6	10.5
30	15.6	12.4	14.5	8.5
40	15.8	13.4	14.2	8.3
50	15.0	12.7	15.2	8.1
60	14.9	12.9	15.5	8.4

As presented in the data sheet, a significantly shorter curing time is observed for PTFE^{500kGy}-EPDM, whereas PTFE^{0,20,100kGy}-EPDM shows an extended curing period. Lower (t_{90}) values

correlate to more rapid cure rates. This indicates that the use of increasing radiation dose of PTFE powder allows faster or incomplete curing. PTFE^{500kGy}-EPDM shows much lower delta torque and optimum curing time. This influence of modification of PTFE powder on some other desired properties will be discussed in detail in the following sections.

4.2.1.2. Compatibility and dispersion behaviour

Figure 33 a) and b) show TEM micrographs of PTFE^{0kGy}-EPDM and PTFE^{500kGy}-EPDM, respectively. The enhanced interfacial compatibility in case of PTFE^{500kGy}-EPDM can be seen in Figure 33 b) where the modified PTFE agglomerate are embedded and partially enwrapped by EPDM.

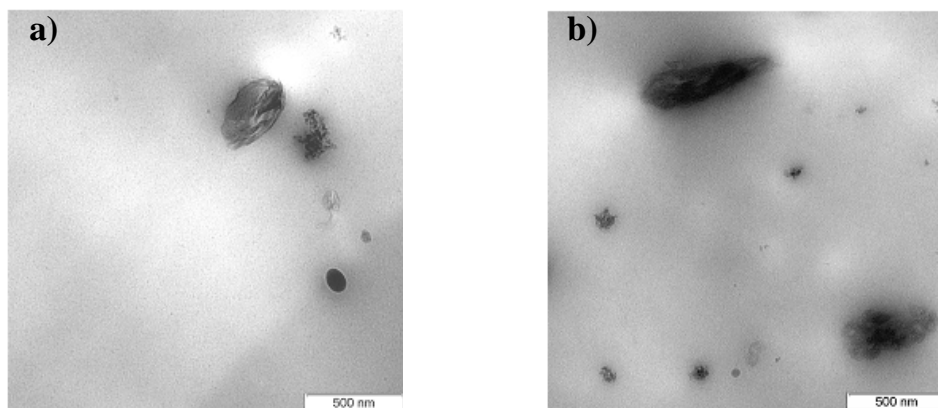


Figure 33. TEM micrographs of a) PTFE^{0kGy}-EPDM and b) PTFE^{500kGy}-EPDM vulcanizates

No clear and visible interphase can be seen between the two incompatible polymers. Slightly light and dark regions around modified PTFE powder are an indication of a reinforced compatible interphase due to radical coupling with EPDM. It is also observed that modified PTFE agglomerate acts as a PTFE core surrounded by EPDM shell. On the other hand, PTFE^{0kGy}-EPDM shows non-modified PTFE powder as solid embedded bodies lacking interfacial compatibility with EPDM. The interface is distinctively separated from each other. No mutual compatible interphase exists as is obvious in PTFE^{500kGy}-EPDM. The modified PTFE particles due to enhanced compatibility and dispersion are slightly oriented under high-shearing during reactive blending. However, non-modified PTFE powder being inert remains as huge rounded agglomerates even under high shearing. This behaviour can also be seen in

microdispersion in EPDM. Figure 34 a) and 34 b) show SEM micrographs of the tensile fractured surfaces of PTFE^{0kGy}-EPDM and PTFE^{500kGy}-EPDM.

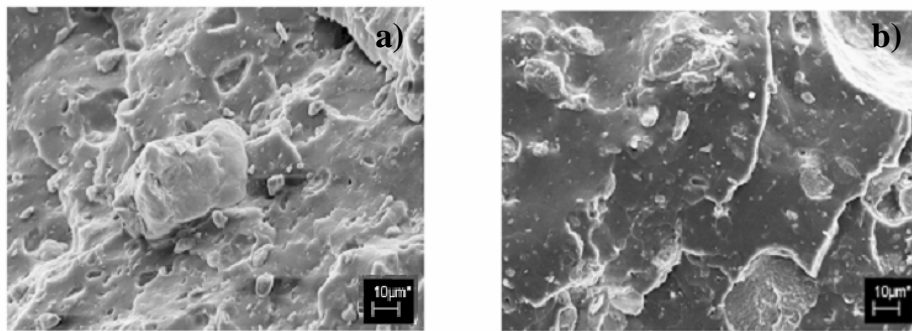


Figure 34. SEM micrographs of the tensile fractured surfaces of a) PTFE^{0kGy}-EPDM and b) PTFE^{500kGy}-EPDM vulcanizates

It is evident that the surface features are apparently distinguishable from each other. PTFE^{500kGy}-EPDM surface is smooth, with agglomerates embedded and homogeneously dispersed in EPDM matrix while PTFE^{0kGy}-EPDM shows an uneven, inhomogeneous surface with large vacuoles on the fractured surface. This indicates that PTFE particles are being pulled out of the matrix on application of stress due to the absence of interfacial interaction or coupling with matrix. It can be observed that non-modified PTFE particles are bigger in size and tend to form huge irregular agglomerates in the EPDM matrix even under high shearing during blending operation. Non-modified PTFE particles lack both the compatibility and the dispersion efficiency. Figure 35 shows the schematics of the state of modified and non-modified PTFE powder in EPDM.

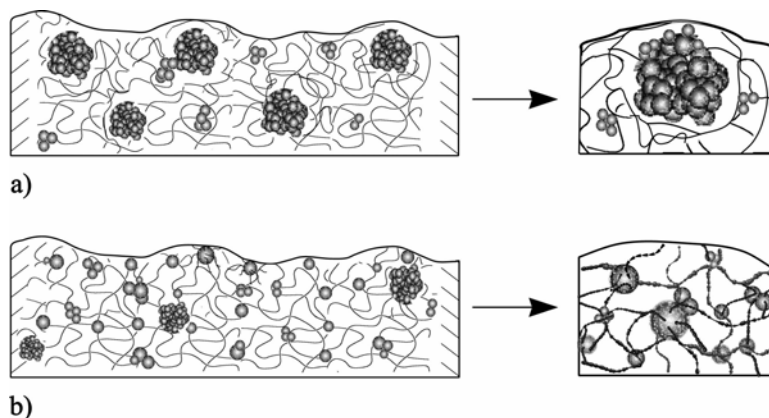


Figure 35. Schematics of the (a) non-modified and (b) modified PTFE powder in EPDM

Non-modified PTFE powder as shown in Figure 34 are huge uncovered agglomerates dispersed as solid rigid bodies in a matrix. Being incompatible they are not covered by EPDM molecules and hence, tend to segregate in EPDM matrix.

Figure 36 shows the thermal traces of (a) non-irradiated and 500 kGy irradiated PTFE powder and (b) corresponding PTFE^{0kGy}-EPDM and PTFE^{500kGy}-EPDM. The crystallization peak of 500 kGy irradiated PTFE powder shifts to a lower temperature of about 303.5°C. Also, the crystallization onset occurred at lower temperature and continued down to approx. 290°C. These distinct variations in 500 kGy in comparison to non-modified PTFE powder is due to the electron beam treatment process which caused degradation of 500 kGy PTFE powder. The molecular weight decreases due to chain scission and leads to PTFE macromolecules of different chain lengths. As a result, the crystallization peak occurs at lower temperatures and the crystallization process continues till much lower temperatures in comparison to non-modified PTFE powder.

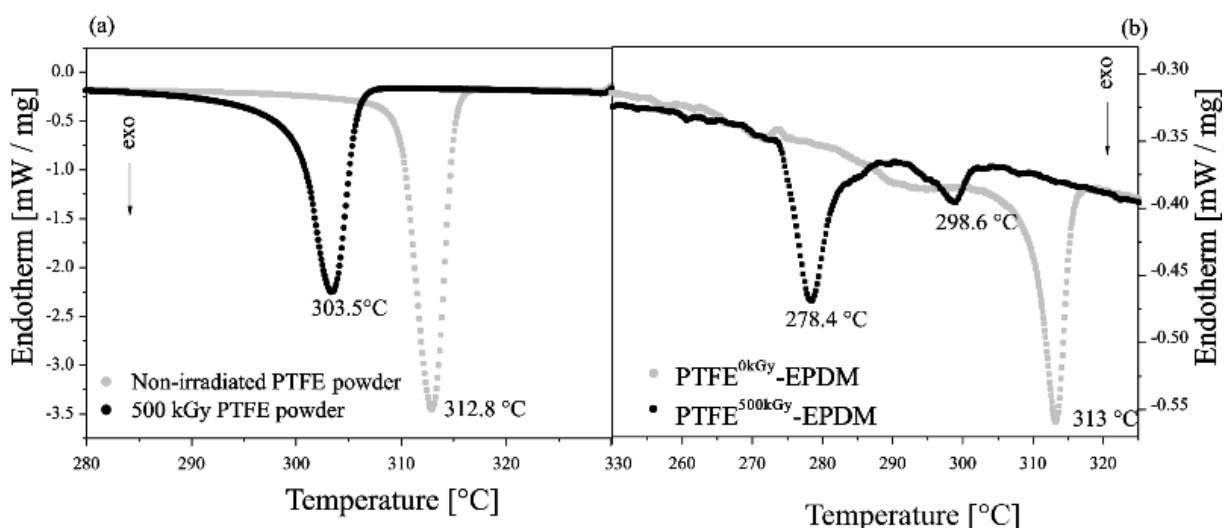


Figure 36. DSC cooling scans of the (a) non-irradiated and 500 kGy PTFE powder; and their corresponding (b) PTFE-EPDM vulcanizates

In case of blends, PTFE^{500kGy}-EPDM shows two crystallization peaks located at distinct temperatures. The second crystallization step at lower temperature also called fractionated crystallization occurred at 278°C along with the bulk crystallization peak at 298°C [110, 111]. The area of the first bulk crystallization peak is smaller as compared to the area of the second peak. However, the crystallization temperature (298.6°C) of the first peak is close to 500 kGy irradiated PTFE powder (303.5°C). The first crystallization peak is attributed to the content of PTFE powder in EPDM having comparatively bigger and incompatible agglomerates. The

PTFE agglomerates could be compatibilized only on the surface and the core consists of pure agglomerated PTFE powder. These agglomerates show crystallization temperatures similar to pure PTFE bulk crystallization. However, for PTFE^{0kGy}-EPDM, no fractionated crystallization except bulk crystallization similar to non-irradiated PTFE powder is observed at 313°C. This stems from the fact that non-irradiated PTFE powder is difficult to de-agglomerate and disperse homogeneously. The variations in the position of the transition-melting peaks observed in PTFE^{500kGy}-EPDM is due to the specific chemical compatibility of the electron beam modified PTFE with EPDM. This unique fractionated crystallization behaviour is mainly due to the fine dispersion of 500 kGy PTFE powder in EPDM. The outstanding dispersion of 500 kGy PTFE powder is also attributed to its comparatively smaller particle size and enhanced compatibility. PTFE^{0kGy}-EPDM on the other hand has significantly poor dispersion and compatibility with EPDM.

4.2.1.3. Physical properties

Figure 37 shows the tensile strength at break as a function of PTFE loading for different electron beam irradiated and non-irradiated PTFE filled EPDM in comparison with the EPDM gum.

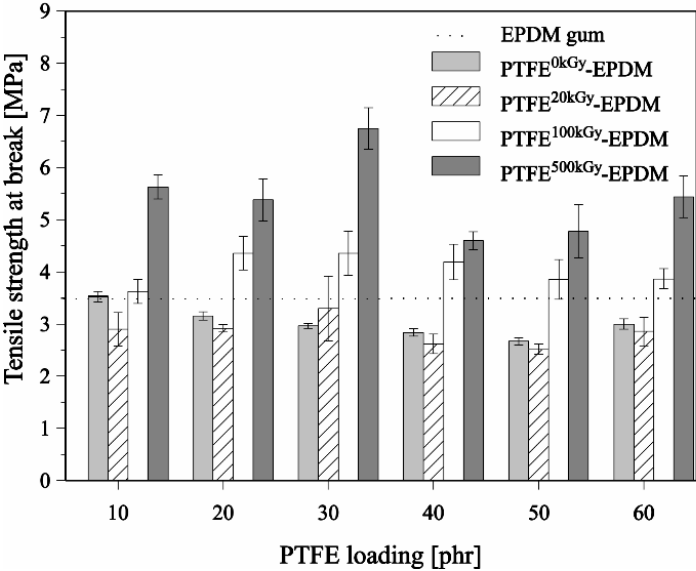


Figure 37. Tensile strength at break as a function of PTFE loading

In case of modified PTFE powder their corresponding EPDM vulcanizates increases by reaching a maximum value up to 30 phr followed by a decrease in the tensile strength above 30 phr loading. For a given formulation, 30 phr loading is the threshold filler loading above

which the poor compatibility and dispersibility of PTFE powder in EPDM results in deterioration of stress-strain properties. On the other hand, tensile strength at break of PTFE^{0kGy}-EPDM gradually decreases with increasing PTFE loading. This clearly indicates the poor dispersion and compatibility of non-modified PTFE powder with EPDM. Due to this reason, tensile strength of PTFE^{0kGy}-EPDM is even lower than EPDM gum. Figure 38 shows the elongation at break as a function of PTFE loading. The elongation at break increases with PTFE loading. Similarly as in the case of tensile strength, a 30 phr PTFE loading provides the maximum elongation followed by a decrease with increasing PTFE loading above 30 phr. Non-modified PTFE powder has elongation similar to that of EPDM gum.

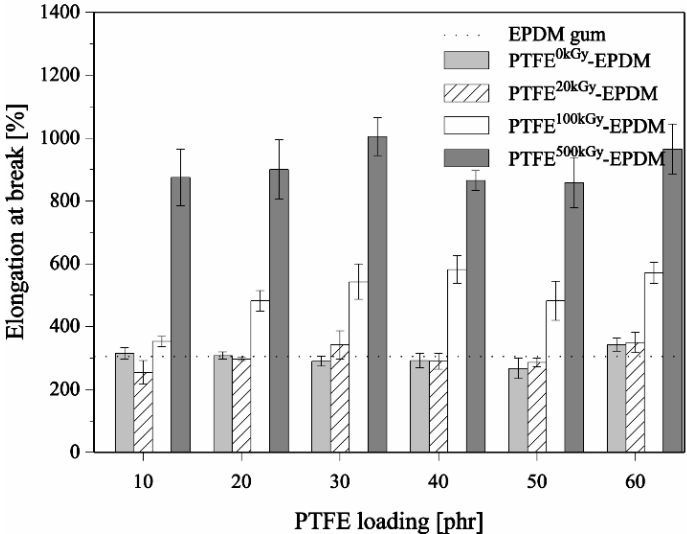


Figure 38. Elongation at break as a function of PTFE loading

In Figure 39 the tear strength is shown as a function of PTFE loading. For modified PTFE powder filled EPDM vulcanizates the tear strength increases both with PTFE loading and irradiation dose.

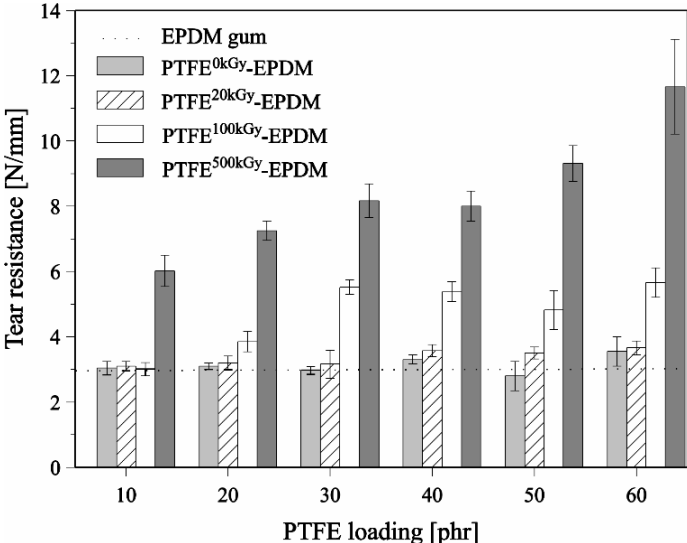


Figure 39. Tear resistance as a function of PTFE loading

However, PTFE^{0kGy}-EPDM vulcanizates did not show any improvement in the tear resistance property. The tear properties of EPDM gum and PTFE^{0kGy}-EPDM vulcanizates are almost the same. The tear strength of PTFE^{500kGy}-EPDM filled with 60 phr PTFE loading increases to almost four folds to that of EPDM gum. It suggests that modified PTFE powder can be effectively utilized in improving the tear strength of low-strength rubbers such as EPDM, EP and Silicon etc. Figure 40 displays the stress at 100% elongation (so-called modulus 100%, M100) as a function of PTFE loading. The M100 decreases significantly for PTFE^{100kGy}-EPDM and PTFE^{500kGy}-EPDM whereas PTFE^{0kGy}-EPDM and EPDM-PTFE^{20kGy}-EPDM shows the highest M100 with increasing PTFE loading up to 30 phr. However, the corresponding values of PTFE^{100kGy}-EPDM and PTFE^{500kGy}-EPDM are lower even than EPDM gum. Above 30 phr PTFE loading M100 decreases to a significant level for all irradiation doses.

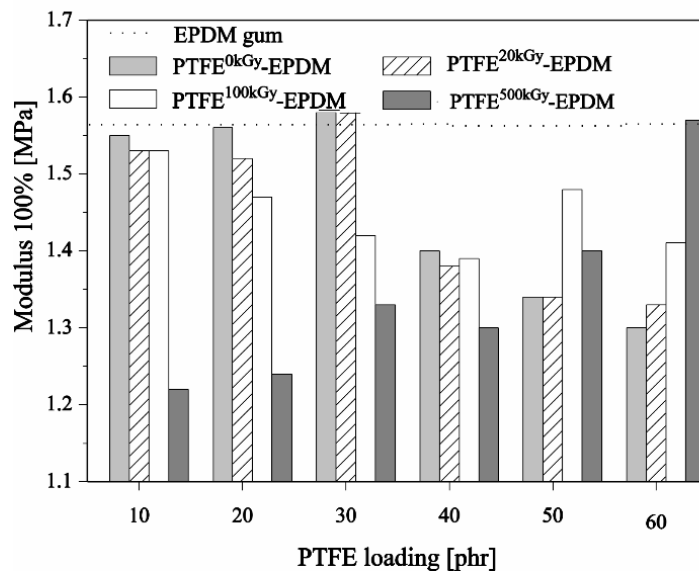


Figure 40. Modulus 100% as a function of PTFE loading

4.2.1.4 Friction and wear behaviour

Beside physical characterization, one important aim of this work is the evaluation of the effects of electron beam modification of PTFE powder on the friction and wear properties of PTFE filled EPDM rubber cured by a radical-initiated peroxide system. Friction and wear properties of EPDM vulcanizates were determined with the help of pin on disk tribometer in sliding contact with a steel-ball at room temperature without lubrication. In the present chapter, the corresponding friction and wear properties for low dose (20 kGy) and high dose (500 kGy) irradiated PTFE powder in comparison with non-irradiated (0 kGy) PTFE powder is investigated. For preliminary study, the effects of PTFE loading, irradiation dose and radiation-induced chemical changes on friction and wear properties of PTFE filled EPDM is discussed. The average friction coefficient (μ)

of EPDM gum and PTFE filled EPDM vulcanizates as a function of PTFE loading is shown in Figure 41. It can be seen that friction coefficient of all PTFE filled EPDM vulcanizates decreases in contrast to EPDM gum. A gradual decrease in friction coefficient can be observed with increasing PTFE loading. The friction coefficient decreased from 2.1 for EPDM gum to almost less than 1.0 for the highest PTFE loading. However, at constant PTFE loading friction coefficient is weakly dependent on irradiation dose as no significant reduction has been achieved with the use of irradiated PTFE. It can be observed that the starting friction coefficient [μ_{initial}] varies differently for PTFE filled EPDM vulcanizates. PTFE^{0kGy}-EPDM and PTFE^{20kGy}-EPDM have almost similar (1.32) and comparatively lower μ_{initial} value for all PTFE loadings. In contrast, PTFE^{500kGy}-EPDM shows the highest μ_{initial} values (1.5 or higher). This variation in friction behaviour

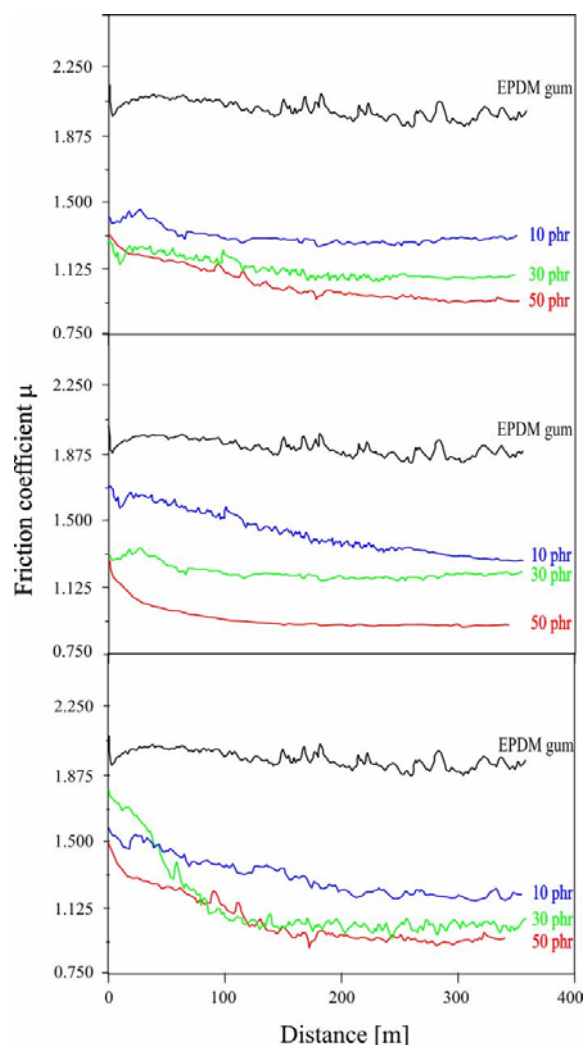


Figure 41. Friction coefficient behaviour of a) PTFE^{0kGy}-EPDM, b) PTFE^{20kGy}-EPDM and c) PTFE^{500kGy}-EPDM for different PTFE loadings in comparison to EPDM gum

could be due to the specific apparent crosslink densities or delta torque (ΔM) values as shown in Figure 32. Both PTFE^{0kGy}-EPDM and PTFE^{20kGy}-EPDM have higher ΔM values and therefore have lower μ_{initial} values. Even a slight variation in ΔM results in different μ_{initial} values. Soon as ΔM decreases as in the case of PTFE^{500kGy}-EPDM, a significant increase in μ_{initial} is observed. With decreasing ΔM , both the modulus and stiffness decreases and the mechanical energy dissipation increases. Both of these bulk properties result in significantly higher μ_{initial} . Lower modulus of the compounds result in larger contact area with the counterbody and therefore high friction coefficient is expected. The decrease in ΔM is primarily caused by the adverse influence of irradiated PTFE powder on the peroxide crosslinking of PTFE filled EPDM compounds. The factors which influence the peroxide curing of EPDM are reported in [72, 77]. However, the main disadvantage of peroxide-induced curing is the undesired interference of free radicals with additives which leads to a reduction of the crosslinking efficiency. Electron beam irradiated PTFE powder reduces the crosslinking efficiency of irradiated PTFE filled EPDM compounds due to the presence of peroxide free-radicals as shown in Figure 26. Since the driving force of peroxide curing is free-radicals, they energetically react with other reactive species to pair with each other. The result is that large number of peroxide free-radicals is consumed wastefully rather than participating in the curing process.

Figure 42 shows the specific wear rate (k) of EPDM gum and PTFE filled EPDM vulcanizates as a function of PTFE loading. Both PTFE^{0kGy}-EPDM and PTFE^{20kGy}-EPDM show significantly lower k values compared to EPDM gum and PTFE^{500kGy}-EPDM. PTFE^{500kGy}-EPDM show increasing k with PTFE loading.

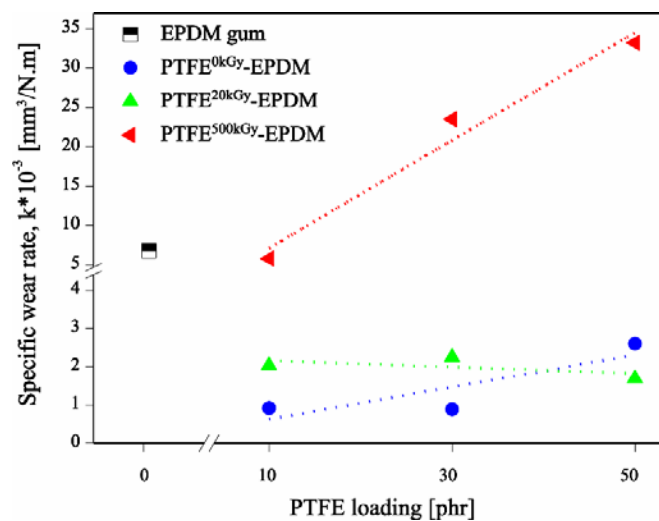


Figure 42. Specific wear rate (k) of EPDM gum and PTFE filled EPDM vulcanizates as a function of PTFE loading

For 30 and 50 phr (parts per hundred of rubber) loading, k was even higher than EPDM gum. For PTFE^{20kGy}-EPDM, k remained constant while PTFE^{0kGy}-EPDM showed the lowest k . The magnitude of friction coefficient values at the beginning of the loading have a significant influence on the wear mechanism during further testing. The specific wear rate (k) clearly indicates a strong correlation with delta torque (ΔM) of the compounds. With increasing ΔM as in the case of PTFE^{0kGy}-EPDM and PTFE^{20kGy}-EPDM k is significantly lower. Soon as ΔM decreases, k increases significantly as in the case of PTFE^{500kGy}-EPDM. The variation in the magnitude of ΔM is strongly correlated to its wear properties. As can be seen in Figures 32 and 42, k varies according to ΔM values. It is also interesting that EPDM gum has significantly higher ΔM than PTFE^{500kGy}-EPDM but shows similar k value as of 10 phr PTFE^{500kGy}-EPDM. This suggests that vulcanizates depending on their unique composition and bulk properties suffered from different modes of wear.

4.2.1.4.1. Analysis of the wear mechanism

In general, particle size, shape and distribution play an important role in the wear of different filled systems [112-114]. The average friction coefficient values are almost similar for PTFE filled EPDM having comparatively different mean agglomerate size and distribution (Figure 28 and 29). Scanning electron micrographs of the wear scars of (a) EPDM gum, (b) PTFE^{500kGy}-EPDM and (c) PTFE^{20kGy}-EPDM vulcanizates are shown in Figure 43.

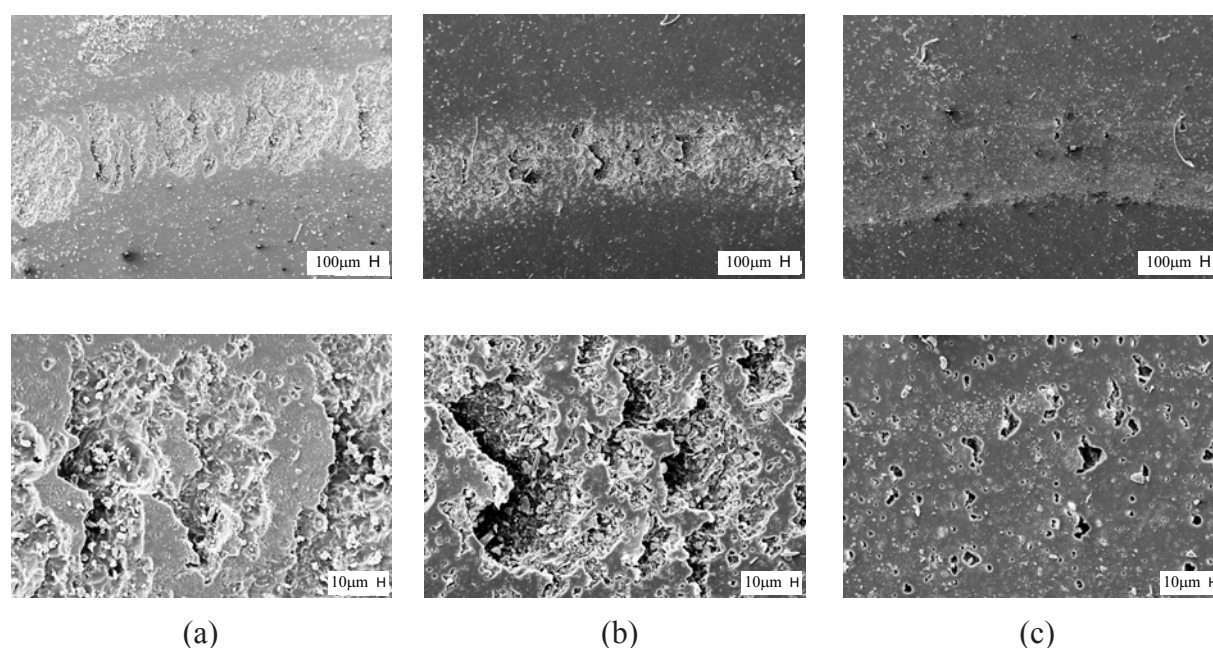


Figure 43. Scanning electron micrographs showing the worn surfaces of: (a) EPDM gum; (b) PTFE^{500kGy}-EPDM; (c) PTFE^{20kGy}-EPDM

The wear-scars suggest that wear in these three different compounds have occurred by different mechanisms. EPDM gum shows a characteristic failure mode due to the absence of PTFE powder. In case of EPDM gum, the solid materials detached from the surface due to adhesion mechanism with the counter-body. However, in presence of PTFE powder the sliding contact area of the PTFE filled EPDM vulcanizates with the counter-surface seems to change apparently. In case of PTFE^{20kGy}-EPDM vulcanizate having higher delta torque (Figure 32) the contact area show smoother surfaces with small detachments around PTFE powder. In this case the wear mechanism is mainly characterized by the detachment of PTFE agglomerates. In contrast, PTFE^{500kGy}-EPDM vulcanizates having significantly lower delta torque (Figure 32), the wear scar is characterized by disruption in deep regions of the EPDM matrix. A wavy pattern exists with fronts transversely oriented to the sliding direction. Figure 44 shows the higher magnification topography of (a) PTFE^{20kGy}-EPDM (b) PTFE^{500kGy}-EPDM vulcanizates. The surface of the PTFE^{20kGy}-EPDM indicates the presence of large PTFE agglomerates. The large agglomerates appear to have been firmly embedded and excessively abraded by the counter-surface. Many unperturbed smaller agglomerates surrounding the huge agglomerate with surprisingly no signs of wear by counter-surface can be seen. In case of PTFE^{500kGy}-EPDM vulcanizates, the worn topography resembles those of the EPDM gum except the presence of PTFE powder. The mode of deformation in these materials has occurred in the deep regions or at the interfaces between the matrix and small particles.

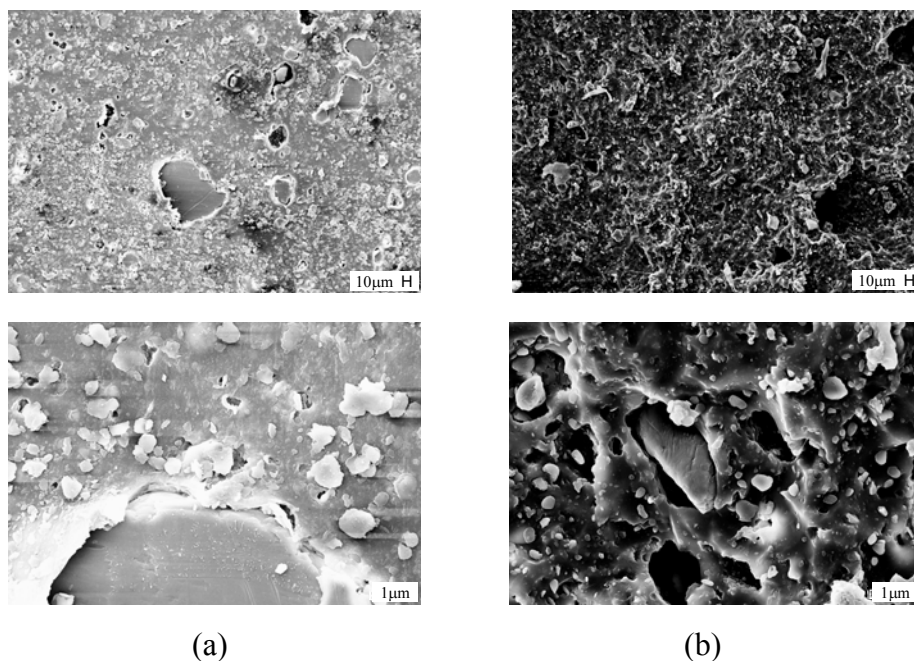


Figure 44. Scanning electron micrographs showing the worn surfaces of: (a) PTFE^{20kGy}-EPDM; (b) PTFE^{500kGy}-EPDM

4.2.1.4.2. Physical-wear property relationship

The physical properties of EPDM gum and PTFE filled EPDM as a function of PTFE loading are summarized in Table 6. PTFE^{500kGy}-EPDM has significantly enhanced tensile strength at break, elongation at break and tear resistance than both PTFE^{0kGy}-EPDM and PTFE^{20kGy}-EPDM but significantly lower hardness. With increasing PTFE loading, hardness increases and specific wear rate (k) is expected to decrease as shown in Figure 42 for PTFE^{0kGy}-EPDM and PTFE^{20kGy}-EPDM. However, it is interesting to note that in case of PTFE^{500kGy}-EPDM with increasing PTFE loading, k increases with increasing hardness. It suggests that another parameter is influencing k. This wear rate controlling parameter could be apparent crosslink density (ΔM). It also suggest that a threshold value of ΔM exists below which k is independent of hardness. The hardness may influence k above this threshold value of ΔM as is the case of PTFE^{0kGy}-EPDM and PTFE^{20kGy}-EPDM. Beside this, numerous other successful correlations of k with various physical properties such as tensile strength, elongation and hardness for various kinds of polymer composites have also been made in the past [115-118].

Table 6. Physical properties as a function of PTFE loading and irradiation dose for different PTFE filled EPDM vulcanizates

PTFE loading [phr]	Irradiation dose [kGy]	σ_B [MPa]	ϵ_B [%]	Tear resistance [N/mm]	Hardness [ShA°]
EPDM gum	-	3.48	304	2.97	54.7
10	0	3.53	315	3.04	60.0
	20	2.90	254	3.10	59.1
	500	5.63	875	6.01	53.2
30	0	2.97	289	2.97	62.3
	20	3.30	342	3.16	61.4
	500	6.75	1005	8.16	55.3
50	0	2.67	267	2.80	63.4
	20	2.52	286	3.50	62.4
	500	4.78	858	9.31	56.9

These investigations have explicitly concluded that the key in developing any such correlation is strictly dependent on unambiguously identifying the dominating properties of the materials which control and inhibit wear. Similar is the case of PTFE^{500kGy}-EPDM vulcanizates where ΔM less than critical value results in significantly higher k. In such case the chemical

composition of the rubber itself, whether filled or unfilled, appears to have no effect in reducing wear. However, it is appropriate to mention that in general the frictional properties of rubber-like materials beside sliding speed, temperature and normal load also depend on the typical surface characteristics of the load counter-face [119]. The results presented in the present work are valid only for the load and sliding speed of 1.0 N and 0.05 ms⁻¹, respectively.

It suggests that the achievement in tribo-performance was at the cost of the most of the mechanical or tribological properties. PTFE^{0kGy}-EPDM vulcanizate shows enhanced wear resistance but has extremely poor tensile strength at break, elongation at break and tear resistance. Thus, with significantly higher irradiation dose, though physical properties increased substantially, it was at the cost of significantly poor crosslinking density and wear performance of the vulcanizate.

4.2.2.3. Conclusions

The existence of compatibility between modified PTFE powder (L100X) and EPDM was revealed by TEM, SEM and DSC. The resultant modified PTFE filled EPDM vulcanizates demonstrate enhanced physical properties by enwrapping of modified PTFE powder by EPDM. The synergistic effect of compatibility and micro-dispersion of PTFE agglomerates due to chemical coupling results in a significant improvement of physical properties of PTFE coupled EPDM compounds.

Friction and wear properties have been improved by incorporating PTFE powder (L100X) as a friction modifier additive in EPDM compared to EPDM gum (No PTFE powder). An optimum PTFE loading of 30 phr in EPDM is sufficient enough in improving physical, friction and dispersion properties. It was found that electron modification of PTFE powder diminish the final cure state and crosslinking density of peroxide-cured EPDM compound. Delta torque (ΔM), a measure of apparent crosslinking density of PTFE filled EPDM compound is identified as an important friction and wear-controlling parameter. Compounds having significantly lower ΔM show poor friction and wear properties due to significantly poor bulk properties (hardness).

4.2.2. Influence of irradiation dose at constant PTFE loading

The preliminary investigations suggest that electron irradiation of PTFE powder undoubtedly influences the friction and wear properties of EPDM through peroxide crosslinking. For this reason in the following chapter friction and wear properties of 30 phr L100X PTFE powder filled EPDM vulcanizates for a complete range of absorbed doses i.e. 20, 100, 200, 300, 400 and 500 kGy are investigated. These investigations are necessary in order to analyze the tendency in friction and wear behaviour of EPDM filled with increasing absorbed dose of L100X PTFE powder. The influence of radiation-induced chemical changes in modified PTFE powder on bulk properties (hardness, mechanical energy dissipation etc) of EPDM and its dependency on friction and wear properties is systematically studied.

4.2.2.1. Curing characteristics

Figure 45 shows the effect of the electron beam modification on the curing characteristics such as delta torque (ΔM) expressed in deci-Newton-meter [dNm] and curing time (t_{90}) in minutes. In general, delta torque allows a qualitative assessment of the state of cure for the determination of crosslinking density of vulcanizates. The magnitude of delta torque corresponds to the degree of crosslink density. As can be seen both t_{90} and ΔM gradually decreases with the use of higher irradiation dose of PTFE powder in EPDM. PTFE^{0kGy}-EPDM shows the highest t_{90} and ΔM followed by EPDM gum, while PTFE^{500kGy}-EPDM shows the lowest values. In other words an inverse relation can be suggested between delta torque and absorbed dose.

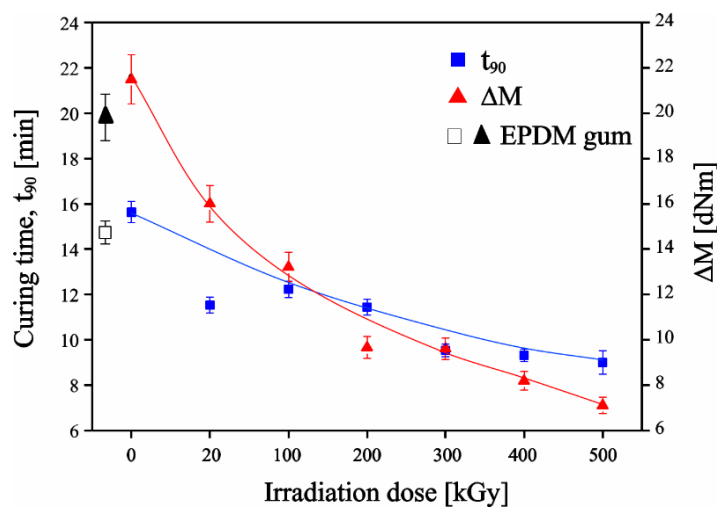


Figure 45. Optimum cure time (t_{90}) and delta torque (ΔM) of EPDM gum and PTFE filled EPDM compounds

4.2.2.2 Physical properties

Figures 46 (a) and 46 (b) show tensile strength and elongation at break of PTFE-EPDM vulcanizates as a function of absorbed irradiation dose. The horizontal line represents EPDM gum. In case of PTFE^{0kGy}-EPDM, tensile strength and elongation at break are lower than modified PTFE filled EPDM. With increasing absorbed dose, tensile strength and elongation at break of modified PTFE coupled EPDM compounds increase systematically. Tensile strength and elongation at break of EPDM gum and PTFE^{0kGy}-EPDM are almost the same because of poor compatibility and dispersion. On the other hand, PTFE^{500kGy}-EPDM shows the highest tensile strength and elongation at break.

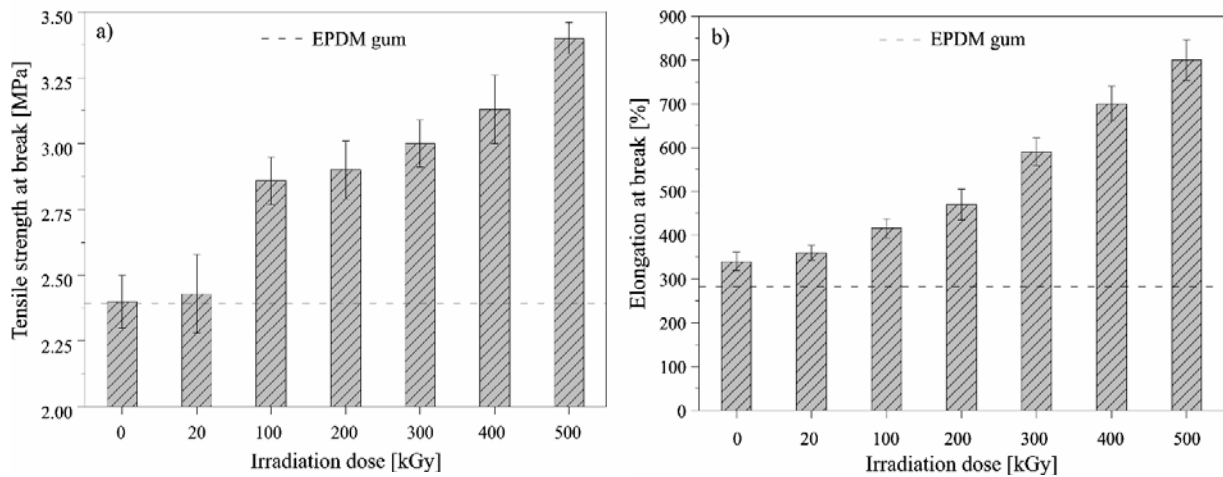


Figure 46. Tensile strength at break (a), elongation at break (b) as a function of dose

Modified PTFE particles having smaller agglomerate sizes and compatible surfaces enhance its degree of dispersion and compatibility. The improvement of physical properties of EPDM filled with electron treated PTFE is essentially due to the synergistic effect of their homogeneous dispersion and desirable compatibility. Figure 47 (a) displays the stress at 300% elongation (so-called modulus 300%, M300) as a function of absorbed dose. The M300 decreases for modified PTFE filled EPDM with increasing irradiation dose. PTFE^{0kGy}-EPDM shows the highest M300. However, the corresponding values of PTFE^{400kGy}-EPDM and PTFE^{500kGy}-EPDM are lower even than EPDM gum. Figure 47 (b) shows the corresponding Shore (A) hardness values of PTFE-EPDM blends. The effect of absorbed dose of PTFE powder on vulcanizate hardness can be seen in their decreasing values of hardness. EPDM filled with PTFE having absorbed irradiation doses higher than 20 kGy results in decreasing hardness values of PTFE-EPDM vulcanizates. PTFE^{20kGy}-EPDM has the highest hardness

while PTFE^{500kGy}-EPDM showed the lowest. It is interesting to note that hardness of the vulcanizates above PTFE^{200kGy}-EPDM is even lower than that of EPDM gum.

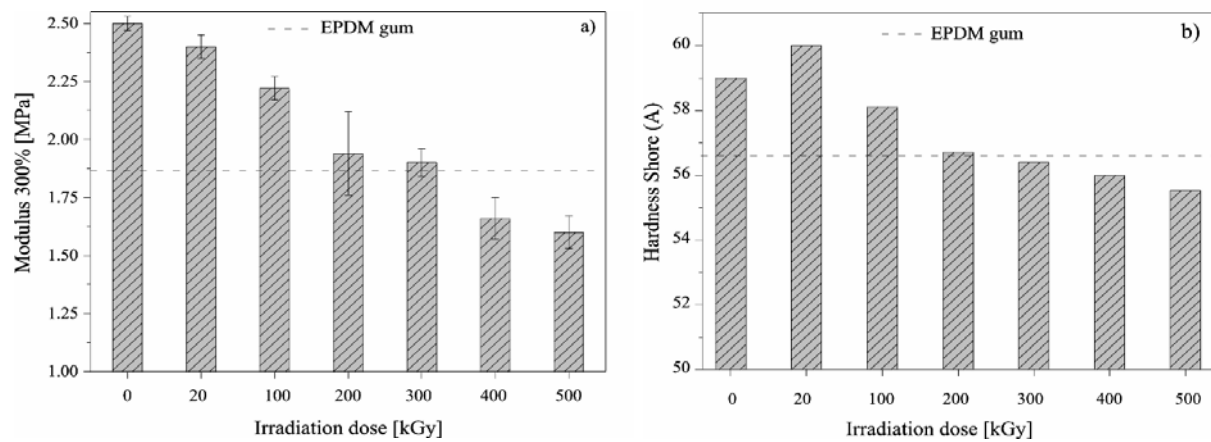


Figure 47. Modulus 300% (a) and hardness (b) as a function of irradiation dose

Surface characterization

Figure 48 shows the XPS results of (a) PTFE^{0kGy}-EPDM and (b) PTFE^{500kGy}-EPDM vulcanizates. On the basis of these investigations the ratio of carbon to fluorine has been calculated. No change in relative fluorine intensity at the smooth surface has been found within the experimental uncertainty.

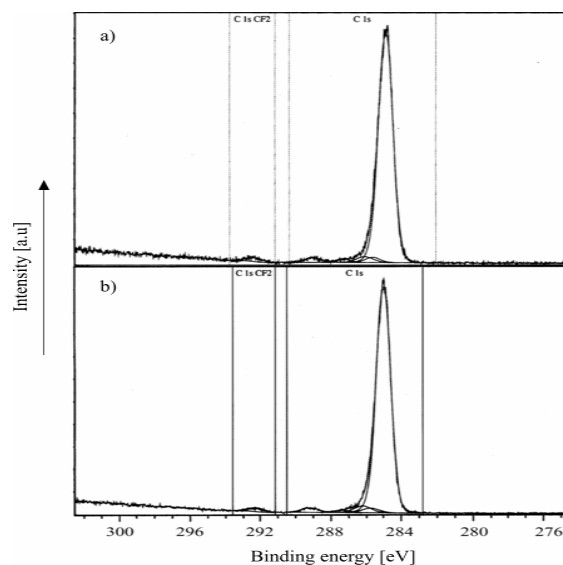


Figure 48. XPS of (a) PTFE^{0kGy}-EPDM and (b) PTFE^{500kGy}-EPDM vulcanizates

The mean surface roughness of unfilled EPDM was 0.1 μm . However, compared to PTFE filled EPDM the root mean square (rms) value was found to be within the range of 0.11 and 0.12 μm .

4.2.2.3. Friction and wear properties

Friction in general is a complex process which characterizes the interaction between surfaces of solid bodies in contact with each other. The molecular mechanical theory unifies well-known deformation and adhesion theory in explaining the complicated interaction between solid bodies in contact. However, friction of viscoelastic elastomers sliding against hard counter-surface results in a more complex behaviour. Beside testing conditions such as temperature, velocity and normal load, their high viscoelastic behaviour results in a spatial distribution of real contact area which varies both locally and temporally during cyclic loading. Generally, the real contact area is only a fraction of the nominal contact regions. The following mechanisms shown in Figure 49 strongly influence both friction and wear behaviour of soft viscoelastic materials sliding against a solid rough counter-surface [120]:

- a) braking-off the adhesive bonds or the boundary layers
- b) plastic deformation of the contacting area zones
- c) plowing due to roughness peaks and wear debris
- d) elastic hysteresis due to damping

The friction and wear properties of the PTFE powder filled EPDM are discussed in the context of the above mentioned mechanisms.

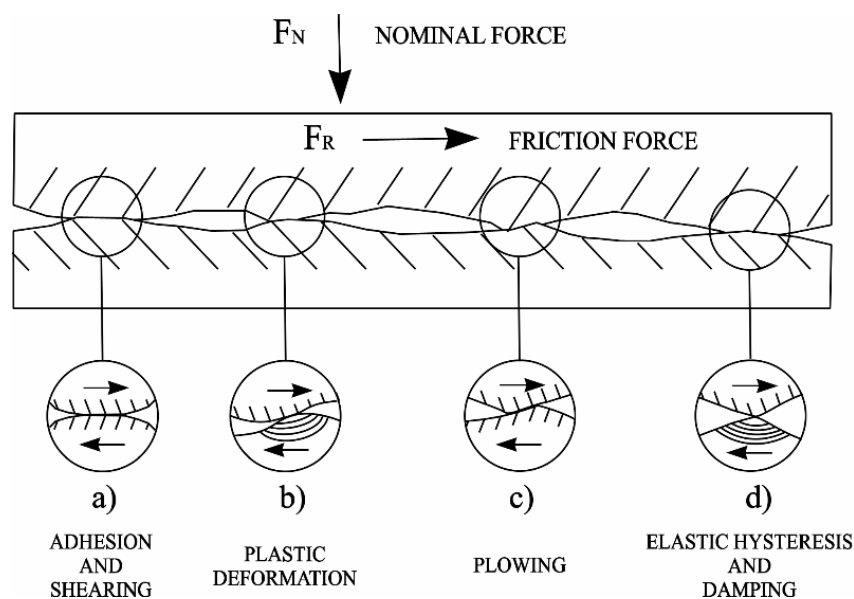


Figure 49. Friction and wear mechanisms involved in viscoelastic solid bodies sliding against a rough counter-surface

Figure 50 a) and 50 b) show the friction coefficient and specific wear rate of PTFE filled vulcanizates in comparison to EPDM gum. Figure 50 a) indicates that the friction coefficient of EPDM gum in comparison to PTFE filled EPDM vulcanizates increased during the course of measurement. All samples display a characteristic run-in process. The friction coefficient values decreased in a range from 9 % to 37 % till the end of the measurements. As shown in Figure 50 b), k increased with absorbed dose or decreasing delta torque. The lowest k value of $0.5 \cdot 10^{-3} \text{ mm}^3/\text{Nm}$ is observed for PTFE^{0kGy}-EPDM having the highest delta torque (Figure 45). Moreover a minor increase in wear rate is observed up to PTFE^{200kGy}-EPDM which corresponds to a delta torque value of approx 10 dNm. Above this threshold, a maximum k value of $12.56 \cdot 10^{-3} \text{ mm}^3/\text{Nm}$ is achieved for PTFE^{500kGy}-EPDM having the lowest delta torque of approx 7 dNm. XPS analysis of PTFE^{0kGy}-EPDM and PTFE^{500kGy}-EPDM surfaces prior to friction and wear testing shown in Figure 48 suggests that the ratio of fluorine to carbon (F/C) is similar with in the experimental uncertainty. This result indicates that the surfaces are chemically similar whether filled with modified or non-modified PTFE powder. On the other hand, evaluation of surface roughness before wear testing supports the fact that the vulcanizate surfaces have almost similar micro-roughness. Both results suggest that the vulcanizates surfaces are chemically and topographically similar before wear testing. This indicates that friction processes are comparable at the beginning of the loading.

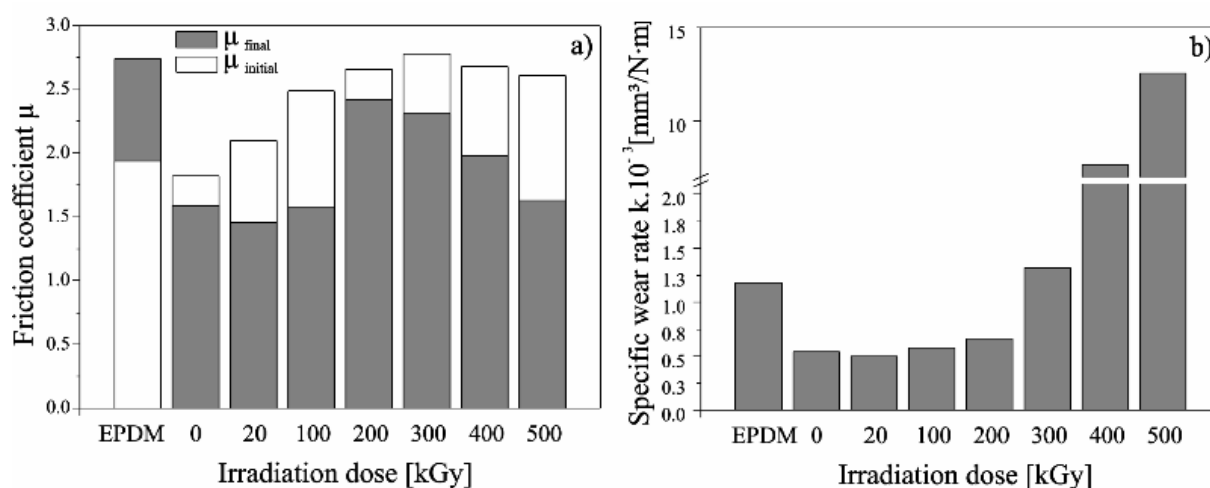


Figure 50. Friction coefficient a) and specific wear rate b) of PTFE powder filled EPDM vulcanizates as a function of irradiation dose in comparison to EPDM gum

For all materials the adhesive mechanism (a) and the plastic deformation (b) should be the main processes. During testing, the variation in friction coefficient values could be influenced by the specific delta torque behaviour. Since delta torque corresponds to the crosslink density

of a vulcanizate, for a qualitative assessment it can be concluded that the crosslink density decreases with increasing absorbed dose. PTFE^{500kGy}-EPDM vulcanizate showed much lower delta torque and t₉₀ values. It can be inferred that the state of cure is strongly dependent on the absorbed dose of PTFE powder.

The magnitude of friction coefficient values at the beginning of the loading have a significant influence on the wear mechanism during further testing. Therefore the friction coefficient at the beginning is correlated to tan delta @ 25°C, hardness and mean agglomerate size. As shown in Figures 51 (a) the friction coefficient (μ) increased with increasing tan delta for modified PTFE filled EPDM vulcanizates. Also PTFE^{0kGy}-EPDM vulcanizate fits well according to this dependency. It suggests that tan delta value of a vulcanizate is influencing the friction coefficient (μ) and could be a friction controlling parameter. The tan delta value characterizes the energy dissipation due to internal friction in these compounds. It was observed that the loss factor increases with absorbed dose of PTFE powder. Assuming that the stiffness and storage modulus of PTFE filled EPDM vulcanizates remains constant, the friction energy produced by the counter body should be better dissipated and therefore friction coefficient should decrease but an increase in friction coefficient was observed. Another reason of increasing tan delta values is the decrease in storage modulus at constant loss modulus. Felhös and Karger-Kocsis report the same tendency that with decreasing stiffness the friction coefficient increases for carbon black filled EPDM [42].

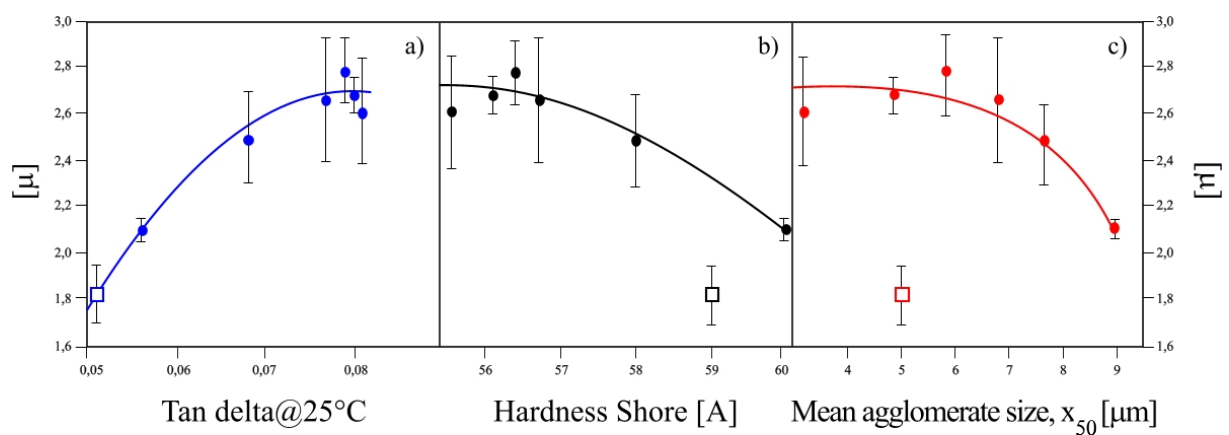


Figure 51. Friction coefficient (μ) values as a function of a) tan delta @ 25°C, b) hardness and c) mean agglomerate size (Unfilled box indicates non-modified and filled box modified PTFE filled EPDM)

Figure 51 b) shows μ as a function of vulcanizate hardness. For modified PTFE filled EPDM vulcanizates μ decreases with increasing hardness. On the other hand, non PTFE^{0kGy}-EPDM

vulcanizate with hardness less than PTFE^{20kGy}-EPDM shows the lowest μ as well as the highest delta torque (Figure 45). This indicates that hardness alone is not influencing the friction behaviour. The gradual decrease in hardness values with increasing dose of PTFE powder in EPDM is due to the influence of modified PTFE powder on the peroxide-induced crosslinking of PTFE filled EPDM. The main factors which influence the peroxide cure efficiency of EPDM are reported in [72, 77]. One disadvantage of the use of peroxide for crosslinking is the undesired interference with additives where they act as radical scavengers, which leads to a reduction of the crosslinking efficiency.

In general, the efficiency of the crosslinking mode depends not only on the chemical composition of the polymer, but also on the presence of additives, such as antioxidants. Electron beam modified PTFE powder seems to have an adverse effect on the crosslinking efficiency of modified PTFE filled EPDM compounds due to the presence of radical and functional groups on modified PTFE powder.

Figure 51 c) shows that for modified PTFE filled EPDM vulcanizates μ decreased steadily with increasing mean agglomerate size. However, PTFE^{0kGy}-EPDM vulcanizate has a lower friction coefficient compared to modified PTFE filled EPDM vulcanizates having the same mean agglomerate size but significantly higher delta torque value. This suggests that the mean agglomerate size of PTFE powder is not a friction controlling property and a further additional parameter is influencing the friction behaviour.

In contrast to the frictional behaviour, the specific wear rate depends both on tan delta and hardness. Figure 52 a) shows k as a function of tan delta.

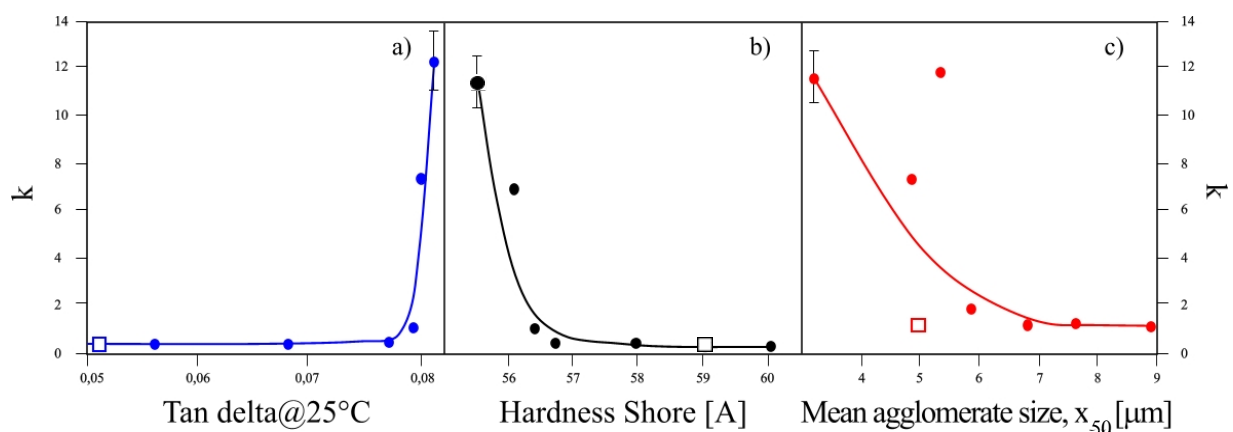


Figure 52. Specific wear rate (k) as a function of a) tan delta @ 25°C, b) hardness and c) mean agglomerate size (Unfilled box indicates non-modified and filled box modified PTFE filled EPDM)

As can be seen, a threshold exists for tan delta values up to which a minor increase in specific wear rate is observed. However, above this limit k increases significantly as observed for PTFE^{300kGy}-EPDM which corresponds to a delta torque value of less than 10 dNm (Figure 45). Figure 52 b) shows wear rate as a function of hardness. Similarly the wear rate increases with decreasing hardness. However, for PTFE^{300kGy}-EPDM and higher it rises significantly. Again this behaviour is due to the significantly lower delta torque value (less than 10 dNm). Figure 52 c) shows k as a function of mean agglomerate size. For modified PTFE filled EPDM vulcanizates k decreased with increasing mean agglomerate size. In contrast, PTFE^{0kGy}-EPDM vulcanizate shows lower k value compared to modified PTFE powder filled EPDM vulcanizate having the same mean agglomerate size but higher delta torque values. This suggests that the delta torque value or cross linking density of these compounds are important wear controlling parameters.

Wear mechanism

Scanning electron micrographs of the wear scars of EPDM gum and PTFE filled EPDM vulcanizates are shown in Figure 53. EPDM gum shows a characteristic failure mode caused by the absence of PTFE powder. EPDM gum failed by detachment of the solid material from the surface by an adhesive mechanism with the counter-body. However, in the presence of PTFE powder in EPDM the sliding contact area of the PTFE filled EPDM vulcanizates with the counter-surface seems to change apparently. In case of PTFE^{0,20,100kGy}-EPDM vulcanizates having delta torque higher than 13 dNm (Figure 45) the contact areas show smoother surfaces with small detachments around PTFE powder and mostly abraded PTFE agglomerates in the matrix as shown in Figures 53 b)-d). In this case the wear mechanism is mainly characterized by the detachment of PTFE agglomerates. In contrast, PTFE^{200.....500kGy}-EPDM vulcanizates having delta torque less than 10 dNm, show contact areas being characterized by a disruption in deep regions of the matrix. A wavy pattern exists with fronts transversely oriented to the sliding direction. The depth of the waves increases with the absorbed dose of the PTFE powder, that means with decreasing delta torque. Due to the presence of many unperturbed smaller PTFE agglomerates with surprisingly no signs of wear by the hard counter-surface a different failure mechanism is involved as can be seen in Figures 53 e)-h).

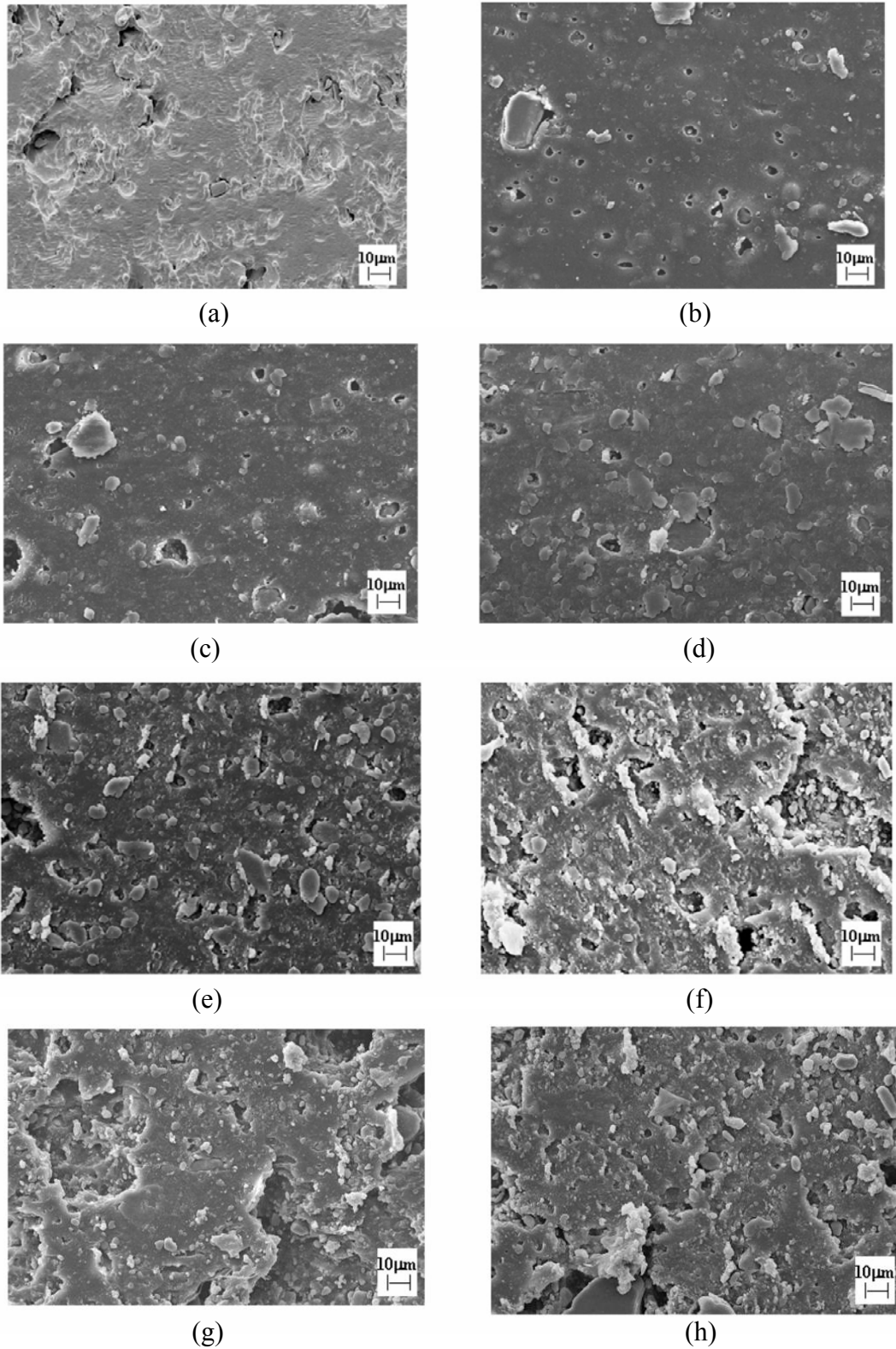


Figure 53. SEM micrographs showing the worn surfaces of: (a) EPDM gum; (b) Non-modified, (c-h) 20,100, 200, 300, 400 and 500 kGy PTFE filled EPDM.

4.2.2.4. Conclusions

The results suggest that friction is primarily related to bulk visco-elastic properties such as hardness, apparent crosslinking density (ΔM) and mechanical energy dissipation ($\tan \delta$). These bulk properties play an important role in friction and wear of PTFE filled EPDM vulcanizates. A critical threshold limit has been found for hardness (58 Shore A) and ΔM (10 dNm) below which chemical composition of the rubber compound either filled with modified or non-modified PTFE powder seems to have no effect in reducing friction and wear. The influence of mean agglomerate size, morphology and electron modification of PTFE powder can be investigated provided PTFE based compounds are produced with comparable bulk properties i.e. hardness and delta torque values.

4.2.3. PTFE micropowder filled EPDM

In previous chapters, properties and characterization of L100X PTFE powder and their corresponding EPDM vulcanizates has been discussed. In the following section, two conventional irradiated PTFE micropowders designated as Zonyl[®] MP1100 and Zonyl[®] MP1200 in EPDM are incorporated and properties investigated for 10, 20 and 30 phr PTFE loading. The reason for studying properties of PTFE micropowders in EPDM is two folds. First, PTFE micropowders have properties not only different than L100X PTFE powder but also from one another. This helps in investigating the effects of microstructure morphology, dispersion and surface activities of different PTFE powders on friction, wear and physical properties provided vulcanizates are produced with comparable bulk properties or hardness greater than the critical threshold. Beside this, the second aim of the present study is concerned with the potential use of variety of commercial PTFE micropowders in rubber compositions.

4.2.3.1. Physical and dynamical mechanical properties

Figure 54 shows the tensile strength, elongation at break and hardness Shore A of MP1100-EPDM and MP1200-EPDM as a function of PTFE loading. The horizontal line indicates EPDM gum.

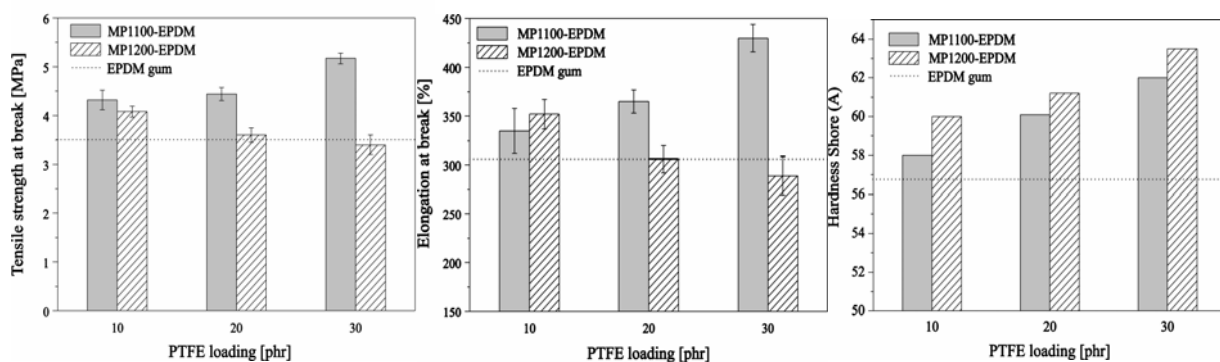


Figure 54. Tensile strength, elongation at break and hardness values of EPDM gum and PTFE-EPDM vulcanizates as a function of PTFE loading

With increasing PTFE loading, tensile strength increased of MP1100 gradually increased while for MP1200-EPDM it decreased. MP1100-EPDM showed the highest tensile strength at break in comparison to MP1200-EPDM and EPDM gum for all PTFE loadings. With

increasing PTFE loading the elongation at break increased for MP1100-EPDM while MP1200-EPDM showed poor elongation behaviour. Even at 30 phr micropowder loading, both elongation and tensile strength at break of MP1200-EPDM remained lower than EPDM gum. On the other hand MP1100-EPDM showed a systematic increase both in tensile strength and elongation at break. The hardness of both MP1100-EPDM and MP1200-EPDM increased with the PTFE loading. MP1200-EPDM showed a similar increment in hardness than MP1100-EPDM for each PTFE loading while EPDM gum showed the lowest hardness.

The variations in tensile strength and elongation at break between MP1100-EPDM and MP1200-EPDM are due to the comparatively higher radical concentration and surface area of MP1100 in comparison to MP1200 as shown in Table 7. Tensile strength and elongation at break of MP1100-EPDM increased due to the availability of excessive radicals for coupling with EPDM per surface area of the PTFE micropowder. The higher the concentration of radicals generated due to electron irradiation, higher the degree of coupling of the smaller PTFE radicals with EPDM due to high surface area. In case of MP1200, bigger micropowder particles having lower surface area resulted in significantly lower physical properties such as tensile strength and elongation at break. The concentration of accessible radicals at the surface of MP1200 is also lower, therefore a lower coupling degree and a comparatively insufficient compatibility with EPDM matrix is expected.

Table 7. Characteristics of PTFE micropowder

PTFE powder properties	MP1100* Emulsion	MP1200* Suspension
Polymerization process	500	500
Irradiation doses [kGy]	4	3
Mean particle size, x_{50} [μm]	7-10	1.5-3
Specific surface area [g/m^2]	7-10	1.5-3
Radical concentration [spin nr/g]	$1.29 \cdot 10^{18}$	$8.15 \cdot 10^{17}$

*commercially irradiated PTFE micropowder

Figure 55 shows the tan delta (E''/E') behaviour of EPDM gum and 30 phr PTFE filled EPDM vulcanizates as a function of temperature. The glass transition temperature (T_g) of -37°C was observed for all the vulcanizates. T_g was not influenced by the addition of PTFE micropowder in EPDM. However, the peak-height of tan delta reduced in case of micropowder filled EPDM in comparison to EPDM gum. MP1200-EPDM showed the lowest

peak-height at the T_g . However above T_g , it increased for MP1200-EPDM at a cross-over temperature of -10°C in comparison to MP1100-EPDM and EPDM gum. In filled system peak-height of tan delta is always lower or equivalent than unfilled system (pure gum) because of the restricted mobility of polymer chains due to the presence of fillers. The presence of filler results in varying tan delta peak-heights due to different polymer-filler interaction.

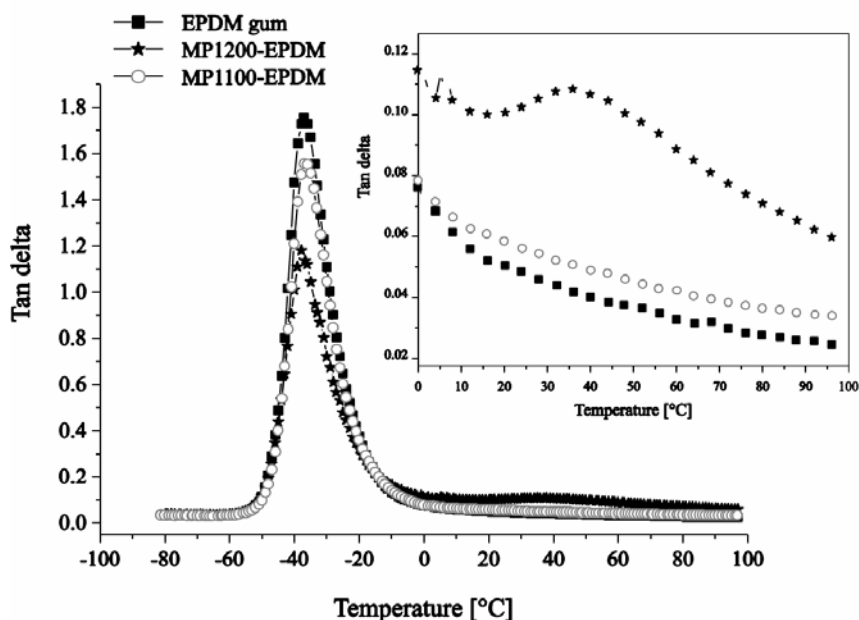


Figure 55. Tan delta behaviour of EPDM gum and 30 phr PTFE micropowder filled EPDM vulcanizates as a function of temperature

Similar is the case in MP1200-EPDM and MP1100-EPDM which depending on their characteristic morphologies and surface activities result in lower tan delta peak-height in T_g zone. In the glassy state the solid granular morphology of MP1200 in EPDM matrix results in higher E' and, consequently, low tan delta peak-height is observed due to restricted mobility of polymer chains. However, above T_g in rubbery region it shows higher tan delta due to its significantly lower compatibility and interaction with EPDM as compared to MP1100-EPDM vulcanizates. Figure 55 also shows the magnified tan delta curves of the compounds from 0°C to 100°C where EPDM gum and MP1100-EPDM have lower tan delta in comparison to MP1200-EPDM. Further, there is a significant difference above 20°C in tan delta behaviour of MP1200-EPDM compared to EPDM gum and MP1100-EPDM.

Above 20°C , MP1200-EPDM increased with temperature and attained a maximum around 37°C followed by a decrease. This upturn in tan delta behaviour of MP1200-EPDM is not observed in EPDM gum and MP1100-EPDM. The main reason for this unique behaviour observed in MP1200-EPDM is not clear and is beyond the scope of current investigation.

However, it is known that radiation-induced changes in PTFE result in unique relaxation processes over a wide range of temperatures [121]. This particular trend in MP1200-EPDM above T_g in rubbery region could be attributed to configurationally changes in the crystallites due to irradiation modification of MP1200 PTFE powder. Since higher tan delta describes higher amount of energy dissipation, different modes of friction and wear behaviour is expected for PTFE-EPDM vulcanizates filled with micropowder having unique dynamic mechanical behaviour.

4.2.3.2. Microstructure and dispersion analysis

Figure 56 shows the microstructure morphology of MP1100 and MP1200 (left hand side) and their corresponding cryogenic fractured blends (right hand side). As is evident from SEM micrographs, the agglomerate microstructure of the two different PTFE micropowders and the surface features of cryogenic fractured surfaces are apparently distinguishable from each other. MP1100 shows cloud-like structures formed randomly by the re-agglomeration of primary PTFE particles. MP1100 produced by emulsion polymerization is a coagulated dispersion that is often referred to as fine-powder or PTFE dispersion. On the other hand MP1200, a solid densely compact agglomerate with rounded morphology is a granular resin produced by suspension polymerization.

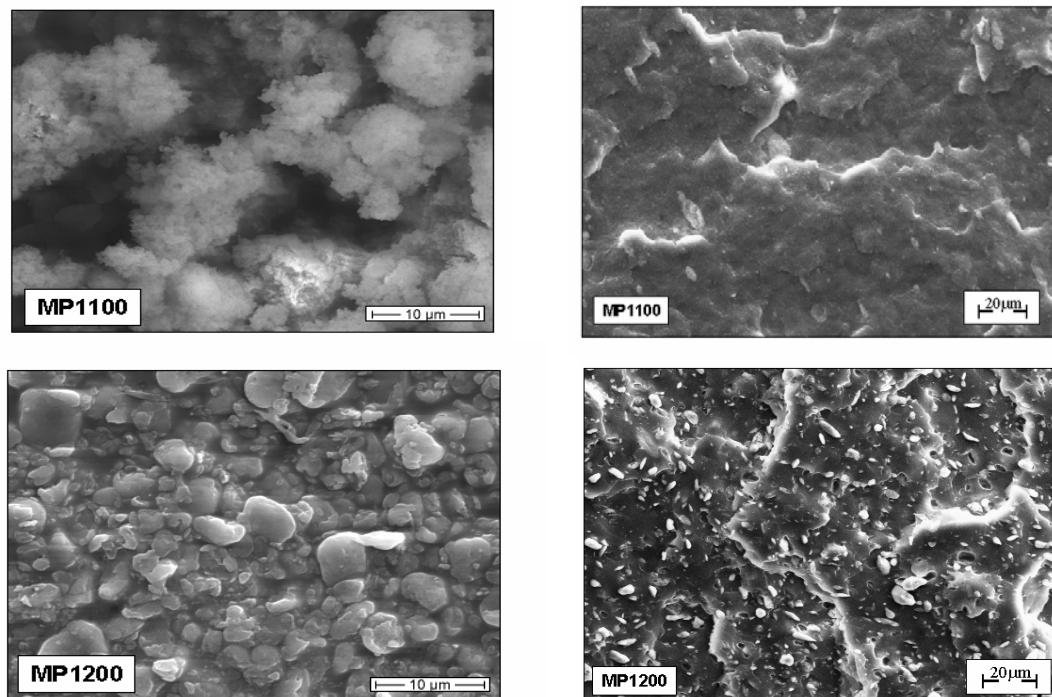


Figure 56. SEM micrographs of the PTFE powder (left hand side) and their corresponding 30 phr PTFE micropowder filled EPDM vulcanizates (right hand side)

Cryofractures investigations of the micropowder filled vulcanizates will direct their mutual interaction with EPDM matrix. As can be seen, MP1100-EPDM has smooth surface profile with particles embedded and homogeneously dispersed in EPDM while MP1200-EPDM show an uneven, coarse surface having small vacuoles and large PTFE particles lying on the fractured surface. This indicates that in case of MP1200-EPDM the particles are being pulled out of the matrix on application of stress. This indicates the poor compatibility of the MP1200 with EPDM as mentioned earlier. This is also due to the difficulty in processing and breaking down of granular structure in EPDM matrix during processing. The fine dispersion of MP1100 is due to its unique morphology and higher active surface (radical concentration) both of which helped to enhance its degree of dispersion and compatibility with EPDM. MP1200 lack both homogeneous dispersion and compatibility owing to its non-conductive micro-structural morphology and insufficient radical concentration for coupling with EPDM. Although, MP1100 powder tends to form agglomerated clumps as shown in Figure 56, they could be easily de-agglomerated and simultaneously dispersed during shear processing or blending operation. This can be seen clearly in Figure 57 which show SEM micrographs of MP1100-EPDM at higher magnification. It shows the presence of fully embedded de-agglomerated particles having particle size even less than 0.5 μm . This also indicates that MP1100 has a homogeneous particle size distribution. MP1200 on the other hand show huge segregated agglomerates in the matrix.

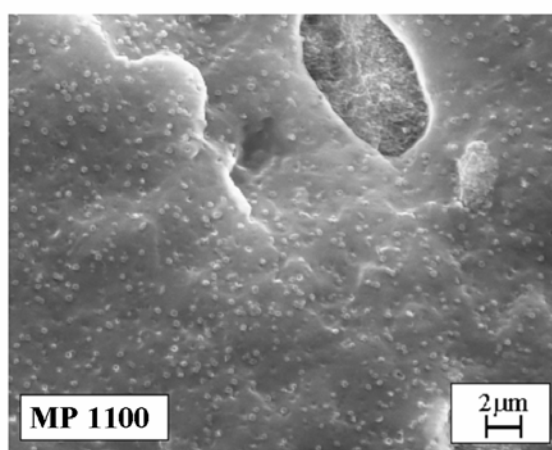


Figure 57. SEM micrographs of MP1100-EPDM vulcanizates at higher magnification

4.2.3.3. Friction and wear properties

The initial friction coefficient (μ_{initial}), steady state final friction coefficient (μ_{final}) and the specific wear rate (k) of EPDM gum and 30 phr PTFE filled EPDM vulcanizates are shown in Figure 58. After a testing time of $t_B = 2$ h, both EPDM gum and MP1100-EPDM attained a similar steady state final friction coefficient values while MP1200-EPDM showed the lowest value. The two important variations in the bulk properties are evident in hardness (Figure 54) and tan delta behaviour (Figure 55). These characteristic bulk properties influence the friction coefficient both at the beginning (μ_{initial}) and later stages (μ_{final}). With decreasing hardness the material becomes softer and μ_{initial} is increased due to plastic deformation in the contact region with counter-surface asperities. EPDM gum with the lowest hardness shows the highest μ_{initial} followed by MP1100-EPDM while MP1200-EPDM with its highest hardness exhibited lower μ_{initial} . Variations in bulk properties are also influenced by specific compatibility of PTFE micropowder with EPDM. Due to enhanced compatibility as in the case of MP1100 the particles are usually surrounded by EPDM as shown in Figure 56 and 57. For MP1100-EPDM, μ_{initial} is increased due to the sliding contact of the counter-surface with EPDM surface. However, MP1200 are less-compatible entities physically embedded in the vulcanizate surface. During sliding contact, the particles interact directly with counter-surface, thereby reducing friction coefficient. This could also lead to the formation of PTFE transfer film on counter-surface which further helps to reduce friction coefficient significantly.

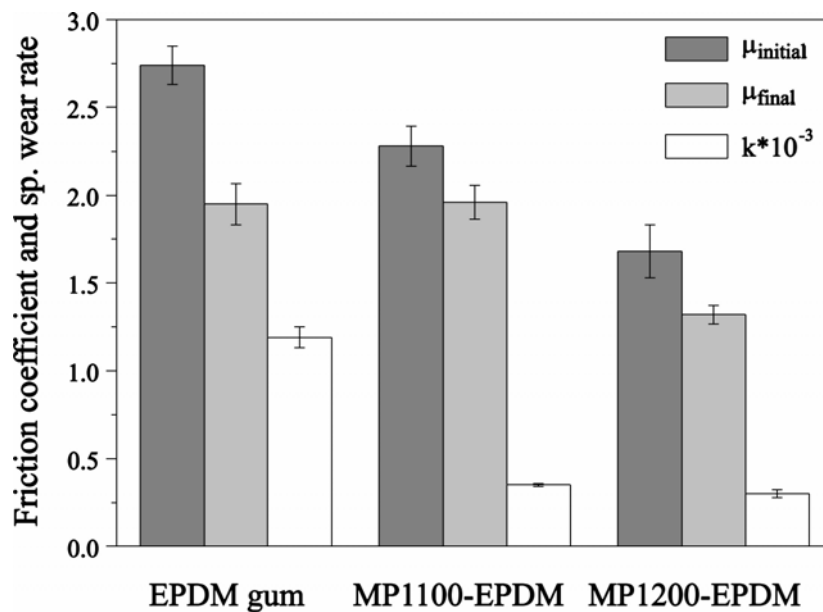


Figure 58. Friction coefficient and specific wear rate of 30 phr PTFE micropowder filled EPDM

The other factor influencing friction behaviour is the heat dissipation during cyclic loading as shown in Figure 55. The tan delta value characterizes the energy dissipation due to internal friction in these compounds. The energy is dissipated when counter-surface exert oscillating forces on elastomer surface. It is interesting to observe that EPDM gum and MP1100-EPDM have lower tan delta values than MP1200-EPDM but shows high friction value than MP1200-EPDM. This suggests that the mode of friction mechanisms were different in these compounds. In case of MP1200-EPDM, the higher hardness may have reduced friction coefficient. However, in case of EPDM gum and MP1100-EPDM the mode of deformation was mainly due to plastic deformation. The vulcanizate hardness is also correlated with specific wear rate.

It can be seen that specific wear rate decreases with increasing hardness. Both MP1100 and MP1200 filled EPDM have almost similar and comparable wear rate because of significantly higher hardness of vulcanizates. Both have hardness higher than the threshold determined for L100X PTFE powder filled EPDM vulcanizates in section 4.2.2. This suggests that different parameters are influencing specific wear rate of these compounds. High wear resistance of MP1200-EPDM is due to the presence of more inert particles. They are firmly embedded on the surface and preferentially interact with the load of counter-surface. The uncovered particles itself are exposed to counter-surface during sliding rather than exposing soft EPDM. However, in case of MP1100-EPDM the decrease in specific wear rate could be due to its comparatively high hardness and lower mechanical energy dissipation. EPDM gum having the lowest hardness results in higher wear rate. Depending on hardness, modulus and tan delta behaviour, different mechanisms including plastic deformation and successive mechanical energy dissipation seem to have been involved in the wear of these compounds.

Wear scar analysis

SEM analyses shown in Figure 59 were performed on the wear scars of (a) EPDM gum (b) MP1100-EPDM (c) MP1200-EPDM vulcanizates. As can be seen, depending on bulk properties, the vulcanizate surfaces experienced different modes of wear. EPDM gum suffered from severe wear while micropowder filled EPDM having similar and low specific wear rate resulted in minor wear. EPDM gum shows a characteristic failure mode caused by the absence of PTFE micropowder. EPDM gum failed due to the detachment of solid material from the surface by an adhesive mechanism with the counter body. In case of micropowder filled EPDM, the wear mechanism is completely different from EPDM gum and from one another. One can observe that the wear-surfaces of both the vulcanizates are different from

each other. MP1200-EPDM showed many smaller vacuoles in the surface while MP1100-EPDM has relatively smooth surface with few big craters formed due to the detachment of significantly large agglomerates. MP1200 are comparatively uncovered particles dispersed as solid rigid bodies in EPDM. Being less compatible they are not fully covered by EPDM molecules. The binding of MP1200 agglomerates is due to the strong physical locking in the EPDM matrix making it difficult for counter-surface to remove during sliding. The surface of MP1100-EPDM is smooth compared to MP1200-EPDM. The particles seem to have been fully embedded in matrix indicating both enhanced dispersion and compatibility. The coupled EPDM concentration at MP1100 surface is much higher than at MP1200 surface.

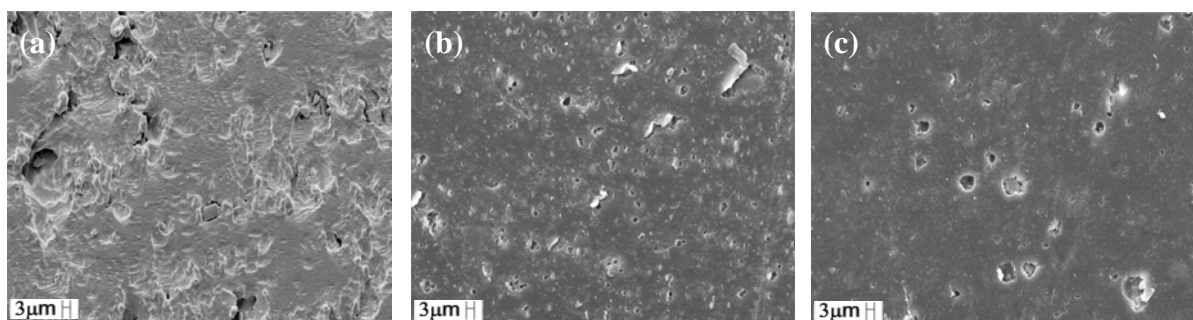


Figure 59. Wear scar micrographs of (a) EPDM gum, (b) MP1200-EPDM and (c) MP1100-EPDM

4.3. Electron beam crosslinked PTFE-EPDM

The present study focuses on using electron irradiation instead of peroxide for crosslinking of EPDM filled with 30 phr L100X (0 kGy), L100X (500 kGy), MP1100 and MP1200. Since ΔM and hardness both influences the friction and wear properties, therefore, PTFE filled EPDM vulcanizates should be produced with hardness higher than the critical value of 58 Shore (A). With the help of electron irradiation for crosslinking, the effect of radiation-induced changes in PTFE powder on peroxide crosslinking of EPDM is significantly reduced. Therefore, any substantial changes in hardness values at a specific crosslinking irradiation dose should arise solely from the PTFE powder itself. The vulcanizates have been produced in a specific and controlled manner so that the influence of morphology, dispersion and surface activity of different PTFE powders on physical and especially on friction and wear properties could be realized. These investigations are of significant importance regarding the application of PTFE powder in rubber compounds.

4.3.1. Characterization with respect to chemical coupling

Optimization of crosslinking dose

In order to investigate the effect of morphology, dispersion and chemical coupling, the vulcanizates should have hardness higher than the critical value of 58 Shore (A). Peroxide crosslinking of PTFE filled EPDM compounds containing electron modified PTFE powder is strongly influenced by the irradiation-induced changes in PTFE powder. Hardness of PTFE filled EPDM vulcanizates vary according to absorbed dose of PTFE powder. For this reason, EPDM has been crosslinked using electron irradiation in order to suppress this undesired effect on vulcanizate's hardness. The dose for irradiation crosslinking was determined relative to the required hardness values of PTFE filled EPDM compounds. This was achieved by monitoring the influence of crosslinking dose on the hardness. Figure 60 shows the influence of absorbed dose on hardness of EPDM rubber and PTFE filled EPDM vulcanizates. It can be seen that the optimum dose for crosslinking of EPDM rubber amounts to about 80 to 120 kGy. Above 120 kGy, hardness decreases due to chain scission of EPDM. However, in the presence of PTFE powder, hardness of PTFE filled EPDM vulcanizates increases as expected.

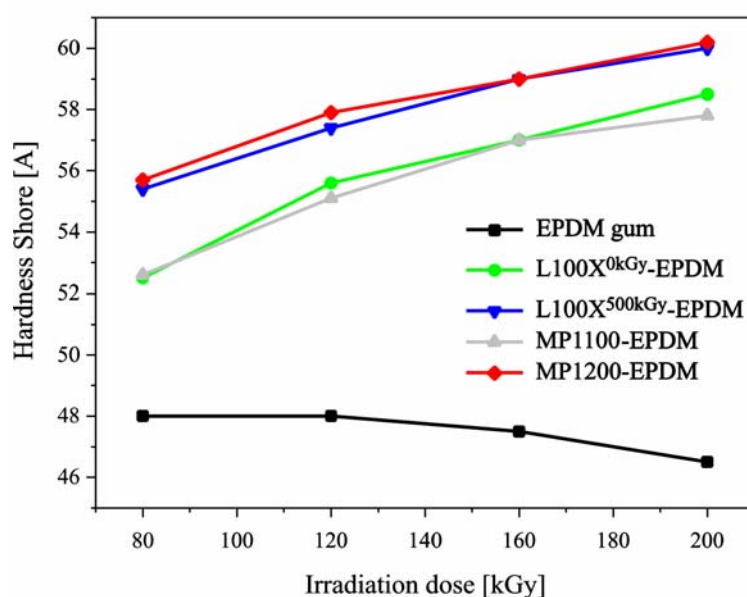


Figure 60. Comparison of hardness values of EPDM gum and PTFE filled EPDM compounds as a function of crosslinking irradiation dose

L100X^{500kGy}-EPDM and MP1200-EPDM show the highest while L100X^{0kGy}-EPDM and MP1100-EPDM show the lowest hardness. This behaviour is in contradiction to that observed in peroxide-induced crosslinking of L100X^{500kGy}-EPDM. It suggests that the variation in hardness of different composites at any specific absorbed dose results from differences in the

chemical coupling between PTFE powders and EPDM. This can be clearly seen in the different hardness values of L100X^{0kGy}-EPDM and L100X^{500kGy}-EPDM. However, at an optimum crosslinking dose of 200 kGy all of the PTFE filled EPDM vulcanizates attained the required minimum hardness value of 58 Shore (A).

Physical and dynamic mechanical properties

The effects of PTFE powders on mechanical properties of PTFE filled EPDM vulcanizates are shown in Figure 61. As expected modified PTFE filled EPDM vulcanizates compared to non-modified (L100X^{0kGy}-EPDM) shows enhanced properties. There is no significant variation in tensile strength and elongation at break values of the modified PTFE filled EPDM vulcanizates. However, L100X^{500kGy}-EPDM shows the highest M100 and M200 followed by MP1200-EPDM and MP1100-EPDM while L100X^{0kGy}-EPDM (horizontal broken lines) shows the lowest. M200 was not achieved by L100X^{0kGy}-EPDM. This reinforcement effect in case of L100X^{500kGy}-EPDM is due chemical coupling of PTFE powder with EPDM. The effect of reinforcement can also be seen in the dynamic mechanical properties.

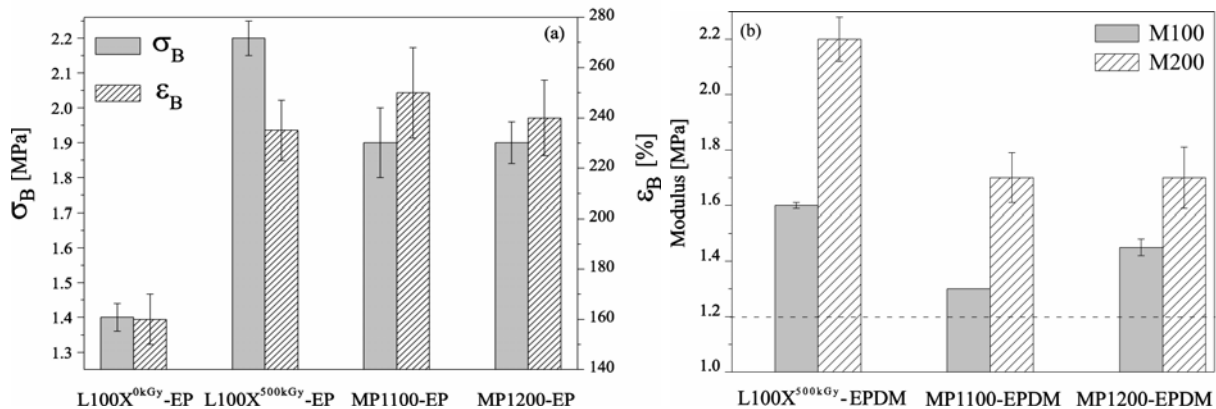


Figure 61. Tensile strength at break & elongation at break (a); modulus, M100 and M200 (b). The horizontal broken lines indicate M100 of L100X^{0kGy}-EPDM

Figure 62 shows tan delta curves of the corresponding PTFE filled EPDM vulcanizates as a function of temperature. As can be seen the glass transition temperature (T_g) is only slightly influenced by addition of different PTFE powders to EPDM. The peak-height increases from MP1200-EPDM to L100X^{500kGy}-EPDM and reaches the maximum value for L100X^{0kGy}-EPDM and MP1100-EPDM. L100X^{0kGy}-EPDM, MP1100-EPDM and MP1200-EPDM show similar T_g of about -38°C whereas L100X^{500kGy}-EPDM has a higher T_g value of about -35°C. This shift in T_g to higher temperature is due to the restricted mobility of the polymer chains.

Figure 62 also shows the magnified tan delta curves of the compounds in the temperature range of friction and wear testing where L100X^{500kGy}-EPDM shows the lowest tan delta while L100X^{0kGy}-EPDM and MP1100-EPDM shows similar behaviour at slightly higher level. The up turn in tan delta behaviour of MP1200-EPDM could be due to the relaxation processes associated with the radiation-induced effects on crystallites structure of PTFE powder.

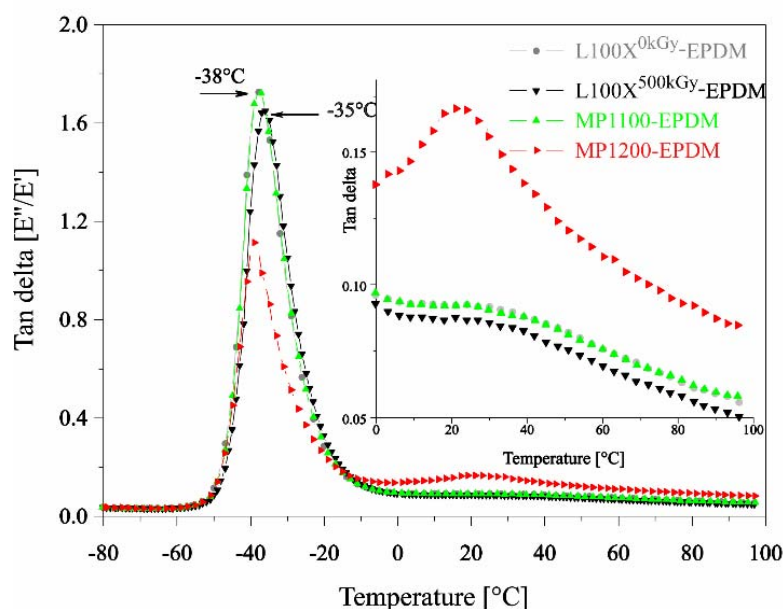


Figure 62. Tan delta behaviour of the vulcanizates as a function of temperature

Compatibility and dispersion

Figure 63 shows the FTIR spectra of PTFE powders. The relative concentration of C=O groups have been determined in the region 1840-1740 cm^{-1} . It can be seen that C=O concentration varies in different PTFE powders. L100X^{0kGy} PTFE powder shows no while L100X^{500kGy} PTFE powder shows the highest concentration of C=O groups. Both MP1100 and MP1200 being three times less compared to that of L100X^{500kGy} PTFE powder have almost similar C=O concentration. Higher C=O concentration in case of L100X^{500kGy} PTFE powder suggests significantly lower contact angle or higher wettability. Lower contact angle corresponds to higher surface energy and enhanced interaction with polar compounds such as water (as shown in section 4.1). However, the enhanced compatibility of irradiated PTFE and EPDM cannot be explained by the presence of these functional groups since EPDM being a non-polar compound does not interact via polar or H-bonding forces. The other influencing factor is the relative concentration of persistent free radicals trapped in the crystalline structure at the surface of irradiated PTFE powders. The radicals affect the properties through radical coupling with the unsaturation in rubber compound. The overall (bulk and surface)

radical concentration of PTFE powders normalized to L100X^{500kGy} PTFE powder (100 %) suggest that MP1100 has the highest (125.6 %) while MP1200 (56.3 %) indicates the lowest radical concentration. However, the degree of chemical coupling might also depend on the amount of radicals available on the surface of PTFE agglomerates for chemical coupling with EPDM. In such case the surface to available radical concentration is of significant importance.

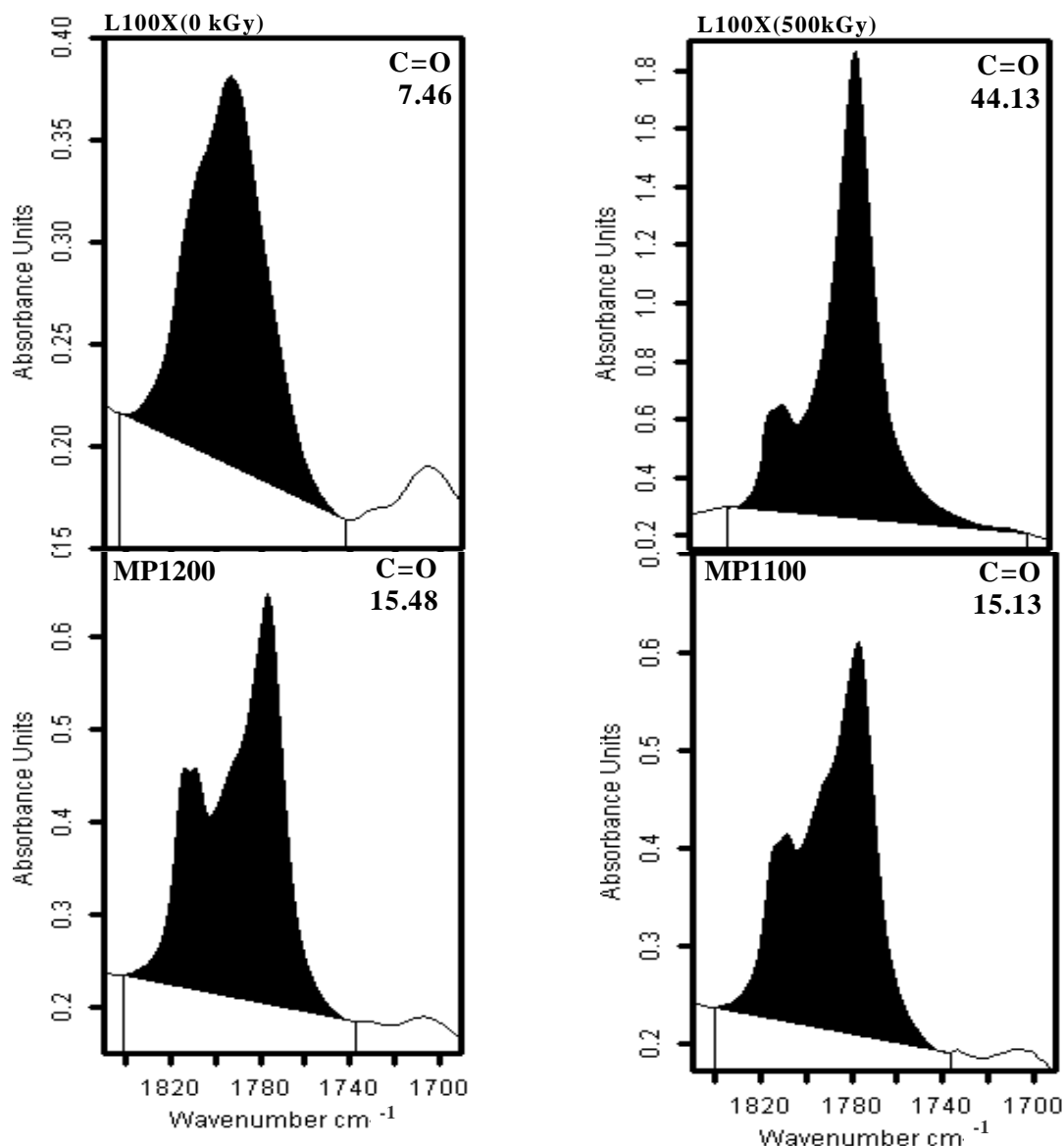


Figure 63. Relative concentration of C=O groups of PTFE powders determined by integrating area under the curve

Figure 64 shows the scanning micrographs of PTFE filled EPDM vulcanizates. It can be seen that L100X^{0kGy}-EPDM demonstrates poor compatibility and dispersion. It shows bigger agglomerates with poor dispersion behaviour in EPDM. This is due to the highly inert and

hydrophobic surface of PTFE powder which lacks interaction and chemical compatibility. For this reason PTFE powder is modified with electron irradiation in order to enhance simultaneously its poor wetting and dispersion characteristics. This can be seen in the enhanced dispersion behaviour of L100X^{500kGy} PTFE powder in EPDM matrix.

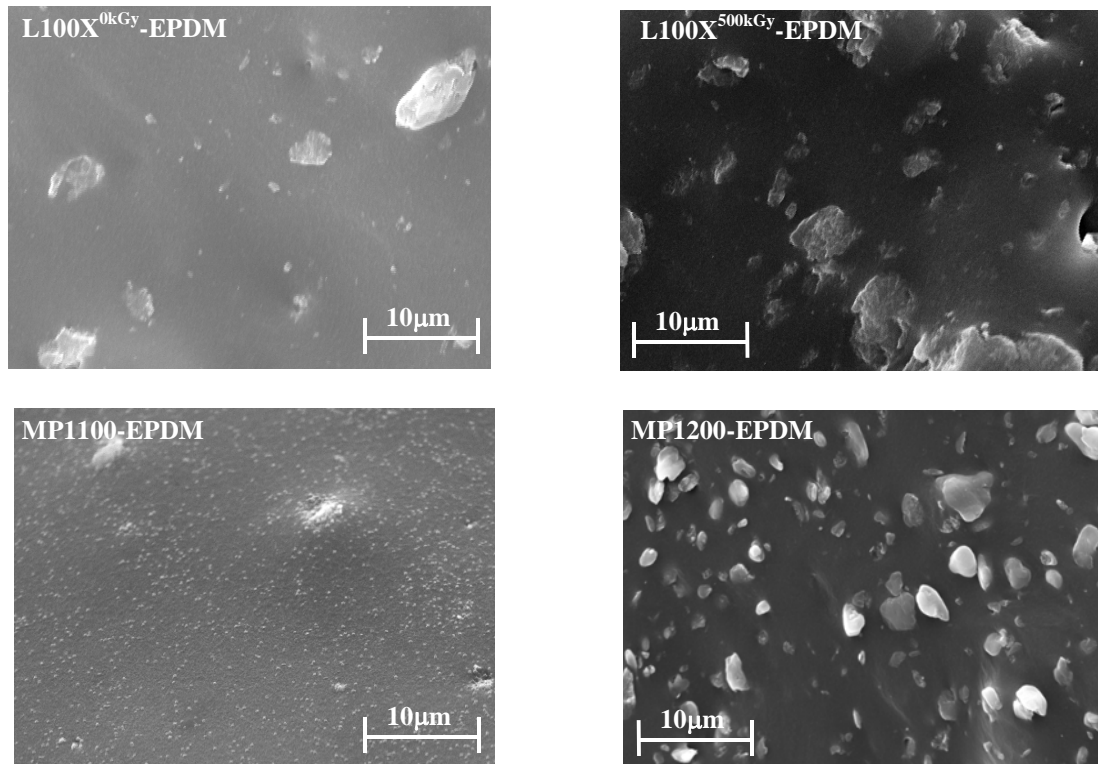


Figure 64. Scanning micrographs of the cryogenically fractured surfaces showing PTFE morphology and dispersion in EPDM

The enhanced compatibility due to the chemical coupling by radical mechanism helps in de-agglomeration and dispersion of PTFE agglomerates during the reactive processing. Grafted EPDM chains on the surface of PTFE particles interact with the EPDM matrix and as such extensive shearing and de-agglomeration provides new active sites for chemical coupling with the olefinic unsaturated diene of EPDM. This help in reinforcement and simultaneously improvement in properties of L100X^{500kGy}-EPDM as shown in Figure 61 and 62. MP1100 shows the most excellent dispersion amongst the PTFE powders investigated. This is mainly due to the ability of this special grade of PTFE powder to de-agglomerate to its primary particle size of 0.2 µm. Both MP1100 and L100X^{500kGy} PTFE powders are embedded firmly in EPDM matrix. However, L100X grade is difficult to disperse uniformly compared to MP1100 even though both are produced by emulsion polymerization. On the other hand MP1200 PTFE powder having solid morphology are difficult to de-agglomerate even under

high shearing. One can observe that MP1200 agglomerates are pulled out of EPDM on application of stress. This clearly indicates the lower degree of compatibility of the bigger MP1200 agglomerates. The surface of EPDM indicates the presence of many PTFE particles. This clearly shows the difficulty in obtaining uniform dispersion of MP1200 in EPDM matrix.

4.3.2. Characterization of friction and wear properties

Friction behaviour

Figure 65 shows the friction behaviour of PTFE filled EPDM vulcanizates sliding against a hard spherical ball. The friction curves demonstrate that the friction coefficients of all vulcanizates decrease during the course of testing. The friction coefficient values decrease from initial to the final friction values within a range of 4 % to 100 %. As can be seen the vulcanizates show different behaviour both at the beginning and during the course of testing time. MP1100-EPDM shows the highest friction values compared to all other compounds. Moreover, a sudden decrease in initial friction coefficient is observed for all compounds except for MP1100-EPDM. After a steady state is achieved, friction coefficient of MP1200-EPDM and L100X^{0kGy}-EPDM remains almost constant up to the end of measurements. On the contrary, MP1100-EPDM shows a gradual decrease in friction coefficient. This behaviour can be approximated by a linear function with a negative slope.

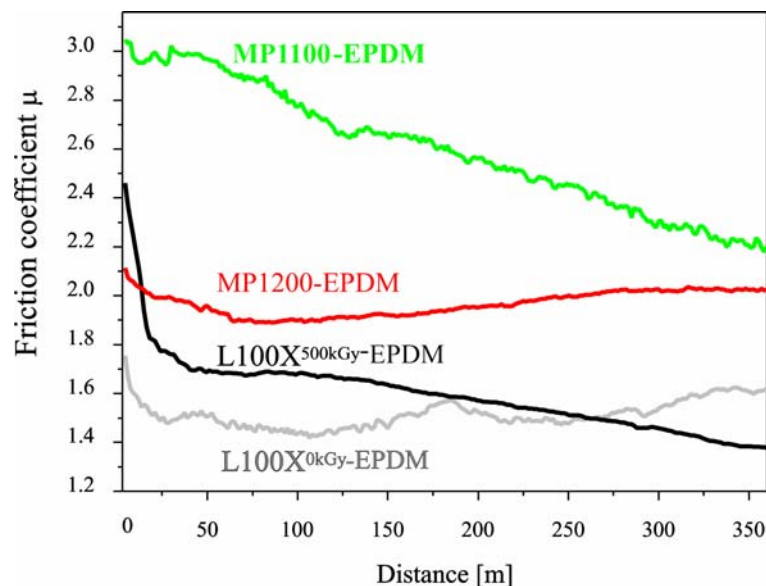


Figure 65. Comparison of the friction behaviour of PTFE-EPDM composites as a function of sliding distance

Similarly, L100X^{500kGy}-EPDM shows the same behaviour after steady state condition has been achieved. However, the slope is less compared to MP1100-EPDM. This clearly shows

the influence of PTFE powders on friction behaviour of EPDM matrix. The higher friction values of MP1100-EPDM could be due to the direct interaction of the counter-body with EPDM. As can be seen in Figure 64, surface of MP1100-EPDM is the smoothest of all the investigated compounds due to its enhanced compatibility and excellent dispersion. There is almost no indication of PTFE particles on the surface. Only a few agglomerates are visible. Thus there is a rare possibility for MP1100 PTFE powders to form a transfer film during sliding contact with counter-body. This results in a significantly higher friction coefficient throughout the testing time. On the other hand, all other vulcanizates show significantly lower friction values. This is due to the presence of PTFE agglomerates on the surface which allows a direct interaction with the counter-surface once EPDM layer is removed. This can be clearly seen in the sudden decrease in friction coefficients shown in Figure 65. Moreover, a further decrease in case of L100X^{500kGy}-EPDM compared to L100X^{0kGy}-EPDM and MP1200-EPDM is observed. This could be due to the interaction of the embedded PTFE agglomerates in wear track of L100X^{500kGy}-EPDM with counter-body. This facilitates in easy sliding of the counter-body against a wear track covered with PTFE particles.

Wear behaviour

Figure 66 shows the specific wear rate (k) of PTFE filled EPDM vulcanizates. As can be seen, specific wear rate responded in accordance with friction behaviour. MP1100-EPDM with its significantly high friction coefficient suffered from higher wear rate.

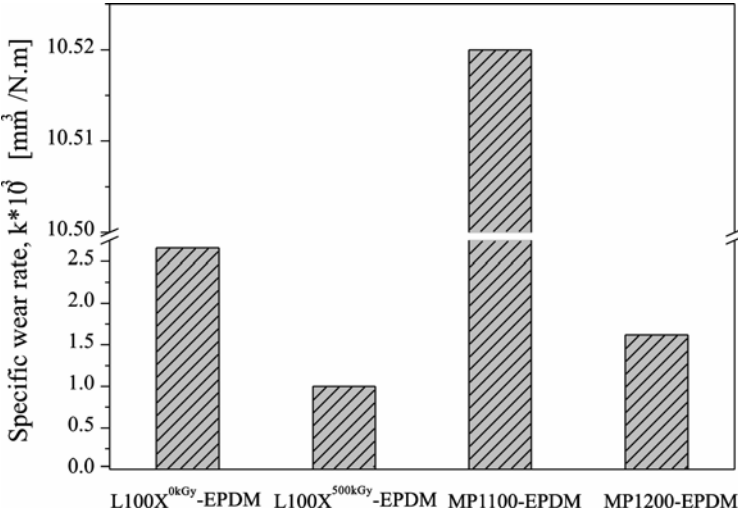


Figure 66. Comparison of the specific wear rate (k) of PTFE filled EPDM vulcanizates

Similarly, L100X^{0kGy}-EPDM and MP1200-EPDM having low friction coefficients show comparatively lower wear rates. Figure 67 shows scanning micrographs of the wear scars of

vulcanizates after repeated sliding of the counter-body. It can be seen that different wear mechanisms have occurred in vulcanizates.

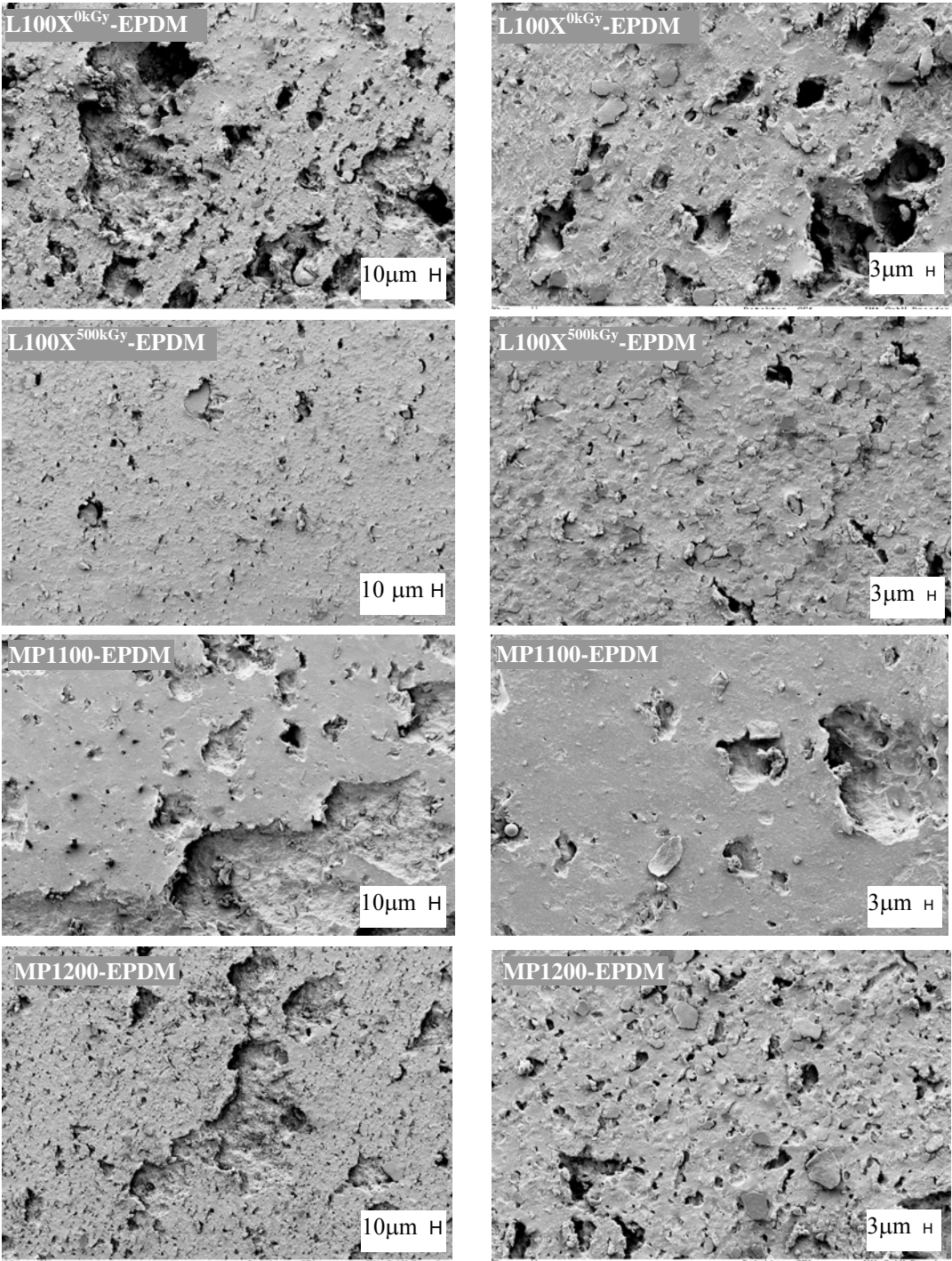


Figure 67. Scanning micrographs of wear track (contact area) showing the wear mechanisms involved in different PTFE-EPDM composites

In case of L100X^{0kGy}-EPDM, wear behaviour is characterized by the detachment of PTFE agglomerates from EPDM due to its significantly poor compatibility with EPDM. At higher magnification it also shows the presence of flattened agglomerates. This indicates that PTFE powder may have been transferred to the counter-surface. However, in case of L100X^{500kGy}-EPDM, the wear track is smooth. It shows the presence of significant amount of embedded PTFE agglomerates that have been flattened or abraded by repeated sliding of the counter-body. This is in accordance with the friction mechanism described before. The interaction of counter-body with PTFE agglomerates results in both the lowest wear rate and friction coefficient. In contradiction, MP1100-EPDM shows a rough wear track due to the detachment of significantly large lumps from the top of the surface. The wear mechanism is similar to the de-lamination type wear that has occurred in the deep regions of EPDM. At higher magnification one can observe that no PTFE agglomerates are visible for contact with counter-body. Thus almost no PTFE has been transferred to the counter-surface. MP1200-EPDM suffered from wear mechanism similar to MP1100-EPDM and L100X^{0kGy}-EPDM. A comparatively smaller lumps compared to MP1100-EPDM have been removed from the top of the surface. On the other hand, MP1200 being bigger and less compatible agglomerates have been removed from EPDM similar to L100X^{0kGy}-EPDM. One can observe the presence of these detached PTFE agglomerates on the wear track surface.

4.3.3. Conclusions

The specific interaction of different PTFE powders with EPDM as well as with the counter-surface (steel-ball) controls physical as well as friction and wear properties of PTFE filled EPDM vulcanizates. L100X^{500kGy}-EPDM shows improved physical, dynamic mechanical and tribological properties due to enhanced chemical compatibility that results from chemical coupling of L100X^{500kGy} PTFE powder with EPDM. The significant improvement in friction and wear properties results from the embedment of L100X^{500kGy} PTFE agglomerates in EPDM matrix. This enable the counter-surface in easy sliding against a wear track covered with embedded PTFE particles. The present investigation implies that friction and wear of PTFE filled EPDM vulcanizates beside other factors, is strongly influenced by PTFE dispersion, PTFE transfer film formation and the corresponding chemical interaction between PTFE powder and EPDM matrix. MP1100-EPDM vulcanizate shows significantly poor friction and wear properties but maintains excellent dispersion while MP1200-EPDM and L100X^{0kGy}-EPDM with comparatively improved friction and wear properties are characterized with poor dispersion and chemical compatibility of PTFE powder with EPDM.

4.4. Chemically coupled PTFE-CR compounds

It has been discussed previously in detail that chemical coupling of the PTFE powder is a prerequisite for effective use of PTFE powder in rubber matrixes. Chemical coupling enhances compatibility of PTFE powder and consequently results in better dispersion and ultimately in improvement of final properties of rubber compound. The following chapter discusses a new class of chemically coupled PTFE filled CR compounds. CR with its inherently outstanding properties (see section 2.6) is categorized as suitable for sealing and gaskets application. CR rubber being highly polar is sufficiently deactivated by electronegative chlorine atom so that the direct chemical coupling with PTFE powder by radical coupling mechanism is not possible. A new approach to the coupling reaction mechanism is proposed based on the Lewis acid concept which is also applicable to crosslinking of CR in the presence of MgO and ZnO. Chemical coupling between CR and modified PTFE is based on the availability of special structures in CR (olefinic unsaturated 3,4-chloroprene structure) and the functional groups in PTFE (carboxylic acid groups). Some new findings and results which have not been previously investigated for CR rubber are reported.

4.4.1. Structure-properties characterization

Figure 68 shows the curing curves of CR gum and PTFE-CR vulcanizates. Optimum curing time (t_{90}) and delta torque (ΔM) both increases with increasing irradiation dose of PTFE.

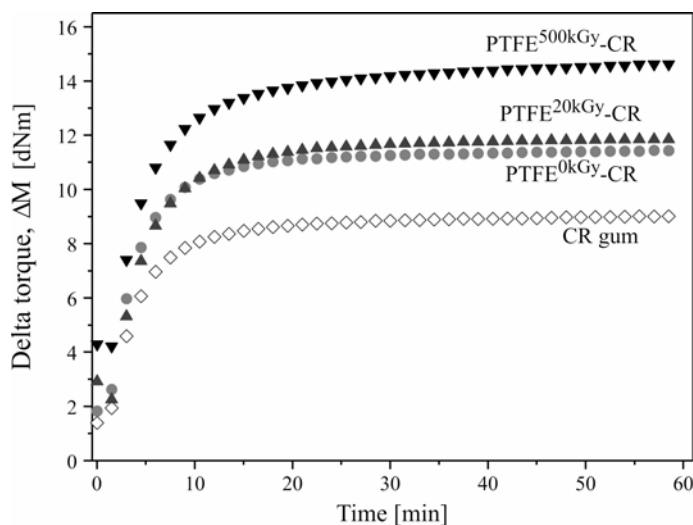


Figure 68. Rheographs of PTFE-CR vulcanizates in comparison with CR gum

This is an important observation because both of the parameters are related to the effect of radiation-induced changes on the state of cure and crosslinking density of CR rubber. t_{90} corresponding to the time required to reach 90% of the delta torque is a useful estimate of the over all cure rate. A higher t_{90} value corresponds to an extended curing time. It can be observed that ΔM values of PTFE-CR vulcanizates are higher than CR gum. However, ΔM increases with the use of increasing irradiation dose of PTFE powder in CR. PTFE^{500kGy}-CR shows the highest while CR gum shows the lowest. Amongst PTFE filled vulcanizates, PTFE^{0kGy}-CR shows the lowest. It should be noticed that ΔM is only a measure of an apparent crosslink density of compounds. It is beyond the scope of the present work to investigate the effective crosslink (physical and chemical). However, for a qualitative assessment it can be concluded that an apparent crosslink density increases or is influenced by the electron beam irradiation of PTFE powder. PTFE^{500kGy}-CR vulcanizate shows the highest ΔM and hence the highest apparent crosslink density. On the other hand PTFE^{0kGy}-CR shows lower ΔM than irradiated PTFE filled chloroprene vulcanizates.

A range of mechanical properties of PTFE-CR vulcanizates as a function of irradiation dose of PTFE powder in CR in comparison with CR gum are shown in Figure 69.

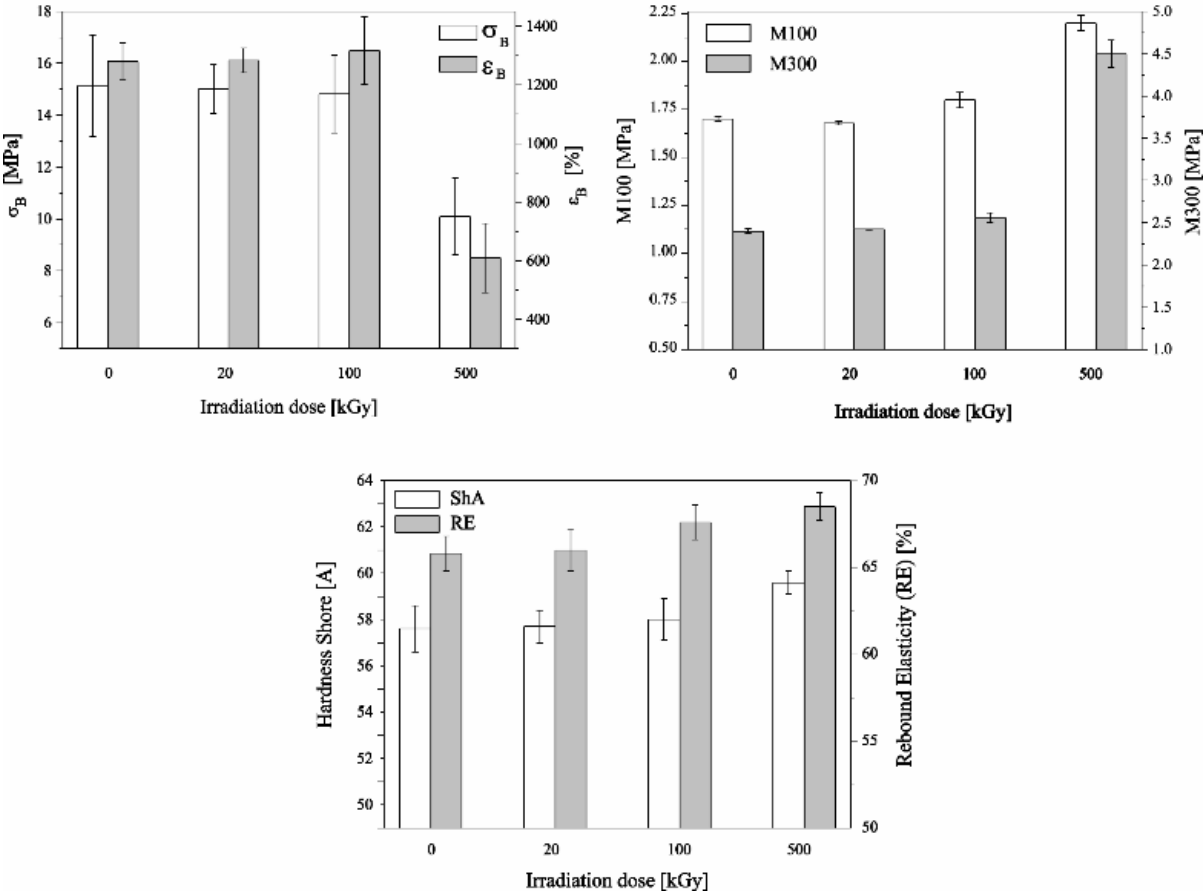


Figure 69. The effect of chemical coupling on mechanical properties of CR compounds

PTFE^{0kGy}-CR, PTFE^{20kGy}-CR and PTFE^{100kGy}-CR having the highest tensile strength (σ_B) and elongation at break (ϵ_B) shows similar values while PTFE^{500kGy}-CR shows even lower than CR gum ($\sigma_B = 11$ MPa, $\epsilon_B = 1210\%$). It can be seen that up to 100 kGy there is no influence of irradiation dose on σ_B and ϵ_B . However, for PTFE^{500kGy}-CR the influence is obviously significant. It shows the highest modulus, hardness and better rebound resilience. This improvement in the properties of PTFE^{500kGy}-CR is due to the highly active surface of PTFE powder which might have enabled in chemical coupling of PTFE powder with CR. With the use of increasing irradiation dose of PTFE powder these properties increases systematically. This indicates that electron beam irradiated PTFE powder in chloroprene provides reinforcement due to chemical coupling.

Other interesting features of elastomeric networks can be revealed using the plots of the reduced stress, $\sigma_{red} = \sigma / (\lambda - \lambda^{-2})$ against inverse extension ratio λ^{-1} . In this case σ is the nominal stress defined as the force divided by the undeformed cross-sectional area and λ is the extension ratio, defined as the ratio of deformed to the undeformed length of the sample stretched in the uniaxial direction as was shown in Figure 25. On plotting the reduced stress (σ_{red}) against inverse extension ratio (λ^{-1}), as shown in Figure 70, the curves obtained are found to be straight in the intermediate region. The intercept at y-axis (C_1), identified as the contribution arising from the chemical crosslinks is shown with dotted lines. For the studied compounds the value of C_1 varies according to the degree of chemical coupling between PTFE powder and chloroprene matrix. Figure 70a shows the comparison of the unfilled chloroprene rubber (CR gum) and chloroprene rubber filled with 10, 20 and 30 phr (parts per hundred of rubber) of non-irradiated PTFE powder. It can be seen that all curves at the y-axis intercept show a similar value of $C_1 \approx 0.22$ MPa. This signifies that non-irradiated PTFE powder is not chemically coupled to chloroprene matrix as expected for these two incompatible polymers. Additionally as the network chains are stretched, a considerable decrease in reduced stress is observed for all chloroprene vulcanizates. This effect is due to reduction in the effectiveness of entanglements due to slippage. At higher elongations, large and rather abrupt upturns in the reduced stress can be seen. This increase in reduced stress is attributed to the finite extensibility of the network chains and due to the induced crystallization of elastomer under stretching by molecular orientation at high strains.

Figure 70b shows the comparison of the C_1 values of PTFE^{0kGy}-CR, PTFE^{20kGy}-CR and PTFE^{500kGy}-CR for 30 phr PTFE loading. It is worthy to note that PTFE^{500kGy}-CR shows higher C_1 value than PTFE^{0kGy}-CR, while there is no influence on the chemical crosslink density of PTFE^{20kGy}-CR due to a significantly lower irradiation dose. However, the

C_1 contribution in the case of PTFE^{500kGy}-CR increases due to the formation of a higher number of chemical crosslinks PTFE powder and chloroprene matrix. The significant improvement in the mechanical and dispersion properties in case of PTFE^{500kGy}-CR is due to higher degree of chemical coupling.

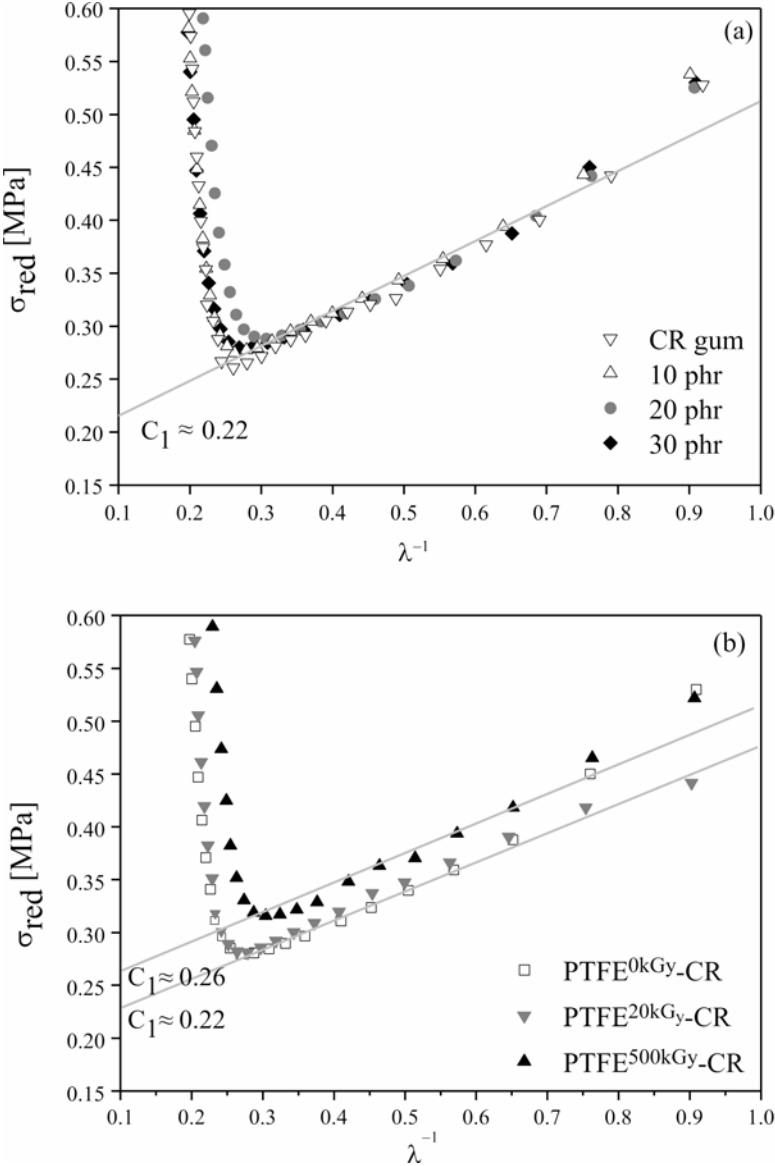


Figure 70. Mooney-Rivlin plots for the (a) chloroprene gum and non-irradiated PTFE filled chloroprene for 10, 20 and 30 phr loading and (b) comparison of PTFE^{500kGy}-CR with non-irradiated (PTFE^{0kGy}-CR) and low-irradiated (PTFE^{20kGy}-CR) for 30 phr PTFE loading

Figure 71 shows the storage modulus (E') and tan delta (E''/E') of CR gum and PTFE-CR vulcanizates as a function of temperature. The dependency of E' on the presence of irradiated PTFE in vulcanizates is obvious both in the glassy and magnified rubbery region. In the

glassy region, E' decreases with the use of increasing irradiation dose of PTFE powder in chloroprene. However, E' increases above glass transition temperature (T_g) in the rubbery region. This augmentation in E' with the use of increasing irradiation dose of PTFE powder in CR can be attributed to PTFE-CR interaction due to chemical coupling. This consistency of E' both at higher and lower temperature is important for elastomeric composites to be used in applications requiring dynamic mechanical properties to be less sensitive to temperature variations. The use of such elastomeric compositions is an important design criterion for automotive suspension systems which can maintain their dynamic characteristics both at low and higher temperature. The corresponding tan delta curves also show a shift in the T_g from -25.5°C for CR gum to -23°C for PTFE-CR vulcanizates. However, a slight decrease in the magnified tan delta peak-height can also be seen with the use of higher irradiation dose of PTFE powder in chloroprene. PTFE^{500kGy}-CR vulcanizate shows the lowest while CR gum shows the highest tan delta peak-height. This suggests that higher irradiated PTFE powder owing to the presence of concentrated functional groups acts as a highly active surface and strongly interacts with the matrix resulting in the lowering of tan delta peak-height. The shift in T_g to higher temperature and the decrease in peak-height of tan delta indicates that the

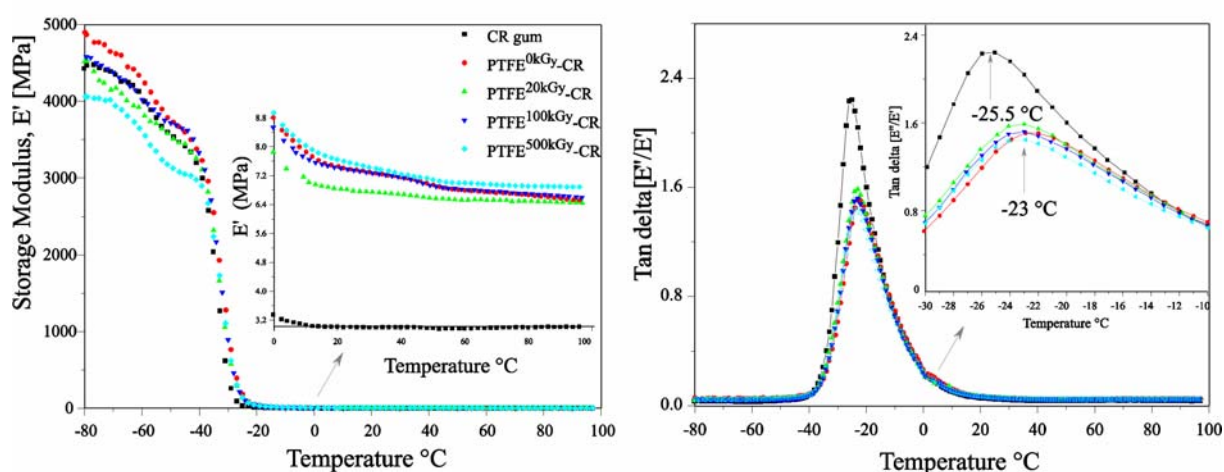


Figure 71. Storage modulus (E') and tan delta (E''/E') of PTFE filled CR vulcanizates in comparison with CR gum

4.4.2. Chemical coupling analysis

4.4.2.1. FTIR spectroscopy

Figure 72 shows the FTIR spectra of a) CR gum, b) 500 kGy PTFE powder, PTFE^{500kGy}-CR and PTFE^{0kGy}-CR compounds. The separation process of PTFE filled chloroprene rubber has

been described in Section 3. As can be seen in Figure 72a, for the CR gum, the characteristic CH-stretching vibrations occur at 3023, 2917 and 2843 cm^{-1} , while the bending vibration can be seen at 1443 and 1430 cm^{-1} . Peaks at 1693 and 1660 cm^{-1} indicate the stretching of the C=C double bonds in the chloroprene matrix. On comparison between 500kGy PTFE powder and its PTFE^{500kGy}-CR blend, as shown in Figure 72b, a significantly stronger chloroprene absorption band in the region 1660 cm^{-1} due to the stretching of the C=C bond in chloroprene is observed.

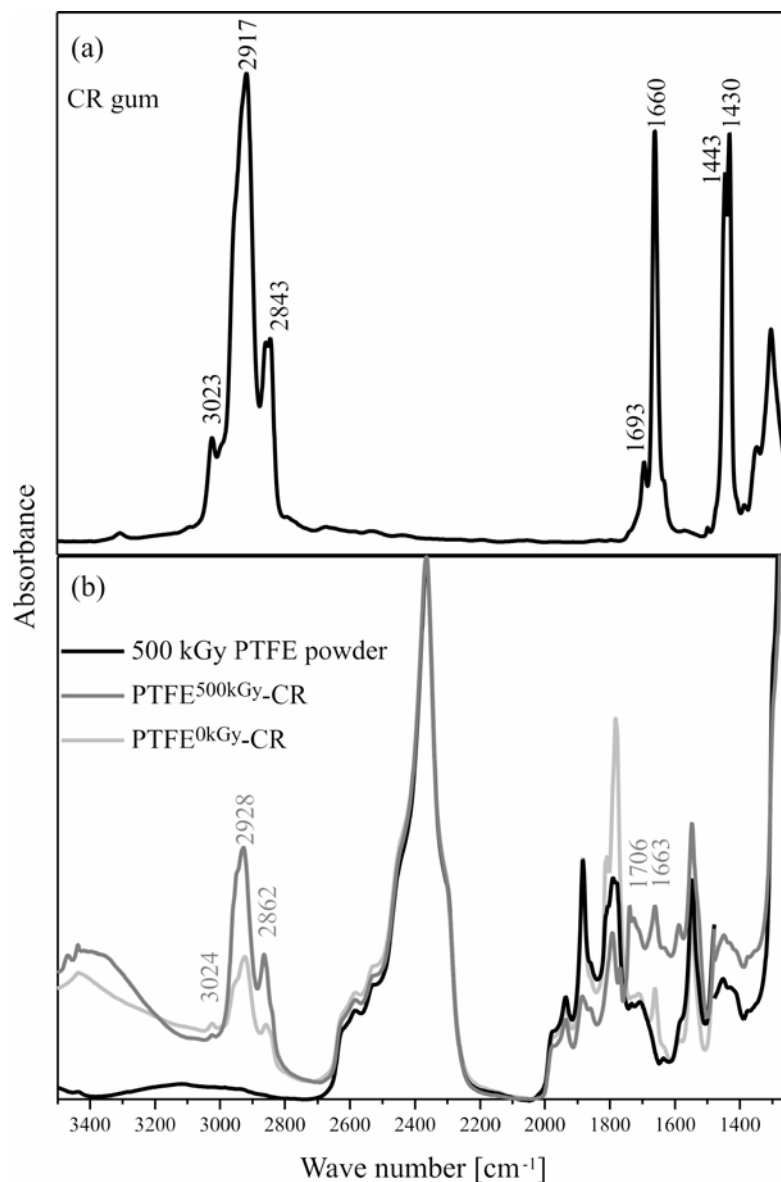


Figure 72. FTIR spectra of a) CR gum, b) 500kGy PTFE powder, PTFE^{500kGy}-CR and PTFE^{0kGy}-CR blend.

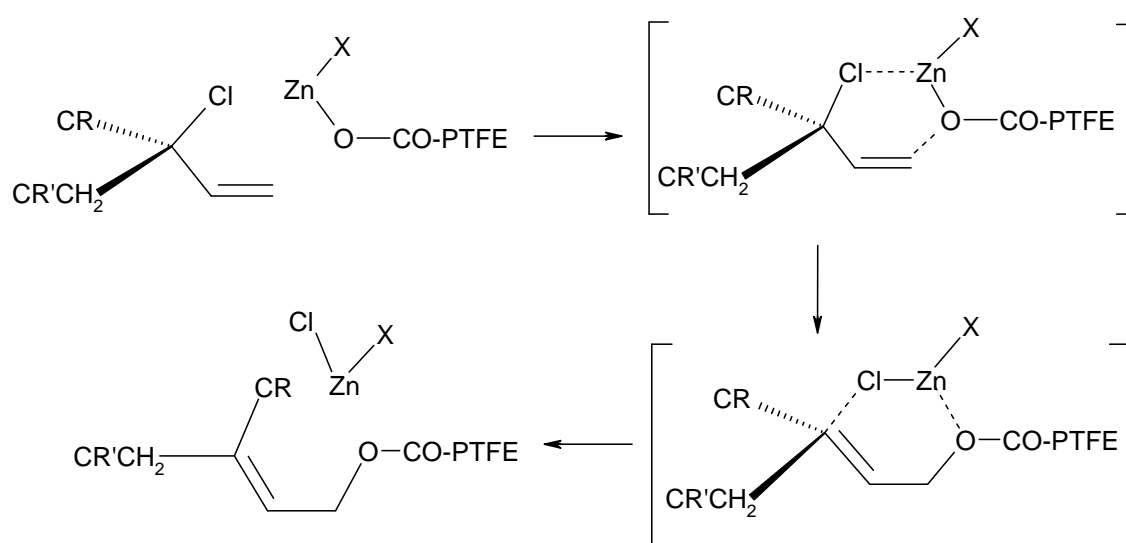
In the case of 500 kGy PTFE powder no such absorption bands are visible. Therefore, this absorption in the FTIR spectra is considered as an indirect indication of the chemical coupling

of chloroprene rubber to irradiated PTFE powder. The presence of CH-absorption bands in PTFE^{500kGy}-CR in the region of 3100-2800 cm⁻¹ blend are not indicative of the coupling of chloroprene rubber to PTFE powder. These bands might have been originated from the materials and solvents utilized in centrifugation and extraction process. The presence of stronger chloroprene absorptions in the PTFE^{500kGy}-CR blend spectrum as opposed to PTFE^{0kGy}-CR blend provides an indication of a stronger chemical coupling between the irradiated PTFE powder and chloroprene matrix. The absorption bands in PTFE^{0kGy}-CR at 1661 cm⁻¹ are significantly weaker than in the PTFE^{500kGy}-CR blend. The FTIR investigations provide only indirect evidence that irradiated PTFE powder is chemically coupled to the chloroprene matrix. Further conclusive investigations are required to obtain a direct evidence of the existence and nature of the chemically coupling between irradiated PTFE powder and chloroprene matrix.

4.4.2.2. Plausible chemical coupling mechanism

The proposed mechanism e.g. for CR rubber vulcanization is up till now discussed as a planar three-component reaction mechanism where structural and special peculiarities have not been fully taken into consideration [99]. A new approach to the coupling reaction mechanism is proposed. Such mechanism can also be applied to vulcanization of CR as well. The new chemical coupling between CR and PTFE is based on the availability of special structures in CR (olefinic unsaturated 3,4-chloroprene structure) and the functional groups in PTFE (carboxylic acid groups: COOH). As mentioned previously, functional groups such as -COOH) at the surface of PTFE particles are generated during irradiation of PTFE in the presence of atmospheric conditions. However, these carboxylic acid groups on PTFE surface itself are inadequately active or inert to initiate a coupling reaction with CR. As a pre-requisite, similar to the initiation of vulcanization process of CR, these carboxylic acid groups require specific activation by the reaction with Zn or Mg salts for chemical coupling with CR. In CR vulcanization, the ZnCl₂ formed acts as strong Lewis acid and can serve to accelerate the reaction. This can be achieved either by activating PTFE^{COOH} with Zn salts prior to reactive mixing with CR or during mixing of PTFE^{COOH} and CR in the presence of ZnO in mixing chamber. The latter procedure for activating PTFE^{COOH} may result either in premature vulcanization of CR with ZnO or either formation of PTFE^{-COOZn)-X}, where X can be -OH, -Cl or another PTFE^{COO-}. The degree of the reactions depends on the processing conditions and kinetics of these reaction processes.

The proposed mechanism is based on a two-component chemical coupling reaction following the chemical bonding (electron redistribution). Figure 73 explains the suggested reaction mechanism, where the interaction of functionalized PTFE powder (PTFE^{-COOZn-X}) with chloroprene matrix during shear blending results in the formation of a six-member ring (Figure 73, right above). Further, the corresponding chemical interaction between the different atoms results in the formation of in-situ conjugated transfer state. After the redistribution of electrons, the formation of a chemically coupled CR-PTFE molecule is then realized with the elimination of the ZnClX compound (Figure 73, right below). The molecular system is then stabilized by the transformation of the carbon atom into CR position 2 from a tetrahedron to a planar configuration.



where X is -OH, -Cl or another PTFE^{COO-}

Figure 73. Plausible reaction mechanism of modified PTFE powder and CR rubber

4.4.3. Compatibility and dispersion

SEM micrographs of the tensile fractured surfaces of PTFE^{0kGy}-CR and PTFE^{500kGy}-CR are shown in Figure 74. The PTFE agglomerates are dispersed in the rubber matrix without much agglomeration. The particle size as shown in the images varies considerably. The average sizes of large agglomerates is in the order of 10-15 μm . The PTFE^{500kGy}-CR vulcanizate surface is smooth and the agglomerates are embedded and homogeneously dispersed in the chloroprene matrix (Figure 74 right), while PTFE^{0kGy}-CR shows the presence of large vacuoles on the fractured surface (Figure 74, left). This indicates that the PTFE particles are being pulled out of the matrix on application of stress.

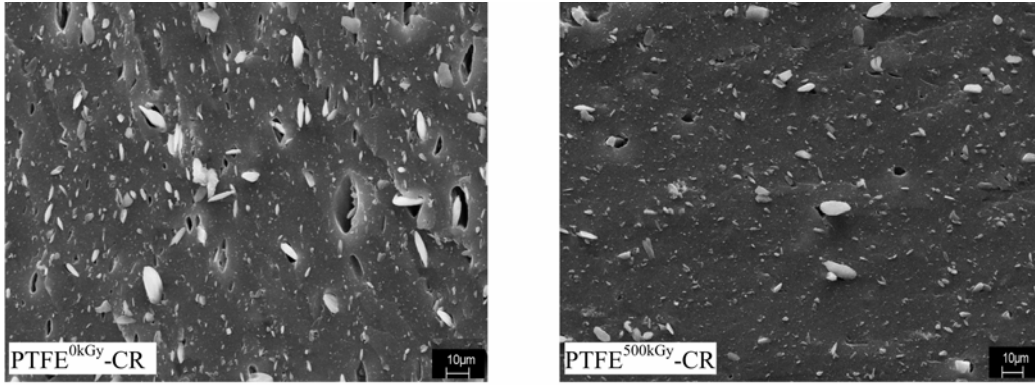


Figure 74. SEM micrographs of tensile fractured surfaces of PTFE-CR vulcanizates

The microstructures of the corresponding rubber composites measured by TEM are shown in Figure 75. The enhanced interfacial compatibility of modified PTFE particles in PTFE^{500kGy}-CR is clearly visible in the corresponding TEM micrographs. The modified agglomerate particles are embedded and partially enwrapped by the chloroprene matrix. No clear and sharp interphase is visible between the two polymeric phases. Slightly light and dark regions around modified PTFE powder are an indication of a reinforced compatible interphase. On the other hand, PTFE^{0kGy}-CR containing non-modified PTFE powder acts as solid rigid bodies lacking interfacial compatibility with polymer matrix. The sharp interface distinctively separates the two incompatible polymers from each other. It is important to note that the filler particles in PTFE^{500kGy}-CR as compared to those in PTFE^{0kGy}-CR are slightly elongated and stretched in a specific direction. Besides strong adhesion or compatibility with rubber matrix, this also proves that the PTFE particles are soft and deformable. The modified PTFE particles due to enhanced chemical coupling with chloroprene have been oriented under the application of strong shearing during reactive blending. However, the inert non-irradiated PTFE particles maintain the spherical shape even under high shearing.

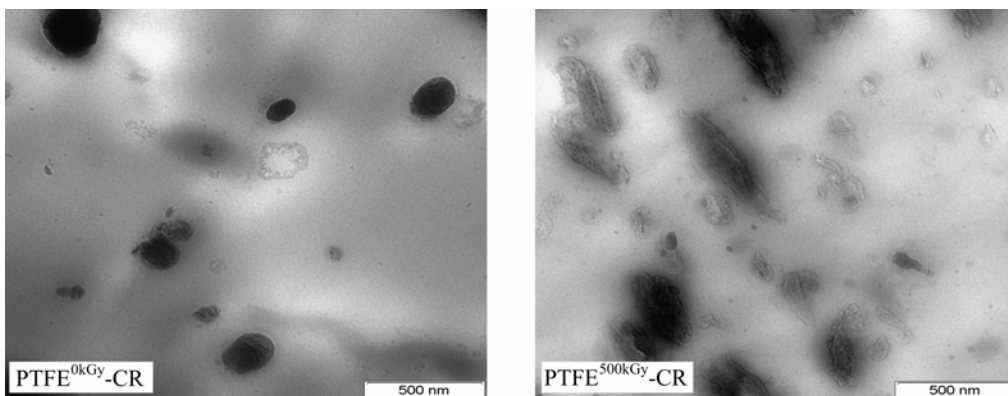


Figure 75. Transmission electron micrographs (TEM) of PTFE filled CR vulcanizates

5. Conclusions & Outlook

The conclusions presented in this thesis have been able to deliver answer to the questions that have been stated above in the aim of the work. PTFE powder can be incorporated as a reinforcing additive in different rubber matrixes where enhanced physical, friction and wear properties are desired. However, different friction, wear and chemical coupling mechanisms in PTFE based rubber compounds have been responsible for their unique behaviour. Morphology, dispersion and chemical coupling of the PTFE powder are critically dominant in controlling friction, wear as well as physical properties. In order to study this aspect, the vulcanizates were produced with hardness values higher than the critical 58 Shore (A) by crosslinking PTFE filled EPDM compounds using electron irradiation instead of peroxide. This was achieved by monitoring the influence of increasing crosslinking irradiation dose on vulcanizate's hardness. The friction and wear properties of L100X, MP1100, and MP1200 EPDM vulcanizates with comparable hardness but different morphologies, dispersion and chemical coupling have been investigated. MP1100-EPDM vulcanizate maintains excellent dispersion but shows significantly poor friction and wear properties while MP1200-EPDM and L100X^{0kGy}-EPDM with comparatively improved friction and wear properties are characterized with poor dispersion and chemical compatibility of PTFE powder with EPDM. On the other hand, L100X^{500kGy}-EPDM shows significantly improved physical, dynamic mechanical and tribological properties. This is attributed to the specific chemical coupling between L100X^{500kGy} PTFE powder and EPDM. The enhanced friction and wear properties results from the embedment of L100X^{500kGy} PTFE agglomerates in EPDM matrix along with its ability to transfer PTFE to wear track. As such a constant source of lubrication due to PTFE transfer phenomenon is formed at the counter-surface which helped in easy sliding of the counter-body against a wear track.

It has been shown that with the help of irradiation the incompatible PTFE surface can be functionalized to enhance its compatibility with rubber matrixes. Besides this, 30 phr PTFE loading has been found sufficient enough in improving physical and friction properties. Further, the influence of radiation-induced free radicals and structure alterations on the properties of rubber compound has been investigated. The radicals generated during irradiation are available for chemical coupling with the unsaturation in EPDM. Low-temperature shear mixing of electron modified PTFE powder with rubber produces PTFE coupled rubber compounds with desired physical properties.

The use of irradiated PTFE powder in EPDM shows enhanced physical properties as compared to non-irradiated PTFE. The existence of compatibility between modified PTFE powder and EPDM is indirectly revealed by Transmission electron microscopy (TEM), Differential Scanning Calorimetry (DSC) and Scanning Electron Microscopy (SEM). TEM shows that modified PTFE powder (500 kGy) is obviously but partially enwrapped by EPDM compared to non-irradiated PTFE powder (0 kGy). This leads to a characteristic compatible interphase around the modified PTFE. The resultant chemically coupled PTFE filled EPDM demonstrate exceptionally enhanced physical properties by partial enwrapping of modified PTFE powder by EPDM. Crystallization studies by DSC also reveal the existence of a compatible interphase in the modified PTFE coupled EPDM. The synergistic effect of enhanced compatibility by chemical coupling and micro-dispersion of PTFE agglomerates results in improvement of physical properties of PTFE coupled EPDM compounds. In summary, an effective procedure both for the modification of PTFE powder as well as the crosslinking of PTFE filled EPDM by electron treatment has been developed to prepare PTFE coupled EPDM compounds with desired properties.

Moreover, PTFE powder was also incorporated in CR rubber. The use of modified PTFE powder as a reinforcing additive in CR results in chemical coupling with CR. Significant improvement in properties for higher irradiation dose of PTFE powder in CR was observed. A new approach to the chemical coupling reaction mechanism is proposed. The coupling between CR and PTFE is based on the availability of special structures (olefinic unsaturated 3,4-chloroprene) in CR and the functional groups in PTFE (COOH groups). These carboxylic acid groups have been chemically activated by Zn or Mg salts for chemical coupling with CR. This can be done either by activating PTFE^{COOH} with Zn salts prior to reactive mixing with CR or during mixing of PTFE^{COOH} and CR in the presence of ZnO in mixing chamber. The latter procedure for activating PTFE^{COOH} may result either in premature vulcanization of CR with ZnO or either formation of PTFE-^{COOZn-X}. The degree of the reactions depends on processing parameters and the kinetics of these reaction processes. In conclusion, PTFE coupled rubber compounds prepared by the described approach offer the potential use of PTFE powder in wide range of rubber compounds for special purpose applications. Accordingly, they are promising in various fields

The state of the art in friction and wear of PTFE filled rubbers include the effects of many important system parameters, such as the composition of the rubber formulation, particle dispersion, bulk mechanical properties, ability of transfer film formation and the chemistry between PTFE powder and rubber matrix. Although, the present study has explicitly

highlighted the potential of PTFE powder in rubber matrixes with significant property improvements in the friction, wear and physical properties, it has simultaneously opened a new field regarding the use of PTFE powder in rubber compounds with some challenging tasks for chemists, engineers and material scientists.

The present work recommends three different subject areas where thorough investigations will further improve our understanding of the governing mechanisms involved in PTFE filled rubber compounds.

- Further investigations in understanding the mechanism/s of chemical coupling are required using well known techniques such as solid state Nuclear Magnetic Resonance (NMR).
- Besides this, investigations concerning the influence of characteristic properties of PTFE powder such as PTFE grade (emulsion, suspension), particle size (surface to volume ratio), and surface activity (functional groups and radicals) on specific chemical coupling mechanism/s during reactive processing is required. This will help in optimizing the modification and compatibilization of PTFE powder as well as preparing PTFE coupled rubber compounds either by controlled reactive mixing as has been adapted in this thesis (two-step process) or by a one-step processing method where modification of PTFE powder using high-energy electrons takes place during mixing process of PTFE based rubber compound.
- The results and experienced accumulated from this fundamental should be applied in technical rubber formulations. However, PTFE powder with its unique properties is exceptionally difficult to disperse and therefore, techniques frequently applied for filler dispersion such as electrical conductivity measurements etc, may seem implausible. The improvement of PTFE dispersion in rubber matrix is certainly desired for further improvement in properties, especially mechanical properties. Such improvements will certainly be helpful to develop PTFE based rubber compounds with satisfactory mechanical properties. These investigations will not only help in understanding friction and wear behaviour but also assist in designing materials for tribological applications based on PTFE-elastomeric composites.

References

- [1] E. Bock; Sealing systems in combustion engine, *GAK Gummi Fasern Kunststoffe* 3 (2004), p. 180-187.
- [2] W. H. Crandell; Evaluation of Silicon Rubber Modified with Teflon, *Rubber World* (1955), p. 236-240.
- [3] M. H. Kaufman, J. Gonzales; Reinforcement of Fluoroelastomers with Halopolymers, *Rubber Chemistry and Technology* 41 (1968), p. 527-532.
- [4] L. M. Magner and J. O. Punderson; U.S patent 3,484,503 Dupont (1969)
- [5] H.C. Nash, E. J. Kohn; Studies on reducing the surface friction of elastomers, Naval Research Laboratories Washington DC (1963); <http://handle.dtic.mil/100.2/AD405838>
- [6] G. F. Paulus, P. Huron; US Patent 3293203 (1966)
- [7] M. H. Kaufman; US Patent 3940455 (1976)
- [8] S. Morita; US Patent 4387168 (1983)
- [9] W. E. Peters; US Patent 4,596,839 (1986)
- [10] W. E. Peters; WO Patent 87/03515 (1987)
- [11] J. A. Dillon; WO Patent 88/04982 (1988)
- [12] E. A. Rubin; WO Patent 97/03812 (1997)
- [13] F. P. Bowden and D. Tabor; *The Friction and Lubrication of Solids*, Clarendon Press, Oxford (1950)
- [14] I. V. Kraghelsky and E. F. Nepomnyashchi; Fatigue wear under elastic contact conditions, *Wear* 8 (1965), p. 303-319.
- [15] Glossary of Terms and Definitions in the Field of Friction, Wear and Lubrication (Tribology), Research group on Wear of Engineering Materials, Organisation for Economic Cooperation and Development (OECD), Paris (1969)
- [16] D. F. Moore; *The Friction and Lubrication of Elastomers*, Pergamon Press, Oxford (1972)
- [17] K. A. Grosch; The relation between the friction and visco-elastic properties of rubber, *Proceedings of the Royal Society of London, Series A* 274 (1963), p. 21-39.
- [18] W. Gwidon, W. Stachowiak and W. A. Batchelor; *Engineering Tribology*, 2nd ed, Bittenworth-Heinemann, Oxford (2001).
- [19] C. W. Bunn, E. R. Howells; Structures of molecules and crystals of Fluorocarbons, *Nature* 4429 (1954), p. 549-551.

- [20] D. L. Burris, B. Boesl, G. R. Bourne, W. Gregory Sawyer; Polymeric nanocomposites for tribological applications, *Macromolecular Materials and Engineering* 292 (2007), p. 387-402.
- [21] A. Schallmach; Friction and abrasion of rubber, *Wear* 1 (1958), p. 384–417.
- [22] A. Schallmach; A Theory of Dynamic Rubber Friction, *Wear* 6 (1963), p. 375-382.
- [23] D. F. Moore, W. Geyer; A review of adhesion theories of elastomers, *Wear* 22 (1972), p. 113-141.
- [24] D. F. Moore, W. Geyer; A review of hysteresis theories of elastomers, *Wear* 30 (1974), p. 1-34.
- [25] M. Barquins, A. D. Roberts; Rubber friction variation with rate and temperature: some new observations, *Journal of Physics D : Applied. Physics* 19 (1986), p. 547-563.
- [26] G. A. D. Briggs, B. J. Briscoe; The dissipation of energy in the friction of rubber, *Wear* 35 (1975), p. 357-364.
- [27] B. N. J. Persson; Theory of rubber friction and contact mechanics, *Journal of Chemical Physics* 115 (2001), p. 3840-3861.
- [28] G. Heinrich; Hysteresis friction of sliding rubbers on rough and fractal surfaces, *Rubber Chemistry and Technology* 70 (1997), p. 1-13.
- [29] G. Heinrich, H. B. Dumler; Wet skid properties of filled rubbers and the rubber-glass transition, *Rubber Chemistry and Technology* 71 (1998), p. 53-60.
- [30] G. Heinrich, M. Klüppel and T. A. Vilgis; Evaluation of self-affine surfaces and their implication for frictional dynamics as illustrated with a Rouse material, *Computational and theoretical polymer science* 10 (2000), p. 53-61.
- [31] M. Klüppel, G. Heinrich; Rubber Friction on Self-Affine Road Tracks, *Rubber Chemistry and Technology* 73 (2000), p. 578-606.
- [32] H. R. Berger, G. Heinrich; Friction effects in the contact area of sliding rubber: a generalized Schallmach model, *Kautschuk Gummi Kunststoffe* 53 (2000), p. 200-205.
- [33] B. N. J. Persson, U. Tartaglino, O. Albohr, E. Tosatti; Rubber friction on wet and dry road surfaces: The sealing effect, *Physical review B* 71 (2005), p. 035428.
- [34] B. N. J. Persson, U. Tartaglino, E. Tosatti et al., Rubber friction on wet rough substrates at low sliding velocity: The sealing effect. *Kautschuk Gummi Kunststoffe* 57 (2004), p. 532-537.
- [35] R. Bjerck, W. Brandon, F. Engelkin and J. Jero; US patent 3,898,361 (1975)
- [36] I. H. Scher and S. I. Ungar; US patent 4,400,423 (1983)
- [37] R. Bjerck, W. Brandon, F. Engelkin and J. Jero; US patent 4045402 (1977)

- [38] M. P. Defrank; US patent 4131590 (1978)
- [39] K. G. Gatos, K. Kameo, J. Karger-Kocsis; On the friction and sliding wear of rubber/layered silicate nanocomposites, *eXPRESS Polymer Letter* 1 (2007), p. 27–31.
- [40] J. Karger-Kocsis, D. Felhös, R. Thomann; Tribological behaviour of carbon nanofiber modified, Santoprenes thermoplastic elastomer under dry sliding and fretting conditions against steel, *Journal of Applied Polymer Science* 108 (2008), p. 724–730.
- [41] D. Felhös, J. Karger-Kocsis, D. Xu; Tribological testing of peroxide cured HNBR with different MWCNT and silica content under dry sliding and rolling conditions against steel, *Journal of Applied Polymer Science* 108 (2008), p. 2840–2851.
- [42] J. Karger-Kocsis, A. Mousab, Z. Major and N. Békési; Dry friction and sliding wear of EPDM rubbers against steel as a function of carbon black content, *Wear* 264 (2008), p. 359–367.
- [43] D. Felhös and J. Karger-Kocsis; Tribological testing of peroxide-cured EPDM rubbers with different carbon black contents under dry sliding conditions against steel, *Tribology International* 41 (2008), p. 404–415.
- [44] N. S. M. El-Tayeb, R. M. D. Nasir; Effect of soft carbon black on tribology of deproteinised and polyisoprene rubbers, *Wear* 262 (2007), p. 350–361.
- [45] A. Koenen, A. Sanon, Tribological and vibroacoustic behaviour of a contact between rubber and glass (application to wiper blade), *Tribology International* 40 (2007), p. 1484–1491.
- [46] H. P. Jost, Lubrication (Tribology) Education and Research, UK Department of Education and Science, HMSO (1966)
- [47] Strategy for energy conservation through tribology, Pub. ASME (1977).
- [48] BMFT Newsletter, High losses for national economy due to friction and wear, English version, (1980)
- [49] H. P. Jost; The tasks of tribology societies on a changing world, Opening Address, *Second World Tribology Congress*, Vienna (2001)
- [50] S. V. Gangal; Tetrafluoroethylene polymers, in '*Encyclopedia of Polymer Science and Engineering*', eds.: Mark. H. F., Bikales N. M., Overberger C. G., Menges G., Wiley, New York, 2 ed., 16 (1989), p. 577–600.
- [51] T. L. Cottrell; *The Strength of Chemical Bonds*, Butterworth, London (1958)
- [52] W. A. Sheppard, C. M. Sharts; *Organic Fluorine Chemistry*, W. A. Benjamin Inc, New York (1969)

- [53] C. W. Bunn, A. J. Cobbold, R. P. Palmer; The fine structure of Polytetrafluoroethylene, *Journal of Polymer Science*, 28 (1958), p. 365-376.
- [54] R. H. H. Pierce, E. S. Clark, J. F. Whitney, W. M. D. Bryant; Crystal structure of polytetrafluoroethylene, Meeting of the American Chemical Society, Atlantic city (1956)
- [55] R. C. Doban, C. A. Sperati and B. W. Sandt; The physical properties of 'teflon', polytetrafluoroethylene, *Society of Plastic Engineer J* 11 (1955), p. 11–30.
- [56] J. Scheirs; *Modern Fluoropolymers*, Wiley, New York (1997)
- [57] D. Lehmann, B. Hupfer, U. Lappan, G. Pompe, L. Häußler, D. Jehnichen, A. Janke, R. Reinhardt, K. Lunkwitz, R. Franke and K. Kunze; New PTFE-Polyamide Compounds, *Designed Monomers and Polymers*, 5 (2002), p. 317-324.
- [58] D. Lehmann, B. Klüpfel DE Patent 10 2004 016 873 A1 (2005)
- [59] D. Lehmann, B. Klüpfel WO Patent 2005/042599 A1 (2005)
- [60] D. Lehmann, B. Hupfer, U. Lappan, U. Geißler, R. Reinhardt, K. Lunkwitz, Neue Polytetrafluoroethylen-Polyamid Compounds, *Materialwissenschaft und Werkstofftechnik* 31 (2000), p. 666-668.
- [61] B. Klüpfel, D. Lehmann, G. Heinrich, C. Linhart, E. Haberstroh, K. Kunze, W. Hufenbach, C. Dallner, R. Künkel, G. W. Ehrenstein; Kopplung von PTFE und Kautschuk- Eine neue elastomere Werkstoffklasse, *Kautschuk Gummi Kunststoffe* 58 (2005), p. 226-229.
- [62] E. Haberstroh, C. Linhart, K. Epping, T. Schmitz; Verbesserte tribologische Eigenschaften von Elastomeren durch PTFE Pulver, *Kautschuk Gummi Kunststoffe* 59 (2006), p. 447-453.
- [63] S. Cheng, D. R. Kerluke; Radiation processing for modification of polymers 'Presented at the 2003 Annual Technical Conference of the Society of Plastic Engineering (ANTEC) IBA, Advanced Materials Division, 7695 Formula Place, San Diego' (2003)
- [64] A. A. Khan, C. W. Stewart; U.S. patent 4,469,864 to Dupont (1984)
- [65] H. Dorschner, U. Lappan, K. Lunkwitz; Electron beam facility in polymer research: Radiation induced functionalization of polytetrafluoroethylene, *Nuclear Instruments and Methods In Physics Research* 139 (1998), p. 495-501.
- [66] U. Lappan, U. Geißler, K. Lunkwitz; Changes in the chemical structure of polytetrafluoroethylene induced by electron beam irradiation in the molten state, *Radiation Physics and Chemistry* 59 (2000), p. 317-322.

- [67] K. Lunkwitz, H. J. Brink, D. Handte and A. Ferse; The radiation degradation of polytetrafluoroethylene resulting in low-molecular and functionalized perfluorinated compounds, *Radiation Physics and Chemistry* 33 (1989), p. 523-532.
- [68] K. Lunkwitz, U. Lappan, U. Scheler; Modification of perfluorinated polymers by high-energy irradiation, *Journal of Fluorine Chemistry* 125 (2004), p. 863-873.
- [69] U. Lappan, U. Geißler and K. Lunkwitz; Electron beam irradiation of polytetrafluoroethylene in vacuum at elevated temperature: An infrared spectroscopic study, *Journal of Applied Polymer Science* 74 (1999), p. 1571-1576.
- [70] U. Lappan, K. Lunkwitz; Radiation-induced functionalization of fluoropolymers, *Zeitschrift für Physikalische Chemie* 191, (1995), p. 209-218.
- [71] W. Bürger, K. Lunkwitz, G. Pompe, A. Petr and D. Jehnichen; Radiation degradation of fluoropolymers: Carboxylated fluoropolymers from radiation degradation in presence of air, *Journal of Applied Polymer Science* 48 (1993), p. 1973-1985.
- [72] P. R. Dluzneski; Peroxide Vulcanization of Elastomers, *Rubber chemistry and Technology* 74 (2001), p. 451-492.
- [73] M. Akiba, A. S. Hashim; Vulcanization and crosslinking in elastomers, *Progress in Polymer Science* 22 (1997), p. 475-521.
- [74] D. S. Ogunniyi; Peroxide vulcanisation of rubber, *Progress in rubber and plastics technology* 15 (1999), p. 95-112.
- [75] R. C. Keller; Peroxide curing of ethylene-propylene elastomers, *Rubber Chemistry and Technology* 61 (1988), p. 238-54.
- [76] T. Yamazaki, T. Seguchi; Electron spin resonance study on chemical crosslinking reaction mechanisms of polyethylene using a chemical agent. V. Comparison with polypropylene and ethylene-propylene copolymer, *Journal of Polymer Science, Part A: Polymer Chemistry* 38 (2000), p. 3383-3389.
- [77] W. C. Endstra, C. T. J. Wreesmann; Peroxide crosslinking of EPDM rubbers, in 'Elastomer Technology Handbook', N. P. Cheremisinoff Ed., CRC Press, Boca Raton (1993), p. 496-518.
- [78] A. S. Basfar, A. A. Abdel Aziz; Comparison of the thermal stability of sulphur, peroxide and radiation cured NBR and SBR vulcanizates, *Polymer Degradation and Stability* 67 (2000), p. 319-323.
- [79] H. F. Mark; Elastomers - past, present, and future, *Rubber Chemistry and Technology* 61 (1988), p. 73-96.

- [80] S. D. Gehman; Network chain distribution and strength of vulcanizates, *Rubber Chemistry and Technology* 42 (1969), p. 659-665.
- [81] J. H. A. Grobler, W. J. McGill; Effect of network heterogeneity on tensile and tear strengths of radiation, peroxide, efficient and conventional cured polyisoprene, *Journal of Polymer Science B: Polymer Physics* 32 (1994), p. 287–295.
- [82] I. Banik, A. K. Bhowmick, V. K. Tikku, A.B. Majali, R. S. Deshpande; Effects of electron beam on the structural modification of the copolymeric and the terpolymeric fluorocarbon rubbers, *Radiation Physics and Chemistry* 51 (1998), p.195-204.
- [83] I. Banik, S. K. Dutta, T. K. Chaki, A. K. Bhowmick; Electron beam induced structural modification of a fluorocarbon elastomer in the presence of polyfunctional monomers, *Polymer* 40 (1999), p. 447-458.
- [84] I. Banik and A. K. Bhowmick; Influence of electron beam irradiation on the mechanical properties and crosslinking of fluorocarbon elastomer, *Radiation Physics and Chemistry* 54 (1999), p. 135-142.
- [85] I. Banik and A. K. Bhowmick; Dynamic mechanical properties of electron beam modified fluorocarbon rubber, *Journal of Applied Polymer Science* 69 (1998), p. 2079-2087.
- [86] M. Aoshima, T. Jinno, T. Sassa; Electron-Beam crosslinking of ethylene-propylene rubber, *Kautschuk Gummi Kunststoffe* 45 (1992), p. 644-646.
- [87] S. Tripodi, J. M. Carella, O. A. Curzio, E. M. Valles; Molecular Weight and Antioxidant Effects on the Structure of Irradiated Linear Low Density Polyethylene *Radiation Physics and Chemistry* 1 (1991), p. 89-94.
- [88] G. G. A. Böhm, J. O. Tveekrem; The radiation chemistry of elastomers and its industrial applications, *Rubber Chemistry and Technology* 55 (1982), p. 575-668.
- [89] M. M. Abdel-Aziz, A. A. Basfar; Evaluation of some antioxidants in radiation vulcanized ethylene-propylene diene (EPDM) rubber, *Nuclear Instruments and Methods in Physics Research B* 185 (2001), p. 346-350.
- [90] M. F. Vallat, F. Ruch, M. O. David; A structural study of EPDM networks—the influence of the crosslinking mode on their microscopic structure, *European Polymer Journal* 40 (2004), p. 1575-1586.
- [91] C. Giovedi, E. S. Pino, M. R. Rossi, L. D. B. Machado; Electron beam irradiation effects on the mechanical, thermal and surface properties of a fluoroelastomer, *Nuclear Instruments and Methods in Physics Research B* 265 (2007), p. 256-259.

- [92] P. S. Majumder, A. K. Bhowmick; Structure-property relationship of electron-beam-modified EPDM rubber, *Journal of Applied Polymer Science* 77 (2000), p. 323-337.
- [93] P. Sen Majumder, A. K. Bhowmick; Friction behaviour of electron beam modified ethylene-propylene diene monomer rubber surface, *Wear* 221 (1998), p. 15-23.
- [94] P. Sen Majumder, A. K. Bhowmick; Electron beam-initiated surface modification of elastomers, *Journal of adhesion science and technology* 12 (1998), p. 831-856.
- [95] R. Aliev; Effect of dose rate and oxygen on radiation crosslinking of silica filled fluorosilicone rubber, *Radiation Physics and Chemistry* 56 (1999), p. 347-352.
- [96] J. G. M. Vangisbergen, M. C. M. Vandersanden, J. W. Dehaan et al.; Influence of electron-beam irradiation on impact properties of polystyrene EPDM rubber blends, *Makromolekulare Chemie-Macromolecular Symposia* 41 (1991), p. 153-164.
- [97] J. W. M. Noordermeer; Ethylene-Propylene-Diene Rubber, *Kirk-Othmer Encyclopedia of Chemical Technology*, 4th ed, 8 (1993), p. 978 – 989.
- [98] R. Karpeles and A. V. Grossi; EPDM Rubber Technology, *Handbook of Elastomers*, 2nd ed., Anil K. Bhowmick and Howard L. Stephens [Editors], Marcel Decker, Inc, New York (2001).
- [99] P. R. Johnson; Polychloroprene rubber, *Rubber Chemistry and Technology* 49 (1976), p. 650-679.
- [100] C. J. Salamone; *Polymeric Materials Encyclopaedia*, CRC Press LLC, Boca Raton, Florida (1999), p. 247-250
- [101] M. Mooney; A theory of large elastic deformation, *Journal of Applied Physics* 11 (1940), p. 582-592.
- [102] R. S. Rivlin and D. W. Saunders; Large Elastic Deformations of Isotropic Materials. VII. Experiments on the Deformation of Rubber, *Phil. Trans. Royal Society of London, Series A243* (1951), p. 251-258.
- [103] G. Heinrich, T. A Vilgis; Contribution of entanglements to the mechanical-properties of carbon-black filled polymer networks, *Macromolecules* 26 (1993), p. 1109-1119.
- [104] E. Guth, O. Gold; On the hydrodynamical theory of the viscosity of suspension, *Physical Review* 53 (1938), p.322.
- [105] U. Eisele, H. K Müller; Eine neue Methode zur Bestimmung der Netzstellendichte von gefüllten Vulkanisaten, *Kautschuk Gummi Kunststoffe* 43 (1990), p. 9-19.
- [106] S. V. Lomov, P. Boisse, E. Deluycker et.al; Full-field strain measurements in textile deformability studies, *Composites Part A: Applied Science and Manufacturing*, 39 (2008), p. 1232-1244.

- [107] J. H. Golden; The degradation of polytetrafluoroethylene by ionizing radiation, *Journal of Polymer Science* 45 (1960), p. 534 – 536.
- [108] M. Hagiwara, T. Tagawa, H. Amemiya, K. Araki, L. Shinohara, T. Kagiya; Mechanism of thermal decomposition of peroxide radicals formed in polytetrafluoroethylene by γ -ray irradiation, *Journal of Polymer Science: Polymer Chemistry* 14 (1976), p. 2167-2172.
- [109] W. K. Fisher, J. C. Corelli; Effect of Ionizing Radiation on the Chemical Composition, Crystalline Content and Structure, and Flow properties of polytetrafluoroethylene. *Journal of Polymer Science: Polymer Chemistry* 19 (1981), p. 2465-2493.
- [110] L. Häussler, G. Pompe, D. Lehmann, U. Lappan; Fractionated crystallization in blends of functionalized poly(tetrafluoroethylene) and polyamide. *Macromolecular Symposia* 164 (2001), p. 411-419.
- [111] G. Pompe, L. Häussler, P. Pötschke, D. Voigt, A. Janke, U. Geißler, B. Hupfer, G. Reinhardt, D. Lehmann; Reactive Polytetrafluoroethylene/Polyamide Compunds. I. Characterization of the Compound Morphology with respect to the Functionality of the Polytetrafluoroethylene Component by Microscopic and differential Scanning Calorimetry Studies, *Journal of Applied Polymer Science* 98 (2005), p. 1308-1316.
- [112] K. Tanaka, S. Kawakami; Effect of various Fillers on the Friction and Wear of PTFE-Based Composites, *Wear* 79 (1982), p. 221-234.
- [113] J. K. Lancaster; The effect of carbon fibre reinforcement on the friction and wear of polymers, *Journal of Physics D* 1 (1968), p. 549-559.
- [114] A. C. M. Yang, J. E. Ayala, A. Bell, J. C. Scott; Effects of filler particles on abrasive wear of elastomer based composites, *Wear* 146 (1991), p. 349-366.
- [115] M. Vaziri, R. T. Spurr, F. H. Scott; An investigation of the wear of polymeric materials, *Wear* 122 (1988), p. 329-342.
- [116] U. S. Tewari, J. Bijwe; On the abrasive wear of some polyimides and their composites, *Tribology International* 24 (1991), p. 247-254.
- [117] J. J. Rajesh, J. Bijwe, U. S. Tewari; Influence of fillers on abrasive wear of short glass fibre reinforced polyamide composites, *Journal of Material Science* 36 (2001), p. 351-356.
- [118] J. Bijwe, S. Awtade, B. K. Satapathy, A. K. Ghosh; Influence of concentration of aramid fabric on abrasive wear performance of polyethersulfone composite, *Tribology letter* 17 (2004), p. 187-194.

- [119] M. Klüppel, G. Heinrich; Rubber Friction on Self-Affine Road Tracks, *Rubber Chemistry and Technology* 73 (2000), p. 578-606.
- [120] O. Pigors; Werkstoffe in der Tribotechnik: Reibung, Schmierung und Verschleißbeständigkeit von Werkstoffen und Bauteilen (1999), ISBN 3-342-00658-7
- [121] D. E. Kline; Nuclear Radiation Effects in Polytetrafluoroethylene, *Journal of Polymer Science: Part A 1* (1963), p. 1621-1626.

Curriculum Vitae

The author of this thesis was born on February 01, 1977 in Peshawar, Pakistan. In 1995 he finished his high school and college education from Abbottabad Public School and College, Pakistan and afterwards started his graduate studies in Chemical Engineering (Bachelor of Science) at the N.W.F.P University of Engineering and Technology Peshawar. After graduating as Chemical Engineer in 2001 he further pursued higher studies (International Master degree in Polymer Science) in 2003 from Martin Luther University (MLU) Halle, Wittenberg Germany. After successful graduation in 2005 from MLU Halle, later he commenced his doctorate studies at the Leibniz Institute of Polymer Research Dresden under Prof. Gert Heinrich, which he completed in March 2009.

Résumé: The present thesis is composed of the following contributions.

Journal Publications

- Khan MS, Lehmann D, Heinrich G. Properties of the EPDM with modified PTFE nanopowder, **Kautschuk Gummi Kunststoffe** 60 (2007) 226-234.
- Khan MS, Lehmann D, Heinrich G. Modification of PTFE nanopowder by controlled-electron beam irradiation: A useful approach for the development of PTFE coupled EPDM compounds, **eXPRESS Polymer Letters** 2 (2008) 284-293.
- Khan MS, Franke R, Gohs U, Lehmann D, Heinrich G. Friction and wear behavior of electron beam modified PTFE filled EPDM compounds, **Wear** 266 (2009) 175-183.
- Khan MS, Lehmann D, Heinrich G, Franke R. Tribological study of peroxide-cured EPDM rubber filled with electron beam irradiated PTFE powder, **Wear** 266 (2009) 200-207.
- Khan MS, Franke R, Lehmann D, Heinrich G. Physical and tribological properties of PTFE micropowder filled EPDM rubber, **Tribology International** 42 (2009) 890-896.
- Khan MS, Lehmann D, Heinrich G, Gohs U, Franke R. Structure-property effects on mechanical, friction and wear properties of electron modified PTFE filled EPDM composite, **eXPRESS Polymer Letters** 3 (2009) 39-48.
- Khan MS, Lehmann D, Heinrich G. Influence of the microstructure of PTFE powder on the dispersion and physical properties of PTFE based EPDM rubber, **Polymers for Advanced Technology** (in press).
- Khan MS, Lehmann D, Heinrich G. Newly developed chloroprene rubber compounds based on electron-modified Polytetrafluoroethylene powder, **Acta Materialia** (submitted, Dec 2008).

Patent:

- Khan MS, Lehmann D, Heinrich G. Polychloroprene-Perfluoropolymer materials and the preparation process for its production (submitted 3rd July 2008).

Selected talks:

- Khan MS, Lehmann D, Heinrich G, Franke R. Development and characterization of PTFE nanopowder- elastomeric composites for tribological applications, **13th European Conference on Composite Materials (ECCM 13)**, 2-5th June, 2008, KTH Stockholm, Sweden.
- Khan MS, Heinrich G, Lehmann D, Franke R. Physical and tribological properties of the modified PTFE nanopowder filled EPDM, **The Polymer processing Society 24th Annual Meeting**, 15-19th June, 2008, Salerno Italy, ISBN: 88-7897-024-7.
- Khan MS, Lehmann D, Heinrich G, Franke R. Development and characterization of PTFE nanopowder-elastomeric composites for tribological applications, **Tribologie-Fachtagung 2008, Reibung, Schmierung und Verschleiß**, 22-24th September 2008, Göttingen Germany. ISBN: 978-3-00-025676-9.
- Khan MS, Heinrich G, Lehmann D, Gohs U, Franke R. Friction, wear and physical properties of PTFE powder-rubber composites: structure-property effects. **Reibung, Lubrikation und Verschleiß**, 8th October 2008, Deutsches Institut für Kautschuktechnologie e.V, Hannover Germany.
- Khan MS, Franke R, Gohs U, Heinrich G, Lehmann D. Electron crosslinking of PTFE powder filled EPDM rubber, **6th Dresden symposium on electron beam technology**, Dresden, 26th – 27th November 2008.

Poster contribution:

- Khan MS, Lehmann D, Heinrich G. Evaluation of EPDM modified with PTFE. **Kautschuk-Herbst-Kolloquium (KHK)**, 8-11 November 2006, Hannover, Germany.
- Khan MS, Lehmann D, Heinrich G, Franke R. Properties of the modified PTFE nanopowder filled EPDM. **12. Problemseminar POLYMERMISCHUNGEN "Gefüllte und verstärkte Polymerblends Nanoblends"**. 28-29th March 2007, Bad Lauchstädt, Germany.
- Khan MS, Lehmann D, Heinrich G, Franke R. Properties of the modified PTFE nanopowder filled EPDM. **Symposium on Functional Polymer Based Materials**, 3-4th April 2007, Jena, Germany.
- Khan MS, Lehmann D, Heinrich G, Franke R. Physical and tribological properties of the modified PTFE nanopowder filled EPDM. **Polymeric Materials in Automotive (PMA)** - 19th Slovak Rubber Conference, 15-17 May 2007, Bratislava, Slovakia.
- Khan MS, Lehmann D, Heinrich G. Properties of the EPDM with modified PTFE nanopowder. **11th Dresden Polymer Discussion**, 16-19th Sept, 2007, Meissen, Germany.